Changes in East Atlantic Deepwater Circulation over the last 30,000 years: Eight time slice reconstructions

Michael Sarnthein, Kyaw Winn, Simon Jung, Jean-Claude Duplessy, Laurent Labeyrie, Helmut Erlenkeuser, Gerald Ganssen

PALEOCEANOGRAPHY, VOL. 9, NO. 2, PAGES 209-267, APRIL 1994

Changes in east Atlantic deepwater circulation over the last 30,000 years: Eight time slice reconstructions

Michael Sarnthein,[1] Kyaw Winn,[1] Simon J.A. Jung,[1] Jean-Claude Duplessy,[2] Laurent Labeyrie,[2] Helmut Erlenkeuser,[3] and Gerald Ganssen [4]

Abstract. Using 95 epibenthic $\delta^{13}C$ records, eight time slices were reconstructed to trace the distribution of east Atlantic deepwater and intermediate water masses over the last 30,000 years. Our results show that there have been three distinct modes of deepwater circulation: Near the stage 3-2 boundary, the origin of North Atlantic Deep Water (NADW) was similar to today (mode 1). However, after late stage 3 the source region of the NADW end-member shifted from the Norwegian-Greenland Sea to areas south of Iceland (mode 2). A reduced NADW flow persisted during the last glacial maximum, with constant preformed $\delta^{13}C$ values. The nutrient content of NADW increased markedly near the Azores fracture zone from north to south, probably because of the mixing of upwelled Antarctic Bottom Water (AABW) from below, which then advected with much higher flux rates into the northeast Atlantic. Later, the spread of glacial meltwater over the North Atlantic led to a marked short-term ventilation minimum below 1800 m about 13,500 ^{14}C years ago (mode 3). The formation of NADW recommenced abruptly north of Iceland 12,800-12,500 years ago and reached a volume approaching that of the Holocene, in the Younger Dryas (10,800-10,350 years B.P.). Another short-term shutdown of deepwater formation followed between 10,200 and 9,600 years B.P., linked to a further major meltwater pulse into the Atlantic. Each renewal of deepwater formation led to a marked release of fossil CO_2 from the ocean, the likely cause of the contemporaneous ^{14}C plateaus. Over the last 9000 years, deepwater circulation varied little from today, apart from a slight increase in AABW about 7000 ^{14}C years ago. It is also shown that the oxygenated Mediterranean outflow varied largely independent of the variations in deepwater circulation over the last 30,000 years.

1. Introduction

The modern Atlantic is characterized by the extensive formation of oxygenated North Atlantic Deep Water (NADW), leading to a deepwater outflow of about 20 sverdrups (Sv) (10^6 m^3s^{-1}), which serves as the "lung" of the world ocean. NADW largely originates from highly saline surface water that is advected from and across the equatorial Atlantic and is downwelled in the Baffin Sea, the Greenland and Iceland Seas, and the Arctic Ocean. Following Stommel [1961] , Rooth [1982], and Emiliani et al. [1978], Broecker et al. [1985a,b, 1990], Broecker and Peng [1989], and Broecker [1992] named this current system the "salinity conveyor belt" (SCB). Except for a restricted region west of the Mediterranean, the present NADW is widely overlain by less ventilated, nutrient-enriched South Atlantic Intermediate Water that is formed in the southern ocean (Geochemical Ocean Sections Study (GEOSECS) data in the work of Bainbridge [1981] and Transient Tracers in the Ocean data (unpublished data, 1987)).

In contrast to today, the Atlantic of the last glacial maximum (LGM) had strongly reduced deepwater ventilation. The lack of ventilation probably resulted from reduced NADW formation [Boyle and Keigwin, 1985; Boyle, 1992; Broecker et al., 1985a,b; Charles and Fairbanks, 1992; Duplessy et al., 1988], which implies an increased spreading of sea ice in the southern ocean [Stocker and Wright, 1991]. This glacial system was paralleled by a better ventilation of the Atlantic Intermediate Water the source of which is still controversial [Zahn et al., 1987; Boyle, 1988, 1992].

Hence the Atlantic, and perhaps the global ocean had perhaps two or three quasi-stable states of general circulation, with each controlled by a different distribution of high-latitude salinity [Rooth, 1982; Broecker et al., 1985 a,b; Bryan, 1986; Maier-Reimer and Mikolajewicz, 1989]. Reversals in the state of ocean circulation, that is changes in the SCB are widely regarded as key to a better understanding of the abrupt climatic changes that marked the transition from glacial to interglacial times. These changes include (1) the heat advection to northern Europe (the "Nordic heat pump"), (2) the temperature regime in the deep Atlantic [Labeyrie et al., 1987, 1992], (3) the deepwater ventilation of the global ocean, and to some extent, (4) the variations in atmospheric CO_2 [Barnola et al., 1987; Michel, 1991; Broecker and Peng, 1992].

It is the strategy of this paper to trace the evolution of Atlantic deepwater masses across various climatic regimes

[1]Geologisch-Paläontologisches Institut, University of Kiel, Germany.
[2]Centre des Faibles Radioactivités, Laboratoire mixte CNRS-CEA, Gif-sur Yvette Cedex, France.
[3]C-14 Laboratory, University of Kiel , Kiel, Germany.
[4]Institut voor Aardtwetenschappen, Vrije Universiteit, Amsterdam, Netherlands.

Paper number 93PA03301.
0883-8305/94/93PA-03301$10.00

over the last 30,000 years by revealing the three-dimensional structure of the $\delta^{13}C$ signal from epibenthic foraminifera in the east Atlantic basins using eight time slice reconstructions (continuing the approach of Zahn et al. [1987] and Duplessy et al. [1988]). This strategy can successfully circumvent common problems linked to assessing the variable net fluxes of deep water from single-core records, that is problems related to local peaks in the vertical flux of particulate organic carbon (POC) or to simple vertical shifts in the mixing zone between Antarctic Bottom Water (AABW) and NADW.

The main objectives of our reconstruction are (1) To study the history of NADW and AABW circulation, especially the link between the SCB and the history of deglacial North Atlantic warming, (2) to trace the impact of meltwater-induced salinity reductions in the North Atlantic on the NADW cell (in the sense of Berger [1977], Berger and Vincent [1986], and Fairbanks [1989]) and, moreover, on European cooling episodes such as the Oldest, Older, and the Younger Dryas (in the sense of Broecker [1992), (3) to explore variations in AABW and NADW flux subsequent to $\delta^{18}O$ event 3.1, close to the buildup of continental ice, which led into the LGM, (4) to measure variability in NADW formation during the Holocene, which may have been linked primarily to changes in high-latitude precipitation. It may have led to a salinity reduction in areas of deepwater formation and thus to a reduction of the SCB [Weaver et al., 1991]. Such internal response mechanisms could account for the climatic variability of the Holocene, and they could explain the marked short-term variability in deepwater ventilation and sea surface temperatures in pre-Quaternary intervals such as the early Pliocene [e.g., Tiedemann, 1991], when climatic forcing by continental glaciations and sea ice formation in the northern hemisphere were less significant, (5) to explore possible linkages (as suggested by Reid 1979) between the evolution of the SCB and variations in the Mediterranean outflow, the strength of which is linked to the degree of Mediterranean/subtropical continental aridity [Zahn et al., 1987].

2. Methods

2.1. Benthic $\delta^{13}C$ Signals

In this study, benthic $\delta^{13}C$ data serve as the major tracer for reconstructing the nutrient (PO_4), the carbon flux, and the ventilation (O_2) of past deepwater masses flooding the deep Atlantic [Broecker and Peng, 1982; Curry and Lohmann, 1982; Duplessy, 1982; Michel, 1991]. The $\delta^{13}C$ values were measured on the benthic foraminifer *Cibicidoides wuellerstorfi* and on *Cibicidoides ariminensis* in cores at less than 1000 m water depth. Lutze and Thiel [1987, 1989] have demonstrated that these species only colonize "elevated" epibenthic microhabitats up to 14 cm above the seafloor [Linke and Lutze, 1992]. Hence their $\delta^{13}C$ test composition serves as a particularly useful "sensor" of the ambient bottom water properties [Graham et al., 1981; McCorkle et al., 1990; Zahn et al., 1986, 1991; Duplessy et al. 1988; Altenbach & Sarnthein, 1989; Boyle, 1992]. By contrast, $\delta^{13}C$ values of many other species, such as *Uvigerina peregrina*, cannot be employed as reliable tracers of deepwater $\delta^{13}C$ because these species live in both (mostly) infaunal and epifaunal microhabitats, depending on the varying conditions of local nutrient supply [Linke and Lutze, 1992]. The $\delta^{13}C$ composition of these foraminifera is thus influenced strongly, but to a varying extent, by the local pore water composition and does not reflect the ambient deepwater chemistry in a predictable manner. This bias is also indicated by the clearly nonlinear relationship between $\delta^{13}C$ values of *Uvigerina peregrina* and *C. wuellerstorfi*, recently confirmed by the data of Zahn et al. [1991].

In a number of cases, however, the $\delta^{13}C$ values of *C. wuellerstorfi* can also deviate from the values of the ambient oceanic water by up to -0.45‰. Based on increased local paleoproductivity estimates [Sarnthein et al., 1988, 1992], we were able to recognize such $\delta^{13}C$ outliers of *C. wuellerstorfi* that clearly resulted from a high local accumulation of ^{13}C-depleted organic fluff. Major fluff layers indeed also affect the epibenthic habitats on the seafloor, in particular, below zones of coastal and equatorial upwelling, which experienced enhanced productivity during the LGM [Sarnthein et al., 1987; Climate: Long-Range Investigation, Mapping, and Prediction (CLIMAP), 1981]. We distinguished (and discarded) the local, possibly fluff-induced ^{13}C depletion by comparing exceptionally low $\delta^{13}C$ data from potential upwelling regions with (1) the paleocarbon flux exceeding 2.0-2.5 g C m^{-1} y^{-1} on the seafloor [Altenbach, 1992; Sarnthein et al., 1988; Sarnthein and Winn, 1990] and with (2) $\delta^{13}C$ values from locations outside, at similar water depths, and below well-known ocean deserts such as the subtropical gyres.

2.2. Reconstruction of Paleoceanographic Transects

The reconstruction of vertical profiles of paleonutrients and deepwater paleoceanography in the east Atlantic was based on the technique of Zahn et al., [1987]. High-resolution epibenthic $\delta^{13}C$ records were obtained from numerous sediment cores that were retrieved from different water depths along vertical transects running across the east Atlantic continental margin, various aseismic ridges and oceanic plateaus, and the Mid-Atlantic Ridge (Figures 1 and 2a). The $\delta^{13}C$ values from each station for any selected time interval ("time slice") were projected (horizontally) onto an imaginary vertical plane running north-south along the central basin axis of the eastern Atlantic, covering water depths from zero to more than 5 km (Figures 1 and 2a). The spatial $\delta^{13}C$ patterns appearing on this plane were interpreted directly as vertical transects of chemical oceanography, based on the assumption that the stratification of water masses in the east Atlantic is essentially horizontal and homogenous from east to west. This assumption is less true in higher latitudes because of enhanced Coriolis forcing. Hence we constructed an additional, NW-SE running transect for Atlantic core sites near 40°-60°N to assess more precisely the local water mass variability in an east-west direction, particularly across the initial track of NADW (Figure 2b). Because of the strong east-west variation in these water masses (see later discussion), we only included those data from the higher latitudes into the north-south running transects (Figure 2a) that were derived from the eastern flank of the Rockall Plateau and further east (east of the divide shown in Figure 1). Only the water masses in this restricted region show properties compatible with the chemical oceanography found throughout the low-latitude east Atlantic basins (as discussed in section 5.2. on modern water masses).

Altogether, we compiled continuous isotopic records from

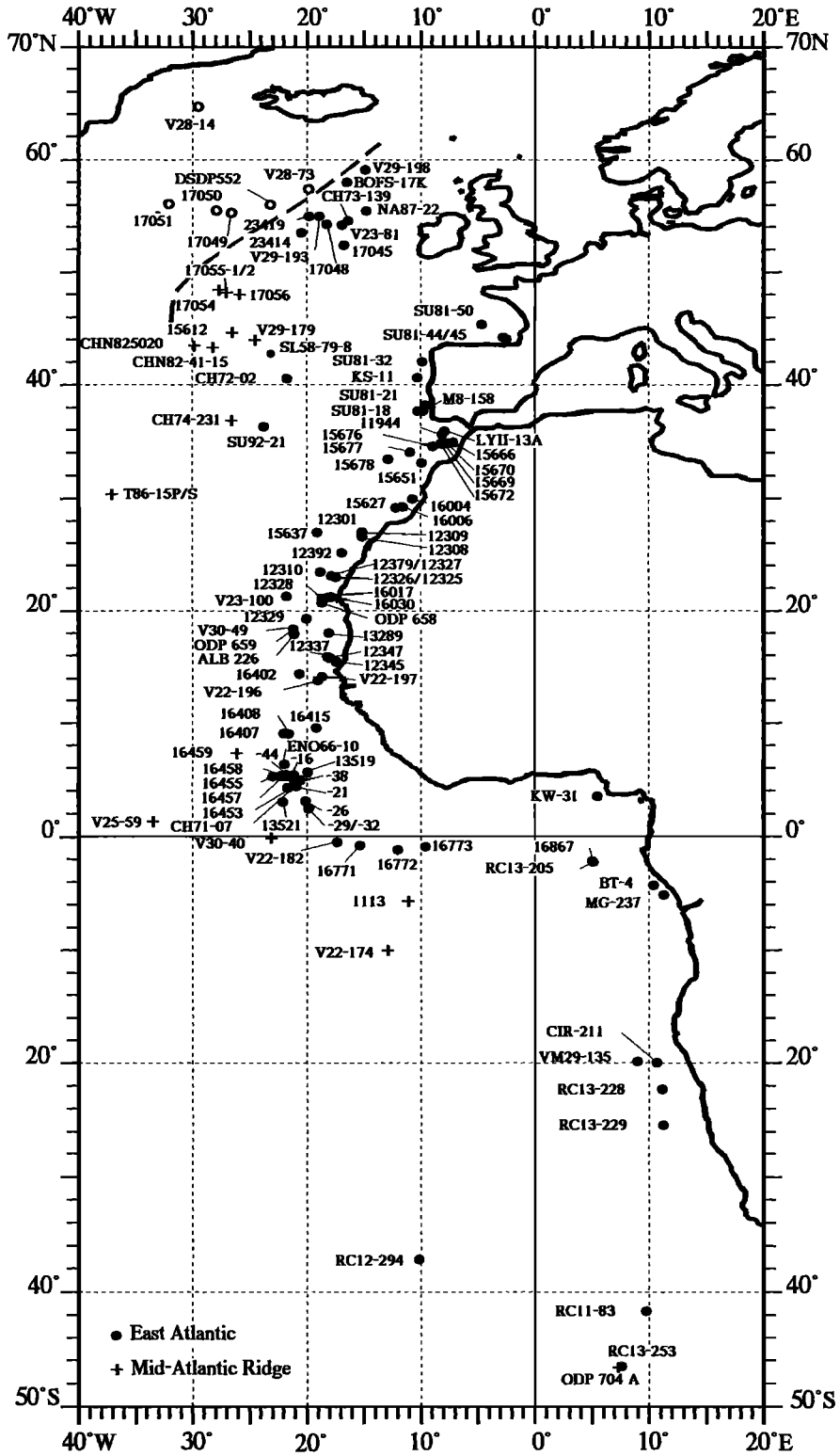

* Hyphenated numbers on Sierra Leone Rise have prefix ENO 66-

Figure 1. Core locations in the east Atlantic. Dashed line separates core locations north of 40°N below east and west Atlantic water masses. Hyphenated numbers on the Sierra Leone Rise have prefix ENO 66-.

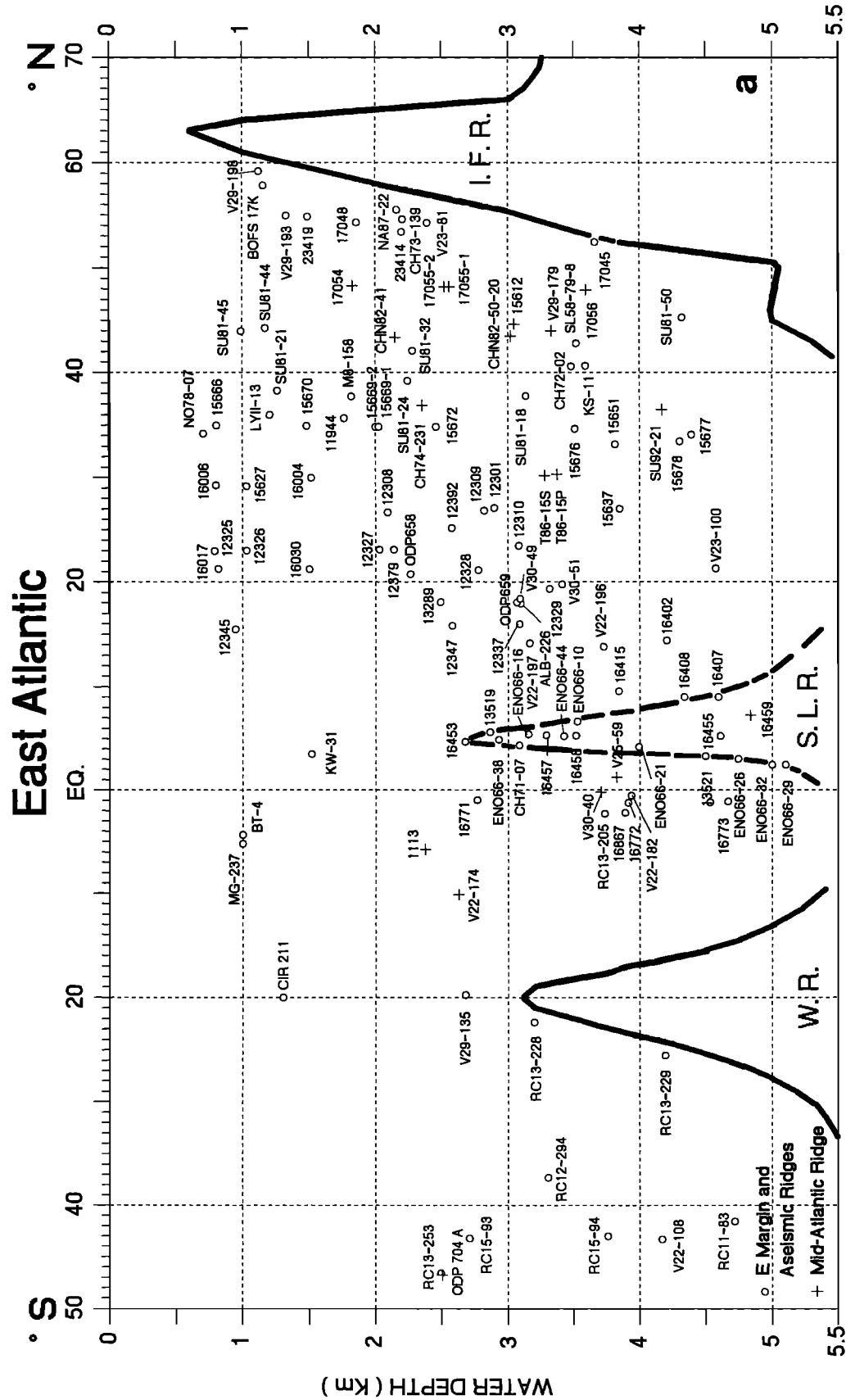

Figure 2. Core locations (Table 1) projected horizontally on vertical ocean transects. (a) N-S transect across east Atlantic. I.F.R., Island-Faeroe Ridge; S.L.R., Sierra Leone Rise; W.R., Walvis Ridge. (b) NW-SE transect across North Atlantic. M.A.R., Mid-Atlantic Ridge; R.B., Rockall Bank; G.B., Gulf of Biscaye.

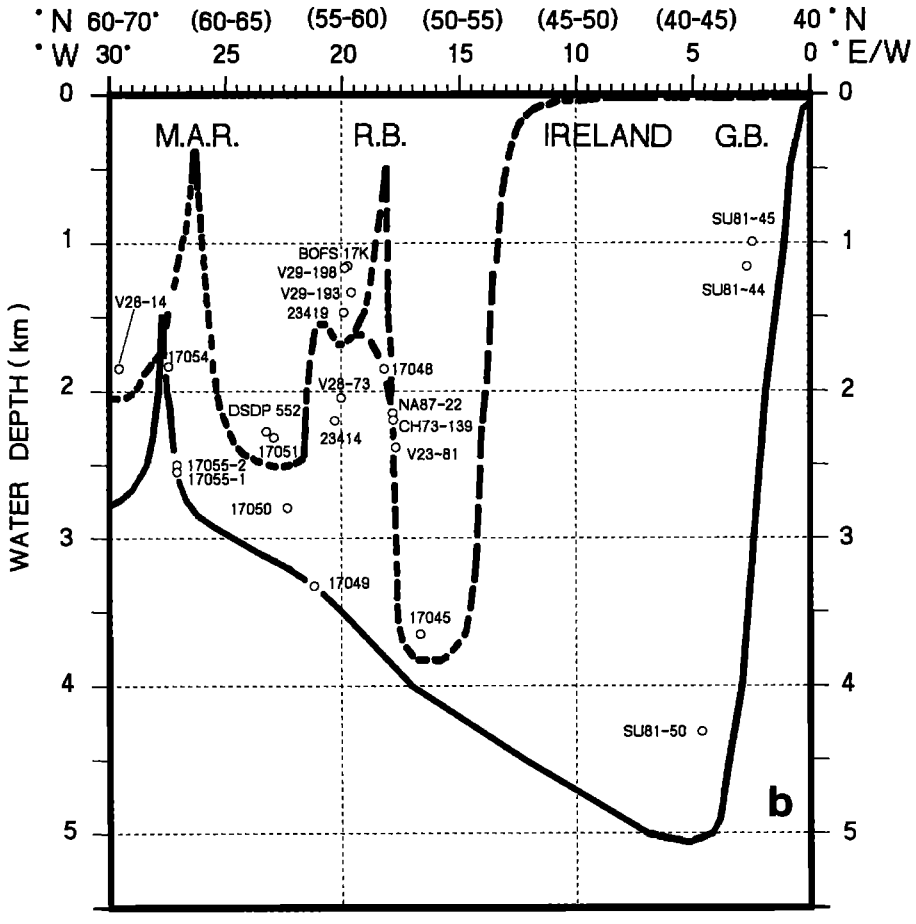

Figure 2. (continued)

about 95 core locations (a number of which were sampled by double and triple cores). In addition, data was included from about 20 stations which only had ("modern") sediment surface samples. The total represents about 4000-5000 epibenthic $\delta^{13}C$ and $\delta^{18}O$ data items for the last 30,000 years.

2.3. Analytical Techniques

Benthic $\delta^{13}C$ and $\delta^{18}O$ values were analyzed according to standard techniques, mostly at the laboratories of the University of Kiel, Kiel, Germany, and the Centre des Faibles Radioactivités, Laboratoire mixte CNRS-CEA, Gif sur Yvette, France (Table 1). In Kiel, sediment samples of known volume were weighed and freeze-dried for the calculation of water content, and then wet-sieved through a 63-mm mesh sieve and then dry-sieved through a 250-mm sieve. A micrometer was used to exclude specimens over 400 mm. Generally, about 5-7 specimens of *C. wuellerstorfi* were picked from the 315- to 400-mm fraction for stable isotope measurements. In the case of rare specimens, some measurements were based on only one or two individuals. Further details of the preparation techniques used are given by Ganssen [1981, 1983].

In Kiel, isotopic measurements were made with a Finnigan MAT 251 mass spectrometer installed at the C-14 Laboratory of the Institut für Kernphysik, Kiel University, Kiel, Germany. This instrument is coupled on-line to a Carbo-Kiel device for automated CO_2 preparation from carbonate samples (down to 10 mg) for isotopic analysis. Samples were reacted by individual acid addition. The system can routinely measure with an accuracy (on the d scale) of ± 0.07‰ for oxygen and ± 0.04‰ for carbon isotopes. Results were calibrated using National Bureau of Standards and Technology, Gaithersburg, Maryland, NBS 20 (and, in addition, NBS 19 and 18) and are reported on the Pee Dee belemnite (PDB) scale.

In Gif-sur-Yvette, analyses prior to 1990 were made on a manually operated VG 602 mass spectrometer. Since 1990, analyses have been run on an automated MAT 251 mass spectrometer using individual acid reactions (such as in Kiel). Results are calibrated using a value of $\delta^{18}O$ = -2.20‰ versus PDB, and $\delta^{13}C$ = 1.95‰ versus PDB for NBS 19 [Hut, 1987], as recommended at the Third Paleoceanography Conference Isotopic Workshop, Cambridge, England, (1989, unpublished). Mean reproducibility is ±0.06‰ for $\delta^{18}O$ and ±0.04‰ for $\delta^{13}C$.

Further benthic stable isotope data were compiled from various published and unpublished sources as listed in Table 1, especially from Curry and Lohmann [1985], Curry et al. [1988], Boyle and Keigwin [1986], N.J. Shackleton (unpublished data, 1986, core V 28-14 and BOFS), G. Ganssen (unpubl. data, 1991, core T86-15b/s), and core NA 87-22, analyzed in a joint project between Gif and the Netherlands' Institute for Sea Research, Texel, Netherlands. The entire $\delta^{13}C$ data file is available on request from the German "Past Global

Table 1. Epibenthic $\delta^{13}C$ Averages for Time Slices 1-8 Listed for 95 Atlantic Deep Sea Cores and 20 Surface Sediment Samples

Core	Latitudes deg	Longitudes deg	Water Depth m	$\delta^{13}C$ (per mil versus PDB) *Cibicidoides wuellerstorfi* [aa]							
				0- 4	7- 8	9.25 -9.8	12.3 -12.8	16.9 -17.1	18.3 -19.3	21.5 -23.5	28.3 -29.5
V28-14[k]	64.78N	29.57W	1855	....	0.69	0.32	0.59	....	1.13	1.39	?0.79 /0.22
V29-198[t]	59.00N	19.00W	1139	1.09[x]	....	....	....	....	1.70	....	....
BOFS 17K[m]	58.00N	16.50W	1150	....	....	....	1.29	....	1.74	....	....
17051[a]	56.16N	31.99W	2295	1.04	0.69	1.04	....	0.47	0.75	1.05	1.04
V28-73[t]	57.00N	20.00W	2063	....	....	....	1.11	....	1.26	....	....
DSDP 552[r]	56.05N	23.23W	2311	....	>1.25	1.29	?>1.00	....	0.94	1.05	1.24
NA87-22[b]	55.50N	14.70W	2161	!1.08	0.94	0.92	0.86	0.30	0.70	0.86	0.83
17050[a]	55.47N	27.89W	2795	0.51	....	0.73	....	....	....	....	?0.54
17049[a]	55.26N	26.73W	3331	0.73	0.99	0.99	0.81	0.27	0.57	....	....
V29-193[t]	55.00N	19.00W	1326	1.32	0.85	1.28[v]	1.31	....	....	1.58[x]	....
CH73-139c[b]	54.63N	16.35W	2209	0.93	!0.81	!0.73	0.89	?0.41	?0.61	0.70	0.47
23419[a]	54.96N	19.76W	1491	....	1.29	1.31	1.15	....	1.56	1.50	1.51
17048[b]	54.31N	18.18W	1859	1.31	1.11	1.24	1.13	0.63	1.26	1.11	1.15
V23-81[n]	54.25N	16.83W	2393	0.93	1.13	?0.96	0.83	0.10	0.61	?0.08	0.70
23414[a]	53.54N	20.29W	2196	1.13	1.17	1.29	0.87	0.65	0.93	0.82	(?)0.98
17045[a]	52.43N	16.66W	3663	0.79	0.77	0.85	....	0.02	0.26	0.13	0.28
17054[a]	48.45N	27.70W	1834	1.32	1.29	1.31	1.08	....	....	....	....
17055-1[a]	48.22N	27.06W	2558	1.24	....	1.32	0.86	0.28	0.97	1.06	?0.89
17055-2[a]	48.21N	27.06W	2510	1.27	1.31	1.26	....	....	....	....	....
17056[a]	48.04N	25.90W	3599	0.93	....	....	....	....	....	....	....
SU81-50[b]	45.38N	04.65W	4320	0.70	0.60	?0.52	....	....	....	....	....
15612[a]	44.69N	26.54W	3050	1.21	?1.25	0.91	0.60	0.52	0.60	0.51	1.10
SU81-44[b]	44.25N	02.70W	1173	....	?1.05	....	0.66	....	1.06	....	....
SU81-45[b]	44.10N	02.48W	994	....	....	....	....	....	1.10	....	....
V29-179[g]	44.00N	24.53W	3331	....	....	....	....	....	0.63	....	....
CHN825020 [h]	43.50N	29.87W	3020	....	1.23	1.07	0.94	0.21	?0.72	0.72	....
CHN824115 [h]	43.37N	28.23W	2151	....	1.24	1.31	1.21	?0.95	1.18	?1.20	....
SL58-79-8[l]	42.83N	23.07W	3520	0.92	....	....	....	....	0.60	....	....
SU81-32[b]	42.10N	09.78W	2280	....	....	0.90	0.69	....	....	....	?0.51
KS-11[c]	40.69N	10.21W	3590	....	0.87	0.95	....	....	0.63	0.69	?0.67
CH72-02[b]	40.60N	21.70W	3485	....	0.90	0.92	....	....	0.80	0.70	0.92
SU81-21[b]	38.25N	09.55W	1260	....	....	....	....	....	?0.98	....	....
SU81-18[b]	37.77N	10.18W	3135	0.77	0.79	0.78	?0.50	?0.10	0.11	....	....
M8-158[l]	37.73N	09.72W	1819	0.95	....	....	....	....	....	....	....
CH74-231[l]	36.87N	26.62W	2354	?1.00	....	....	....	....	....	....	....
SU92-21[a]	36.57N	23.74W	4170	....	....	?0.94	0.59	-0.23	-0.10	0.04	-0.41
LYII-13A[a]	35.97N	07.82W	1201	....	....	....	....	0.66	1.58	1.57	1.51
11944[a]	35.65N	08.06W	1765	1.21	1.21	0.99	0.64	0.53	1.07	1.01	0.88
15666[a,w]	34.96N	07.12W	803	1.27	1.25	1.27	1.29	1.35	1.60	1.76	1.53
15670[a]	34.91N	07.58W	1482	....	0.97	0.95	0.98	0.73	....	....	1.29
15669-1[a]	34.89N	07.82W	2022	1.09	1.12	1.15	0.84	0.34	0.81	0.90	0.61
15669-2[a]	34.89N	07.81W	2001	1.04[y]	....	....	....	....	....	....	....
15672-1/2[a]	34.86N	08.12W	2455	1.18	1.14	1.11	0.76	0.34	0.68	0.65	0.77
15672-2[a]	34.86N	08.13W	2435	0.90[y]	....	....	....	....	....	....	....
15676[a]	34.66N	08.85W	3515	1.10[y]	....	....	....	....	....	....	....
15677[a]	34.13N	10.83W	4410	0.88[y]	....	....	....	....	....	....	....
15678[a]	33.47N	12.76W	4305	0.85[y]	....	....	....	....	....	....	....

Table 1. (continued)

Core	Latitudes deg	Longitudes deg	Water Depth m	$\delta^{13}C$ (per mil versus PDB) *Cibicidoides wuellerstorfi* [aa]							
				0-4	7-8	9.25 -9.8	12.3 -12.8	16.9 -17.1	18.3 -19.3	21.5 -23.5	28.3 -29.5
15651[a]	33.19N	09.83W	3816	0.95[y]	....	....	....	....	....	....	....
T86-15P[f]	30.43N	37.07W	3375	....	....	0.95	0.73	....	0.53	0.47	0.74
T86-15S[f]	30.33N	36.95W	3280	1.15	....	....	....	....	....	....	....
16004[a]	29.98N	10.65W	1512	1.19	0.92	0.79	....	0.56	1.16	1.11	1.05
16006[a,w]	29.27N	11.50W	796	1.20	1.03	1.01	1.22	0.90	1.50	1.48	1.34
15627[a]	29.17N	12.09W	1024	....	?0.97	0.70	....	....	1.45	1.35	1.31
12301[a]	27.05N	15.05W	2896	1.08[y]	....	....	....	....	....	....	....
15637[a]	27.01N	18.99W	3849	....	0.93	0.91	0.55	0.13	?0.04	....	0.29
12309-1[a]	26.83N	15.11W	2849	1.14[y]	....	....	....	....	....	....	....
12309-2[a]	26.84N	15.11W	2820	1.10	!0.92	0.87	0.55	0.16	0.15	0.27	0.21
12308[a]	26.65N	15.05W	2090	1.15[y]	....	....	....	....	....	....	....
12392[a,s]	25.17N	16.85W	2575	1.02	1.01	0.96	0.70	0.25	0.43	0.50	0.38
12310-3/4 [a]	23.50N	18.72W	3080	1.06	0.82	0.52	!0.50	....	0.35	-0.07	0.33
12310-1[a]	23.50N	18.72W	3075	1.16[y]	....	....	....	....	....	....	....
12379[a]	23.14N	17.75W	2136	1.06	0.91	0.68	0.40	0.15	0.43	0.43	0.41
12327[a]	23.13N	17.74W	2032	0.98[y]	....	....	....	....	....	....	....
12326[a]	23.04N	17.41W	1024	1.20[y]	....	....	....	....	....	....	....
12325[a]	22.99N	17.33W	787	0.92[y]	....	....	....	....	....	....	....
V23-100[e]	21.30N	21.68W	4579	0.59	....	....	....	-0.03	?0.12	?0.07	?0.27
16017[a]	21.25N	17.80W	812	0.99	1.04	1.01	0.77	0.95	1.13	1.08	0.82
16030[a]	21.24N	18.06W	1500	0.94	0.89	0.71	0.80	?0.95	1.04	0.86	0.79
12328[a]	21.15N	18.57W	2778	0.86	0.58	0.50	0.48	0.03	0.23	0.35	0.28
ODP 658[a]	20.75N	18.58W	2263	0.79	0.68	0.63	0.57	0.30	0.48	0.51	0.44
12329-6[a]	19.37N	19.93W	3320	0.82	0.90	0.81/ ?0.57	0.47	?0.34	0.18	0.20	0.66
12329-2[a]	19.37N	19.93W	3314	0.85[y]	....	....	....	....	....	....	....
V30-49[p]	18.43N	21.08W	3093	....	0.84	0.48	....	....	0.18	0.23	0.28
ODP 659[a]	18.08N	21.03W	3069	0.99	!1.04	0.87	....	?0.11	?0.16	?0.33	0.61
13289[a]	18.07N	18.01W	2490	0.95	....	0.92	0.49	0.21	0.48	0.50	0.33
ALB-226[d]	17.95N	21.05W	3100	0.88	0.73	0.56	0.37	....	0.04	0.19	0.45
12337[a]	15.95N	18.13W	3088	0.67	0.55	0.58	0.10	-0.10	....	....	....
12347[a]	15.83N	17.86W	2576	!0.81	0.97	0.64	0.51	-0.28	0.23	....	....
12345[a]	15.48N	17.36W	945	0.75	0.58	?0.52	....	0.47[w]	0.85	?0.92	....
16402[a]	14.42N	20.57W	4203	0.64	0.43	0.61	?0.04 /?0.32	-0.17	-0.03	-0.18	0.00
V22-197[k]	14.17N	18.58W	3167	....	0.62	0.74	0.37	0.36	0.19	0.21	0.03
V22-196[g]	13.83N	18.97W	3728	....	....	0.86	0.67	?-0.07	-0.19	....	....
16415[a]	09.57N	19.11W	3841	0.55	0.68	0.84	0.20	0.08	-0.20	0.07	....
16407[a]	09.04N	21.96W	4596	?0.75	0.20	0.85	....	....	?0.03	....	....
16408[a]	09.01N	21.50W	4336	0.71	0.48	0.41	0.48	?-0.04	-0.14	-0.25	....
16459[a]	07.28N	26.19W	4835	0.58	0.71	0.50	0.24	-0.19	-0.13	0.03	0.22
ENO66-10[j]	06.65N	21.90W	3527	....	....	0.82	....	....	0.47	0.40	?0.50
13519[a]	05.66N	19.85W	2862	1.05	0.97	0.97	?0.63 /!0.88	?0.39	0.37	0.52	0.62
ENO66-16[j]	05.46N	21.14W	3152	....	0.94	0.99	?0.57	....	0.38	0.47	0.84
16457[a]	05.39N	21.72W	3291	1.11	0.94	0.88	0.88	0.13	0.29	?0.31	....
16458[a]	05.34N	22.06W	3518	0.90	?0.34!	0.89	0.77	?0.36	0.34	?0.02	0.42
16455[a]	05.27N	22.87W	4160	0.65	0.93	0.40	0.76	?0.08	-0.06	....	....
ENO66-44[j]	05.26N	21.71W	3428	....	....	1.05	....	....	?0.60	0.45	0.57
ENO66-38[j]	04.92N	20.50W	2931	....	1.05	1.24	0.89	....	0.41	?0.64	?0.62
16453[a]	04.73N	20.95W	2675	1.17	!1.04	!1.13	0.92	....	?0.36	0.43	0.60

Table 1. (continued)

Core	Latitudes deg	Longitudes deg	Water Depth m	$\delta^{13}C$ (per mil versus PDB) *Cibicidoides wuellerstorfi* [aa] 0-4	7-8	9.25 -9.8	12.3 -12.8	16.9 -17.1	18.3 -19.3	21.5 -23.5	28.3 -29.5
CH71-07[b]	04.38N	20.87W	3083	1.08	....	....	....	....	0.28	0.32	0.51
ENO66-21[j]	04.23N	21.63W	3995	.... (0.4-0.7k)	0.83	0.90	?0.69	!0.17	0.12	0.12	0.09
KW-31[b,z]	03.52N	05.57E	1515	?0.29	....	-0.35	0.19	0.22	0.62	0.48	0.19
ENO66-26[j]	03.09N	20.02W	4745	....	....	?0.52!	?0.24	....	0.15	-0.16	0.07
13521[a]	03.02N	22.03W	4504	....	!0.74	0.89	?0.16	....	-0.13	-0.42	....
ENO66-32[j]	02.47N	19.73W	5003	....	....	0.91	?0.60	....	0.04	-0.20	0.22
ENO66-29[j]	02.46N	19.76W	5104	....	....	0.85	?0.48	....	-0.04	-0.16	?0.27
V25-59[o]	01.37N	33.48W	3824	0.86	....	0.92	0.71	0.02	0.06	0.06	-0.02
V30-40[q]	00.20S	23.15W	3706	....	?0.91[x]	0.88	0.58	....	0.11	-0.16	-0.06
V22-182[l]	00.55S	17.27W	3937	0.67	....	....	....	....	....	....	....
16771[a]	00.82S	15.51W	2764	1.26	....	....	....	....	....	....	....
16773[a]	00.97S	09.44W	4662	0.76	0.75	0.84	?0.25	0.32 /0.19	....	....	....
16772[a]	01.21S	11.96W	3912	0.86	0.85	0.71	....	....	-0.18	!-0.32	-0.03
16867[a]	02.20S	05.10E	3891	0.81	0.65	0.87	0.67	....	-0.22	-0.67	-0.31
RC13-205[l]	02.28S	05.18E	3731	0.98	....	....	....	....	....	....	....
BT-4[k]	04.33S	10.43E	1000	....	0.33	0.43	?0.12	-0.06	0.24	0.00	0.19
MG-237[b]	05.20S	11.33E	1000	-0.11	-0.19	-0.25	-0.15	-0.07	-0.10	....	....
GeoB 1113[a]	05.75S	11.04W	2374	0.93	0.92	0.99	?0.66	....	0.45	0.44	0.36
V22-174[l]	10.07S	12.82W	2630	0.80	....	....	....	....	....	....	....
V29-135[a,c]	19.60S	08.88E	2675	0.65	0.66	0.72	0.27	?0.09	?-0.11	0.12	0.20
CIR-211[b]	20.00S	10.75E	1300	0.24	....	....	....	....	0.28	....	....
RC13-228[k]	22.33S	11.20E	3204	0.56	0.59	0.12	....	-0.25	0.09	-0.15	0.17
RC13-229[k]	25.50S	11.30E	4194	....	0.30	!0.41	0.20	-0.15	-0.47	-0.44	-0.42
RC12-294[l]	37.27S	10.10W	3308	0.86[x]	....	....	....	....	-0.23	....	....
RC11-83[i]	41.60S	09.72E	4718	....	....	0.10	0.00	-0.83	-0.68	-0.81	....
RC13-253[l]	46.60S	07.63E	2494	?0.62	....	....	....	....	....	....	....
ODP 704[u]	46.88S	07.42E	2532	0.58	....	....	....	....	-0.26	-0.50	....

Derivation and averaging of time slice values from analytical data is marked on $\delta^{13}C$ records in Figure 3. PDB, Pee Dee belemnite.

[a] University of Kiel (published and unpublished),
[b] Centre des Faibles Radioactivités, Laboratoire mixte CNRS-CEA, Gif-sur Yvette Cedex, France.(published and unpublished),
[c] Abrantes (unpublished data, 1993).
[d] Bornmalm (unpublished data, 1993).
[e] Fairbanks (unpublished data, 1992).
[f] Ganssen (unpublished data, 1992).
[g] Shackleton (unpublished data, 1992).
[h] Boyle and Keigwin [1985, 1987].
[i] Charles and Fairbanks [1992].
[j] Curry and Lohmann [1985].
[k] Curry et al. [1988].
[l] Duplessy et al. [1984].
[m] Labeyrie et al. [1992].
[n] Jansen and Veum [1990].
[o] Mix and Ruddiman [1985].
[p] Mix and Fairbanks [1985].
[q] Oppo and Fairbanks [1987].
[r] Shackleton and Hall [1984].
[s] Shackleton [1977],
[t] Oppo and Lehman [1993].
[u] Hodell [1993].
[w] *C. wuellerstorfi* and *P. ariminensis.*
[x] *C. kullenbergi.*
[y] living rose bengal stained *C. wuellerstorfi*, [Ganssen, 1983].
[z] *C. pseudoungerianus.*
[aa] Time slices are in 1000 calendar years.

Changes" (PAGES-) marine data repository SEDAN (grobe @ awi-bremerhaven.de).

In addition, $\delta^{13}C$ data of total dissolved CO_2 in east Atlantic ocean water was compiled to validate the modern benthic $\delta^{13}C$ record as a tracer of ocean chemistry. Most of the data on water samples came from Duplessy [1972] and Kroopnick [1985], with few additional data from a study by the Kiel group (H. Erlenkeuser and M. Sarnthein, unpublished data, 1993) from the northeastern Atlantic. A comparison of data produced by the different studies at nearby stations in the northwestern and

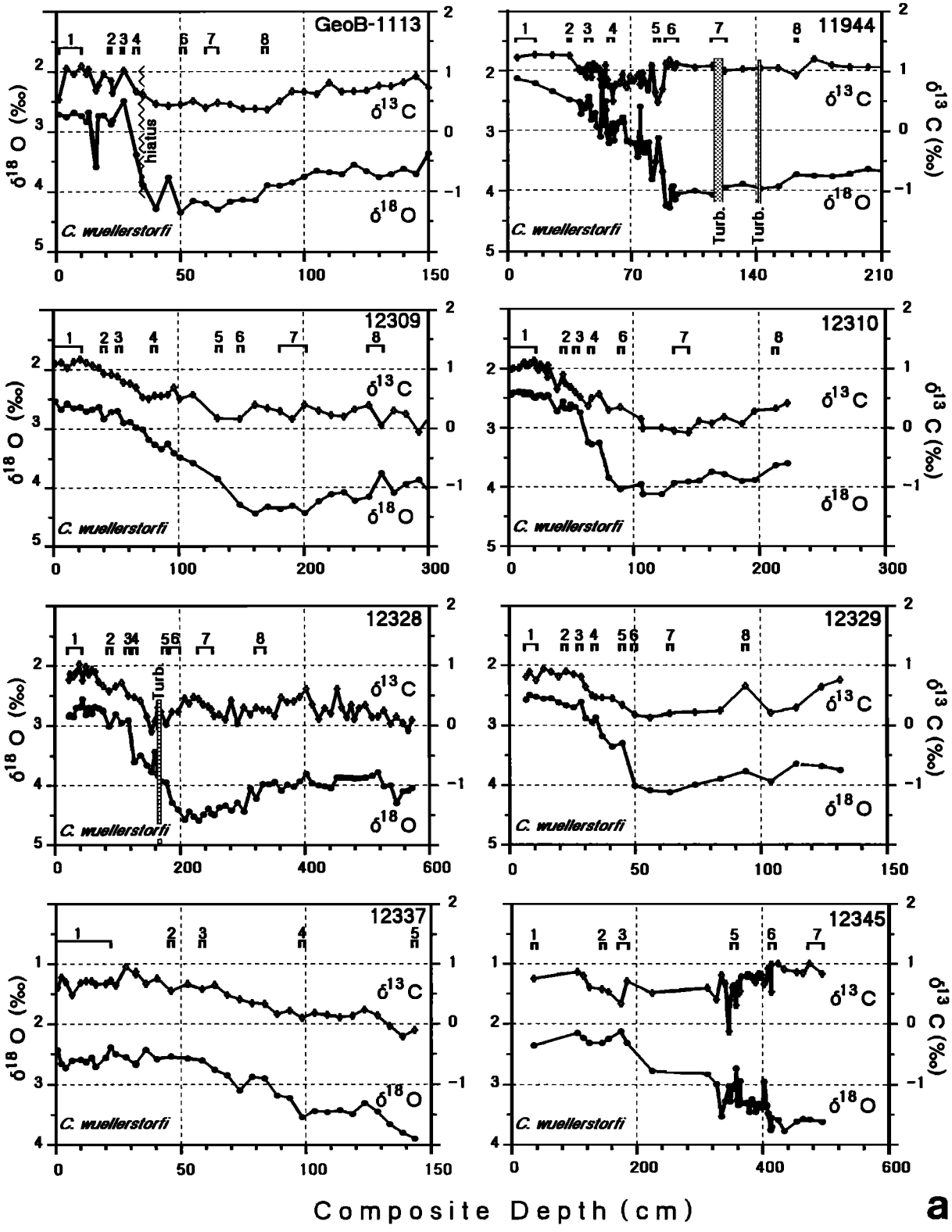

Figure 3. The $\delta^{13}C$ and $\delta^{18}O$ records of *C. wuellerstorfi* in east Atlantic deep-sea cores. Vertical zigzag lines in various records show hiatuses. Numbered bars mark time slices 1-8. Core locations and $\delta^{13}C$ data averaged over the time slices are listed in Table 1.

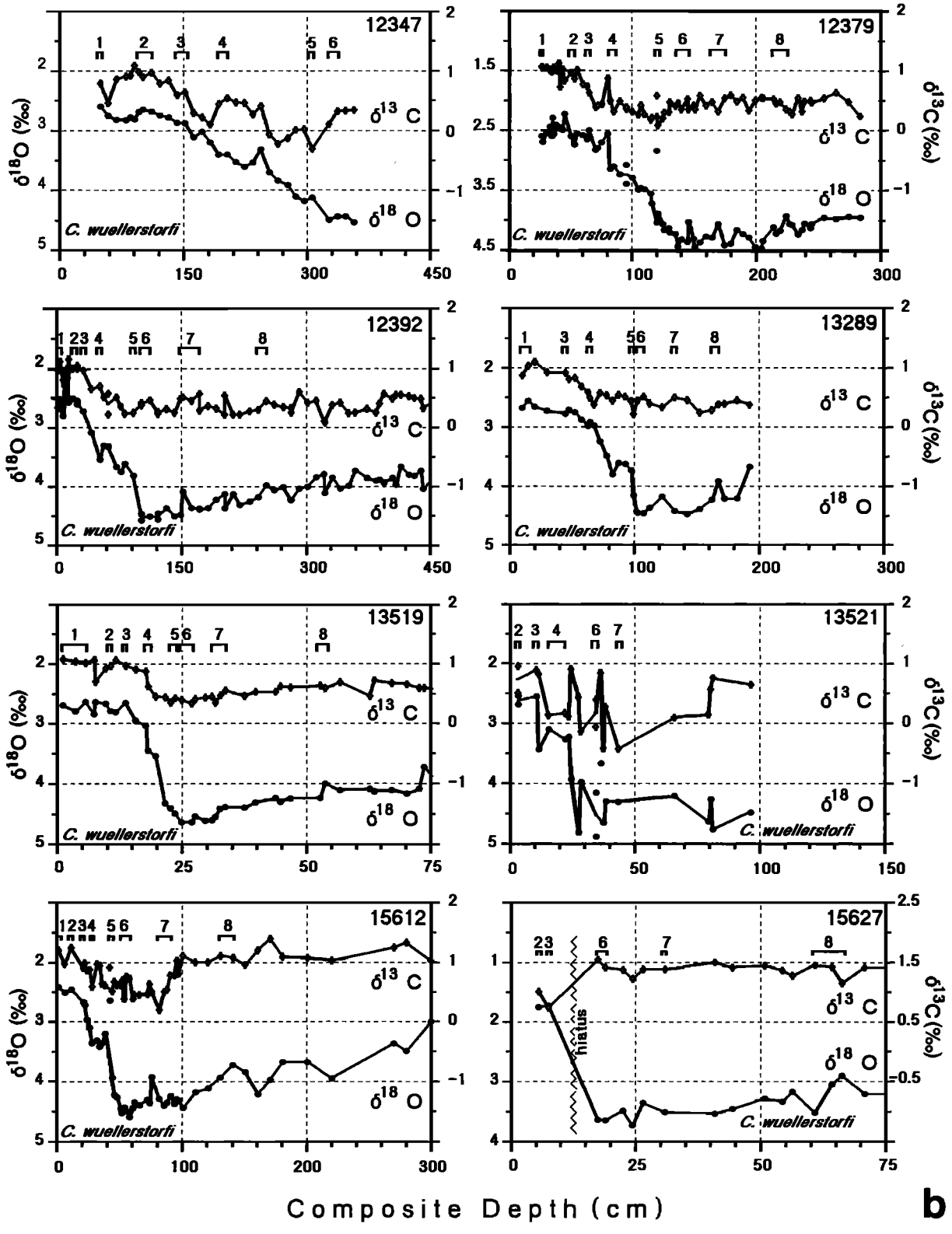

Figure 3. (continued)

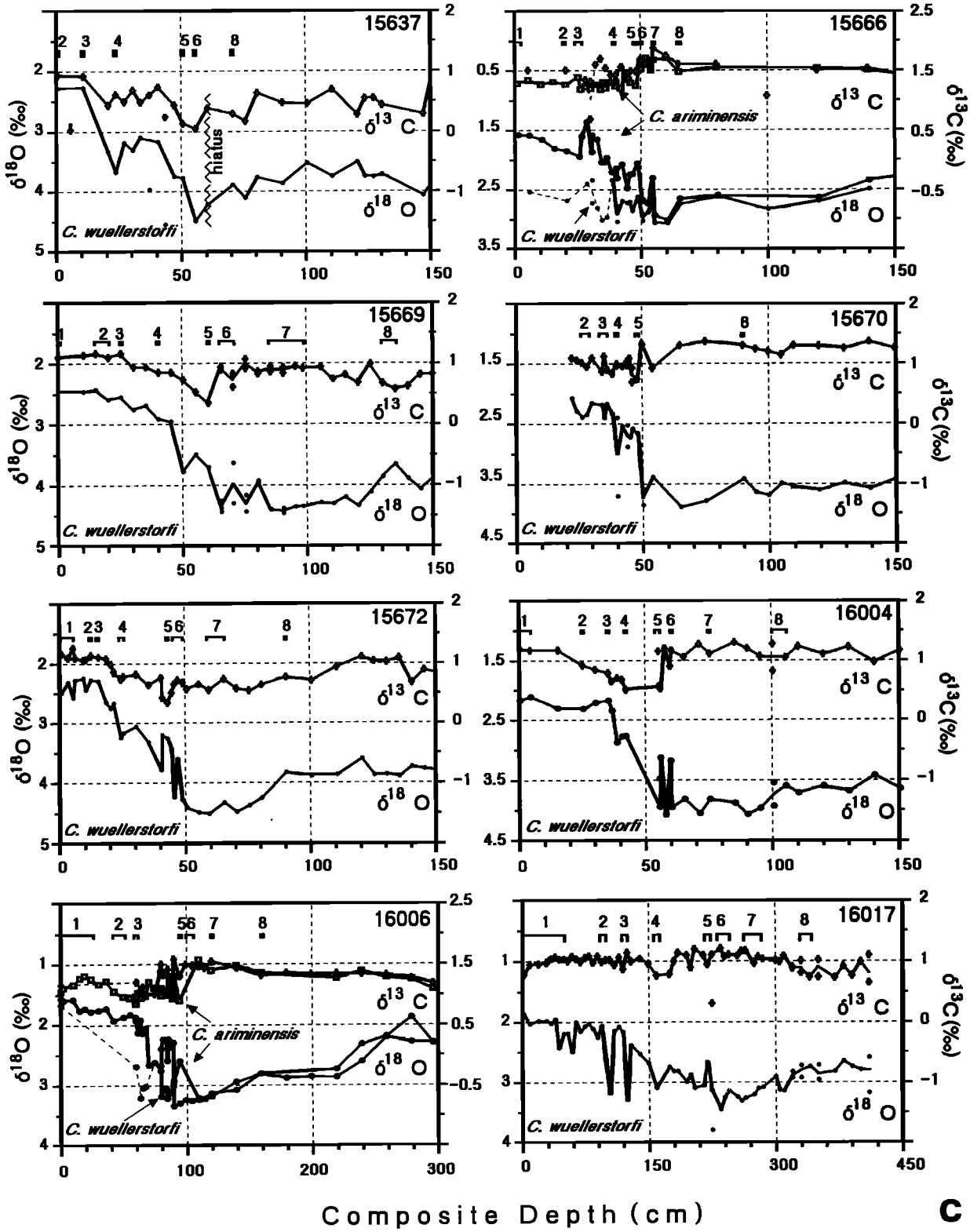

Figure 3. (continued)

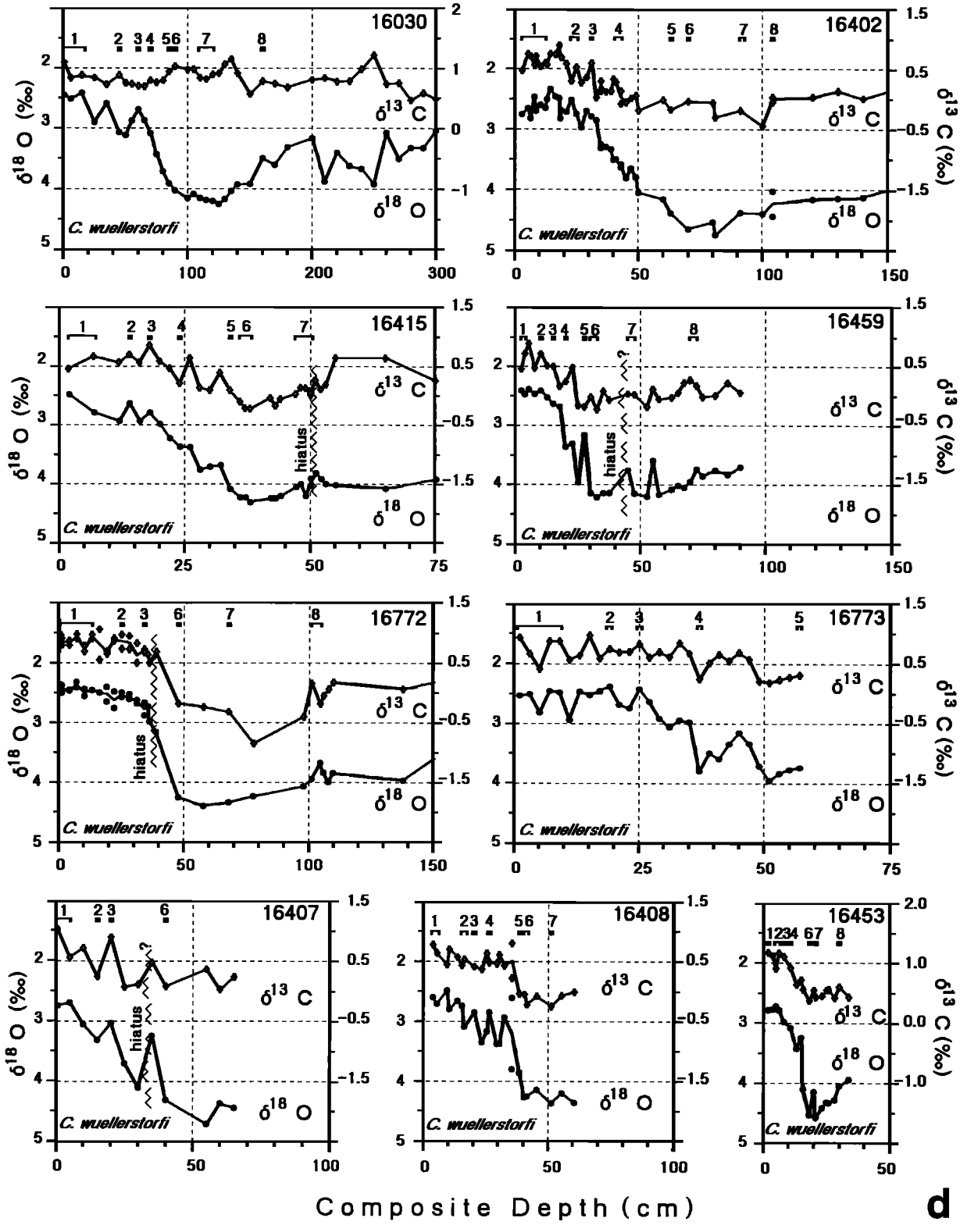

Figure 3. (continued)

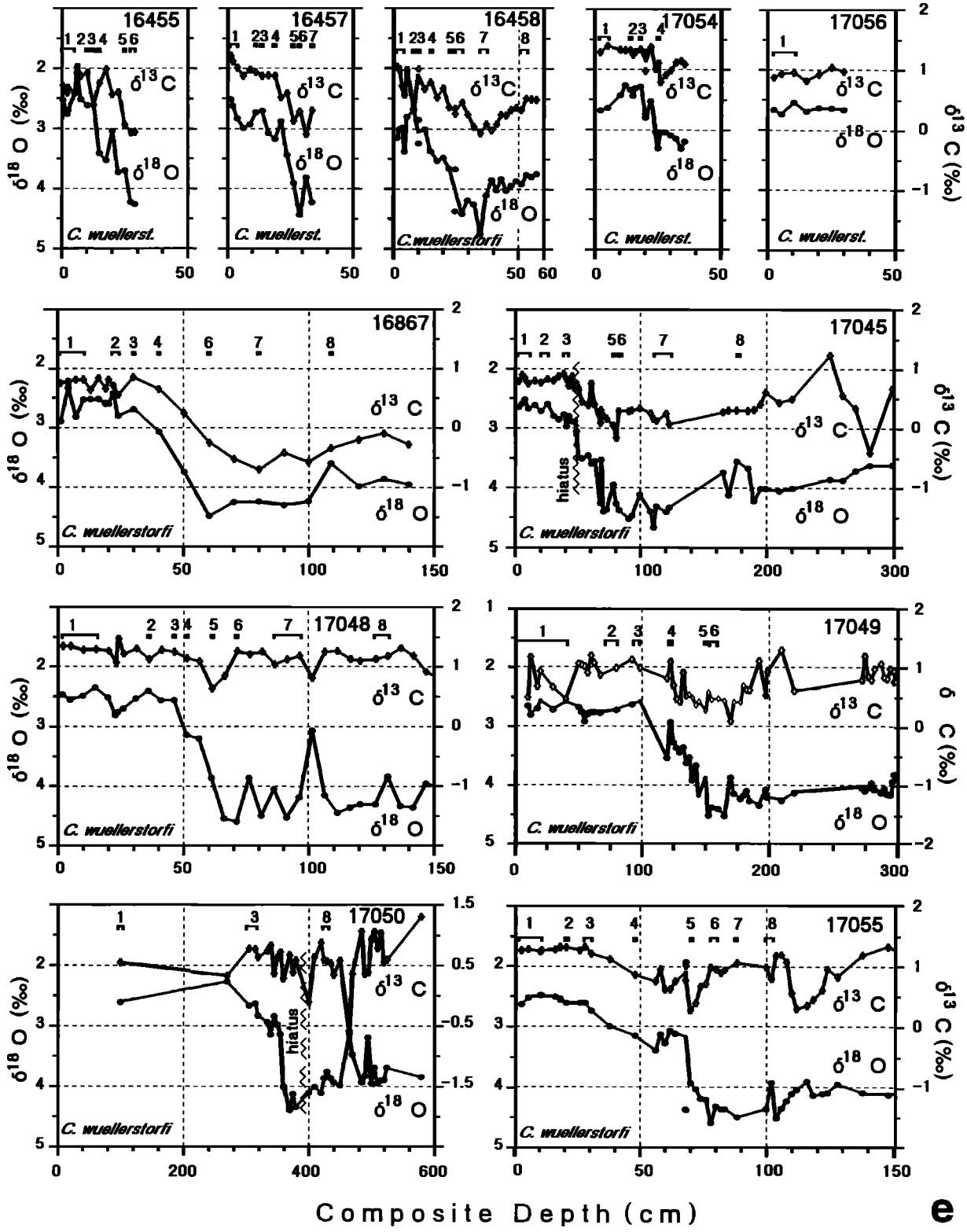

Figure 3. (continued)

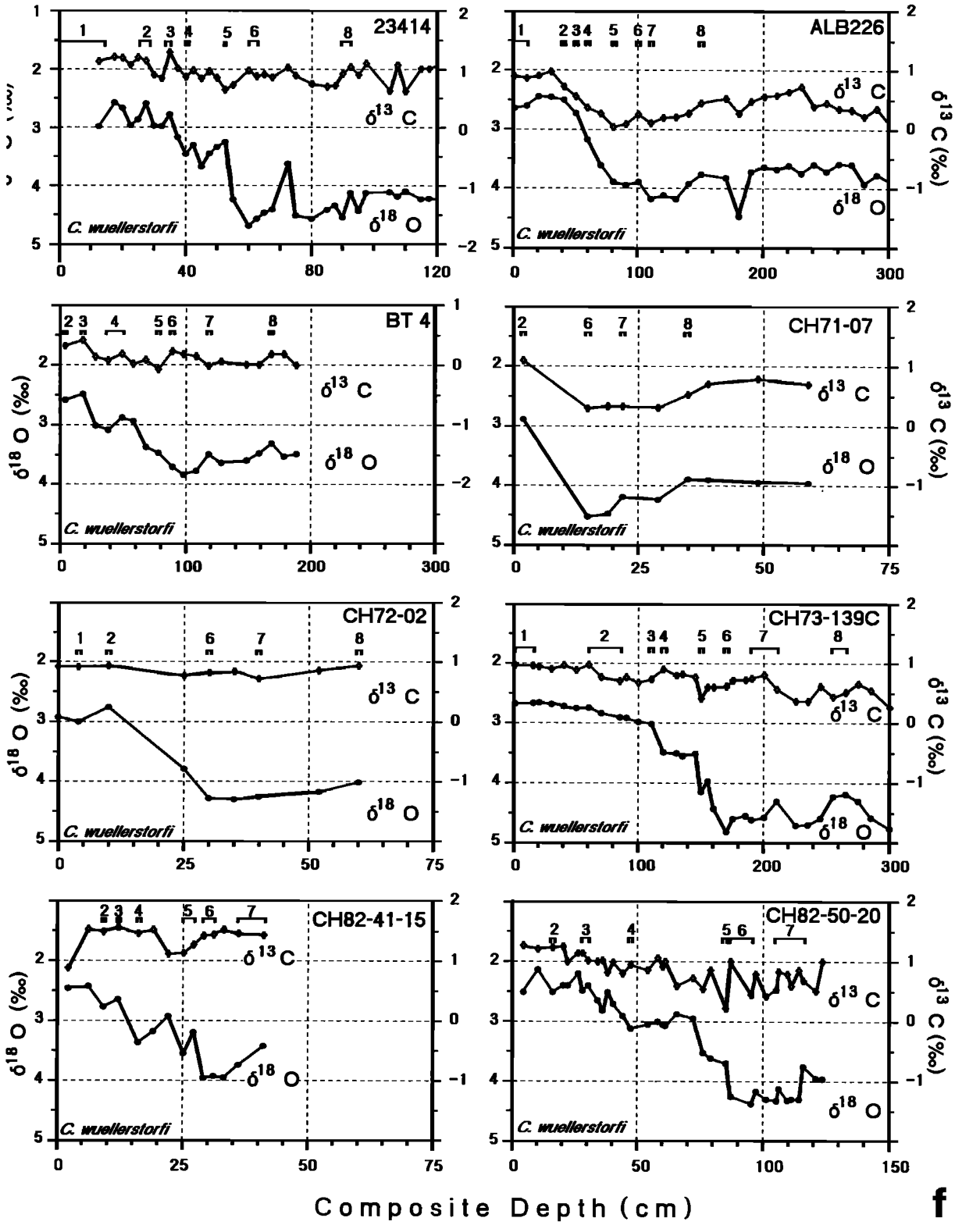

Figure 3. (continued)

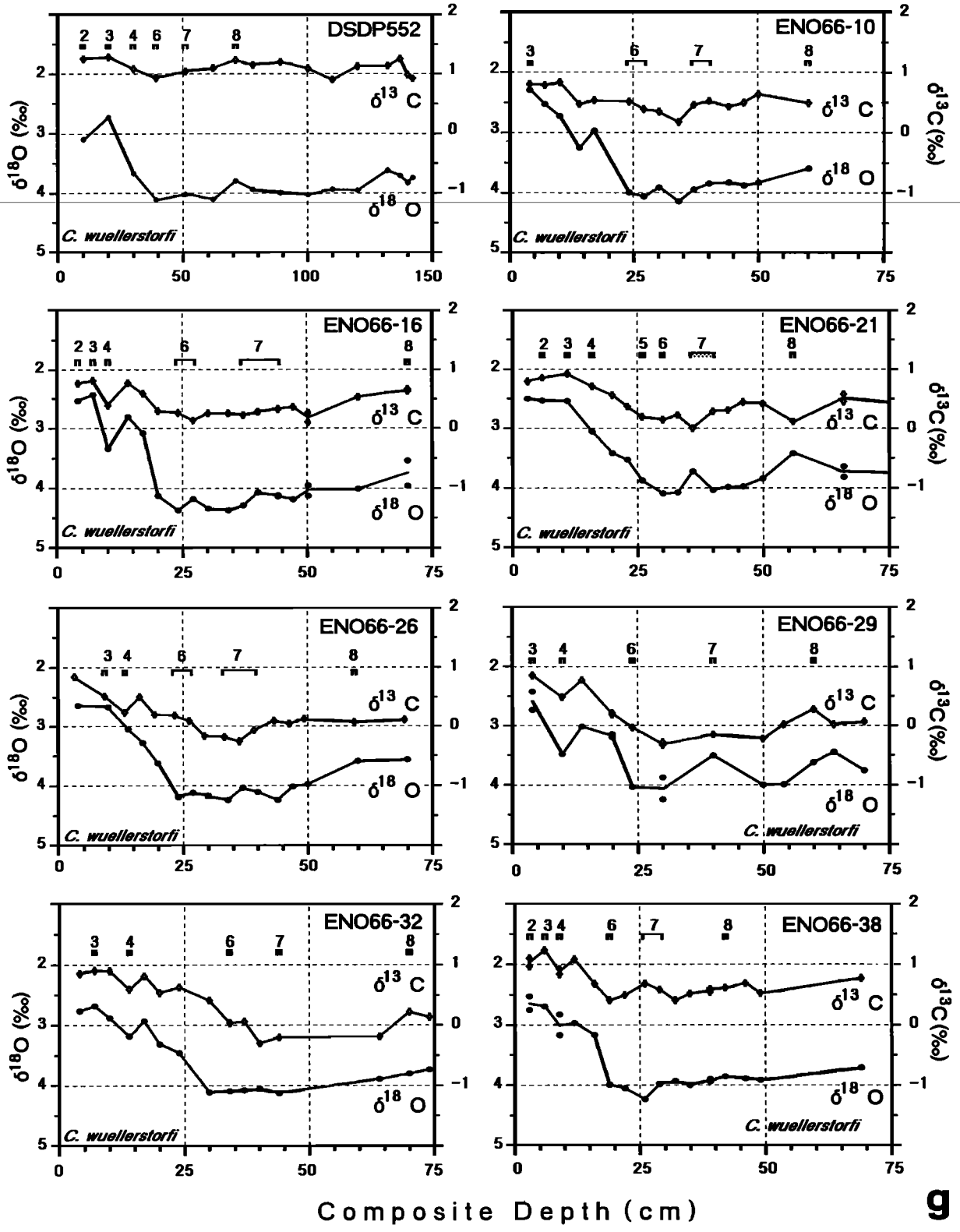

Figure 3. (continued)

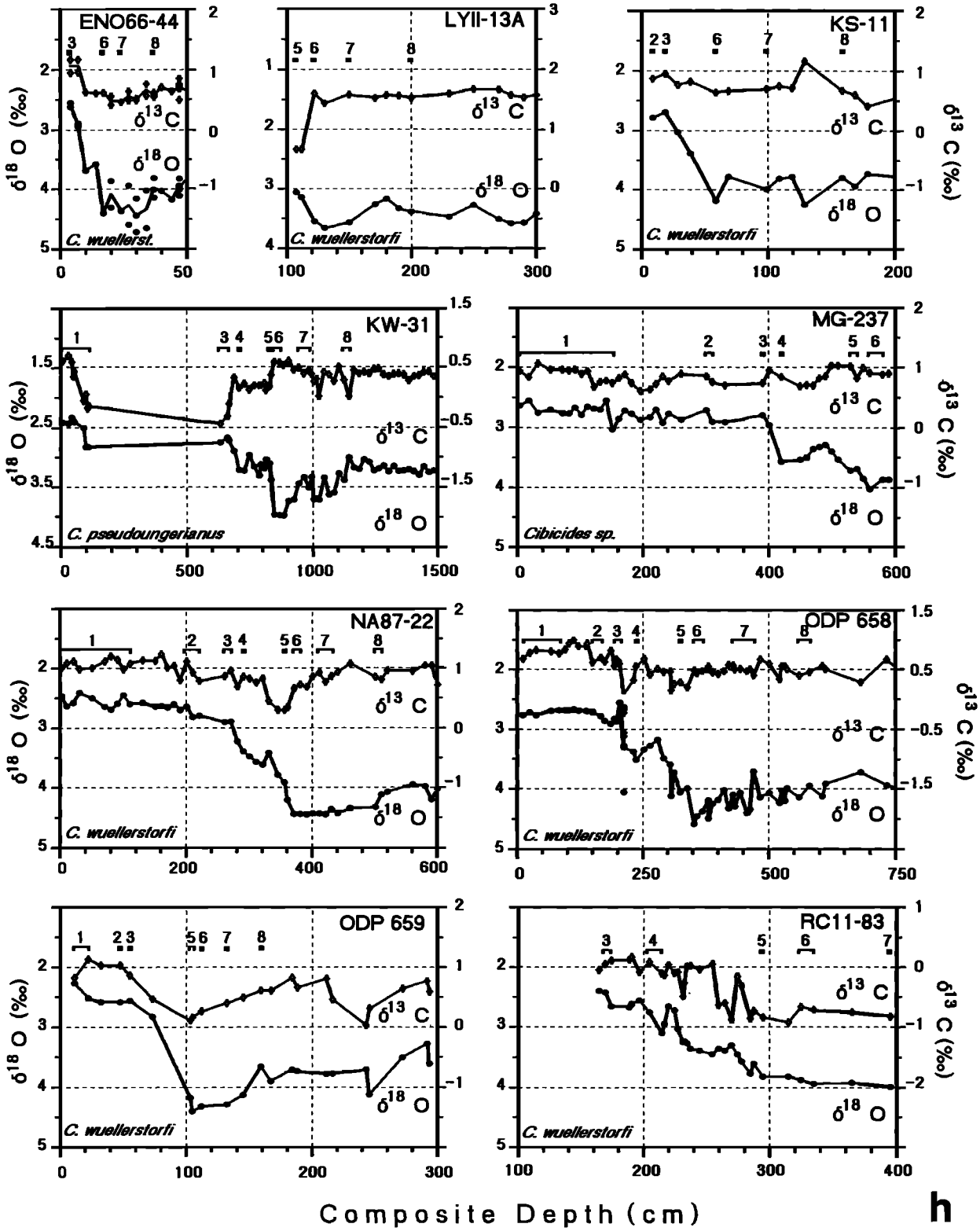

Figure 3. (continued)

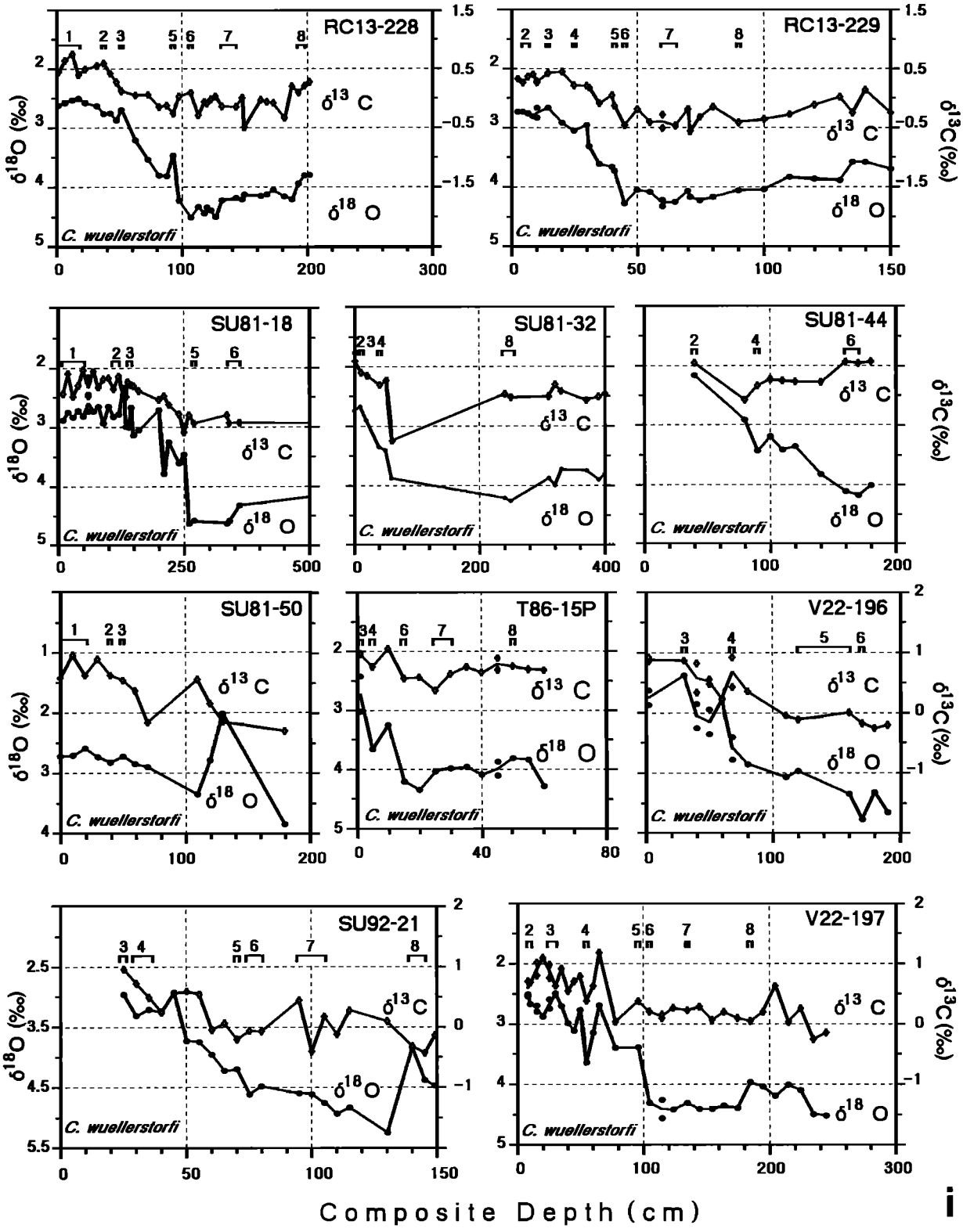

Figure 3. (continued)

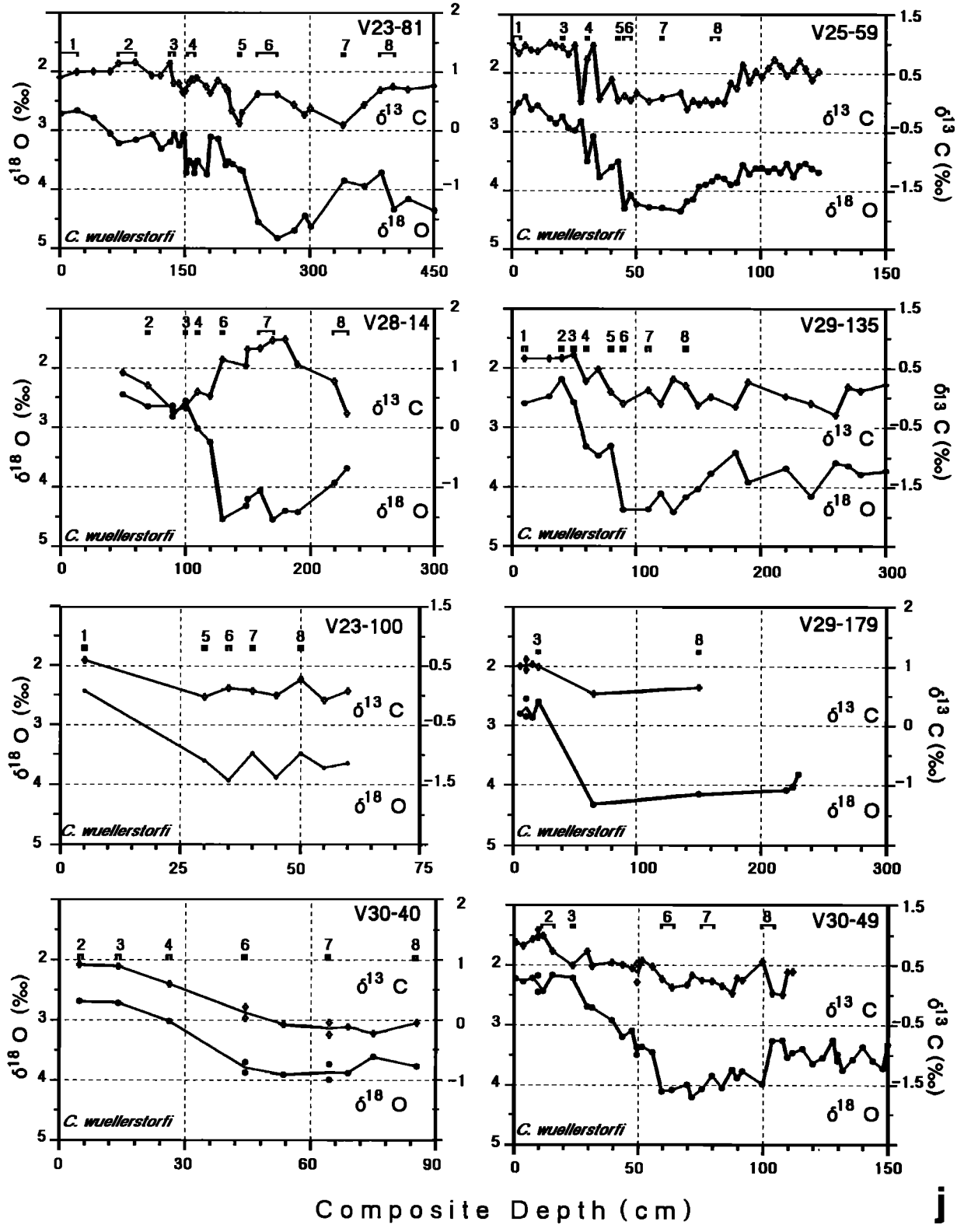

Figure 3. (continued)

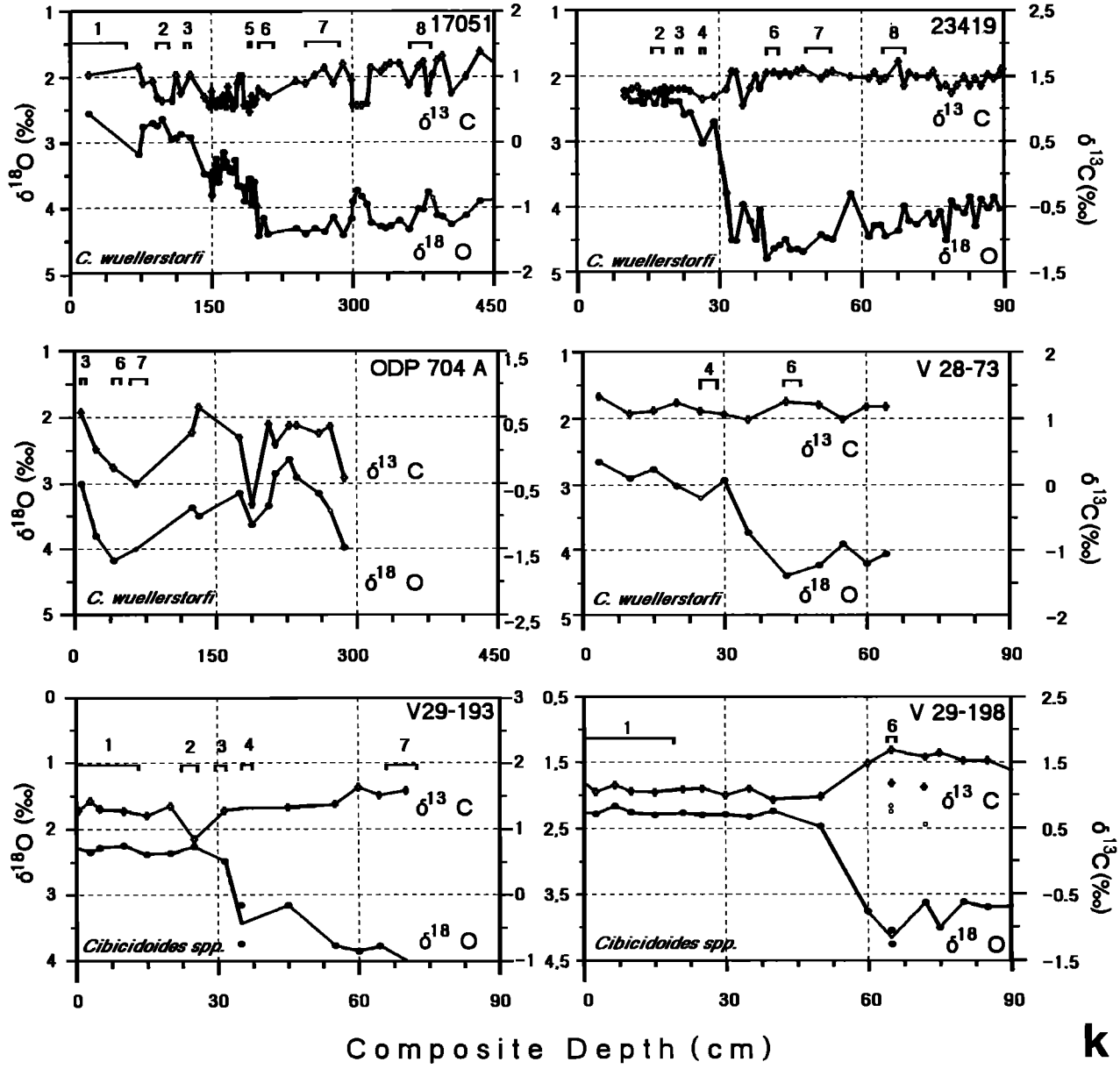

Figure 3. (continued)

the equatorial east Atlantic [Duplessy, 1972; Kroopnick, 1985; Kroopnick et al., 1972] suggests a general agreement of the analytical data, with deviations of less than 0.1‰.

3. Age Control

The age control and stratigraphic correlation of more than 90 sediment cores were based on benthic $\delta^{18}O$ records of *C. wuellerstorfi*, where a detailed event stratigraphy was defined for the last 30,000 years (Figure 3) (a full documentation of the stratigraphy in most Kiel $\delta^{18}O$ records is presented by Winn et al., 1991). In six benthic $\delta^{18}O$ records from the study area the event stratigraphy was dated directly by accelerator mass spectrometry (AMS) ^{14}C ages (Figure 4).

Based on the average ages of six ^{14}C dated events, we defined a detailed framework of age control points for $\delta^{18}O$ records, comprising (1) 9100 years B.P. for the end and (2) 10,400 years B.P. for the beginning of termination Ib, (3) 13,600 years B.P. for the end and (4) 14,800 years B.P. for the beginning of termination Ia, (5) 20,000 years B.P. for a $\delta^{18}O$ minimum in the middle of $\delta^{18}O$ stage 2, and (6) 26,000 years B.P. for $\delta^{18}O$ event 3.1 (Figure 4). This stratigraphic framework allowed us to estimate "AMS ^{14}C analogue ages" [Winn et al., 1991] for the vast majority of benthic isotope records not directly dated by radiocarbon ages.

Special problems occur with dating the surface sediment samples ("core tops") from gravity, piston, and kasten cores, where the top 10-20 cm of sediment are usually lost or disturbed. Precise surface ages and complete late Holocene sediment sections were reconstructed by means of a detailed core fit with neighboring box cores or multicorers, both of which typically

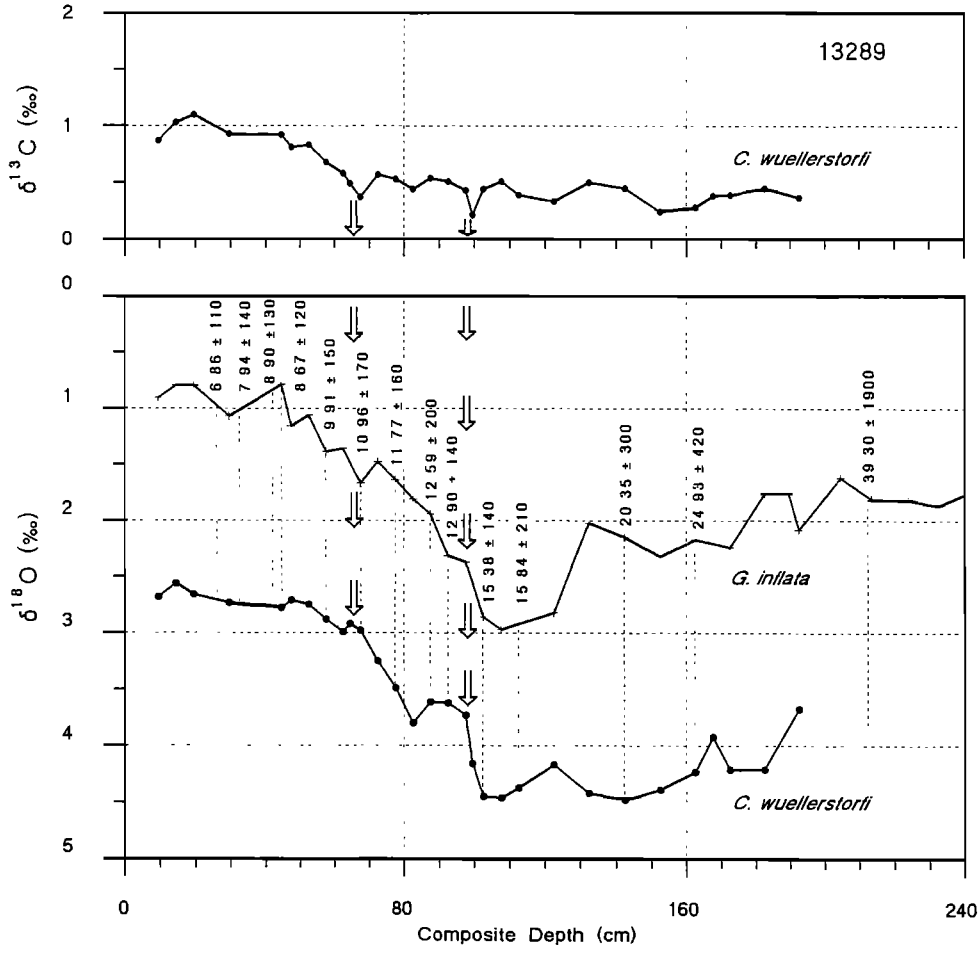

Figure 4. Accelerator mass spectrometry (AMS) ^{14}C dated (in kiloyears) $\delta^{18}O$ records of various planktonic foraminiferal species and $\delta^{13}C$ and $\delta^{18}O$ records of *C. wuellerstorfi* from cores 13289, 17045, CH73-139c, RC 11-83 , SU81-18, V23-81, and Ocean Drilling Program holes 658 A/B. Vertical arrows mark the end of marked $\delta^{13}C$ minima during termination I related to ^{14}C plateaus. Zigzag line in core 17045 marks hiatus. AMS -^{14}C ages were measured at Gif-sur-Yvette, except for ages in core RC11-83 [Charles and Fairbanks, 1992].

contain largely undisturbed sediment surfaces corresponding to an age of zero calendar (not ^{14}C) years.

Linear interpolations were applied between the selected age control points to obtain ages of the sediment in between. This was essential if the correct depths were to be selected for each time slice. This, however, causes further problems: Based on findings of Bard et al. [1990], any direct interpolation of ages and sedimentation rates between ^{14}C ages are invalid because of the fact that the conversion of ^{14}C years into calendar years is nonlinear, particularly across glacial termination I (14,800-9,100 ^{14}C years B.P. equating to 18,300-9,800 calendar (cal) years B.P.), as there are at least two major "^{14}C plateaus," that is hundreds of years with no ^{14}C change. The first of these occurs between 9,000 and about 10,300 ^{14}C years B.P. [Becker et al., 1991], and a further plateau probably lies near 12,500-13,000 ^{14}C years B.P. [Lotter et al., 1992].

Based on these findings, prior to interpolations between the age control points, we converted the ^{14}C age control points into calendar ages using the tree ring conversion scheme of Stuiver et al. [1991] for the Holocene and the conversion into U/Th years between 10,000 and 30,000 years B.P., as published by Bard et al. [1990]. The simplified conversion scheme of ^{14}C to calendar ages is based on six age switch points at 9.1 ka to 9.8 ka, 10.0 ka to 11.6 ka, 10.4 ka to 12.4 ka, 13.0 ka to 15.0 ka, 13.6 ka to 17.1 ka, and 26.0 ka to 29.5 ka (for further details see the work by Winn et al. [1991]). It was found that this method of selecting the range of the time slices was far superior to the conventional straightforward interpolation on the nonlinear radiocarbon age scale, as shown by the reduced downcore variability of sedimentation rates and also by clearly improved stratigraphic correlations between different cores. Finally, the interpolated calendar ages were converted back into ^{14}C ages to facilitate general comparisons with published ^{14}C dates for readers unfamiliar with the calendar age of common climatic events. We are aware of the fact that the details of the calibration scheme between radiocarbon and "calendar" years currently are rapidly improving. Because these changes [e.g., Bard et al., 1993] are ongoing, however, they cannot be considered anymore in this paper.

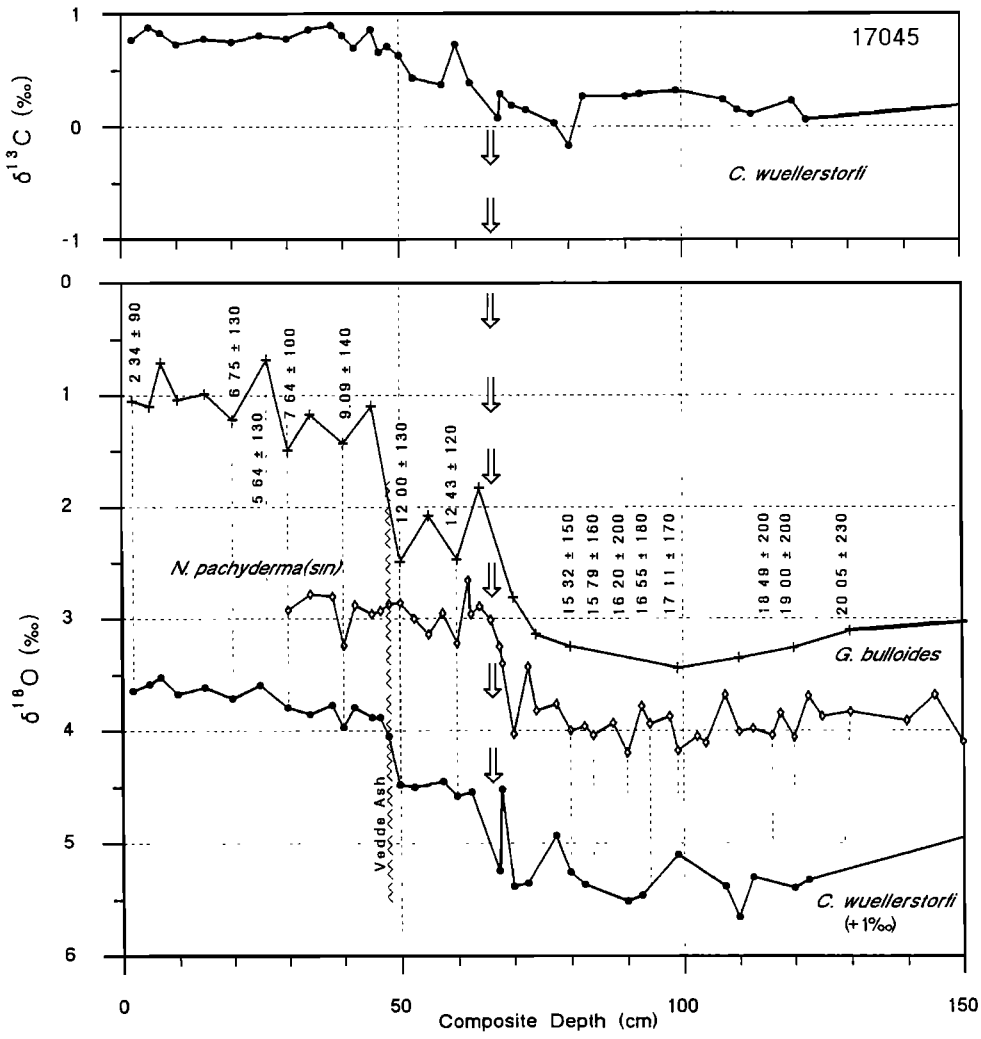

Figure 4. (continued)

Generally, we were encouraged by the fact that an increase in sampling density, time resolution, and stratigraphic accuracy led to increased internal consistency, simplicity, and greater predictability of the $\delta^{13}C$ patterns presented in the various transects.

4. Time Slice Selection

In this study, the evolution of Atlantic deepwater oceanography is traced by examining eight "time slices" over the last 30,000 years. These time intervals, which each may average several isotopic data points, have been selected in view of the following aspects (compare Figure 3):

The interval 0-3600 ^{14}C years (0-4000 cal years) ago approximates the regime of modern sedimentation and serves for "calibrating" the epibenthic $\delta^{13}C$ record with $\delta^{13}C$ data of dissolved inorganic carbon (DIC) in the modern ocean water. The long duration of this time interval takes into account both the frequent loss of the actual sediment surface in many cores and the need to test the modern $\delta^{13}C$ distribution pattern at as many sites as possible. At a few sites, $\delta^{13}C$ values of "living," that is, rose bengal stained specimens of *C. wuellerstorfi* (l) [Ganssen, 1983], illustrate the actual modern $\delta^{13}C$ signal.

The interval 6100-7200 ^{14}C years (7000-8000 cal years) ago was selected to investigate the climatic fluctuation between the early and middle Holocene climatic optimum, which is recorded in a minor ^{13}C minimum in many high-resolution $\delta^{13}C$ records.

The interval 8350-9100 ^{14}C years (9250-9800 cal years) ago corresponds to the sudden onset of the Holocene peak conditions, as indicated by the benthic $\delta^{18}O$ records (Figure 3), immediately subsequent to the last solar insolation maximum in the northern hemisphere.

The interval 10,350-10,800 ^{14}C years (11,800/12,300-12,800 cal years) ago represents the Younger Dryas cooling event. The "^{14}C plateaus" toward the end of and subsequent to this time [Kromer and Becker, 1992; Bard et al., 1990] may have led to inaccuracies in the extension of the absolute age range. The end of this time slice is well defined in the $\delta^{18}O$ records by the end of the *C. wuellerstorfi* based "$\delta^{18}O$ plateau" near 3.4‰, dividing glacial termination I.

The narrow interval 13,400-13,600 ^{14}C years (16,900-17,100 cal years) ago is marked by the first $\delta^{18}O$ minimum immediately subsequent to the LGM and is picked by a precise

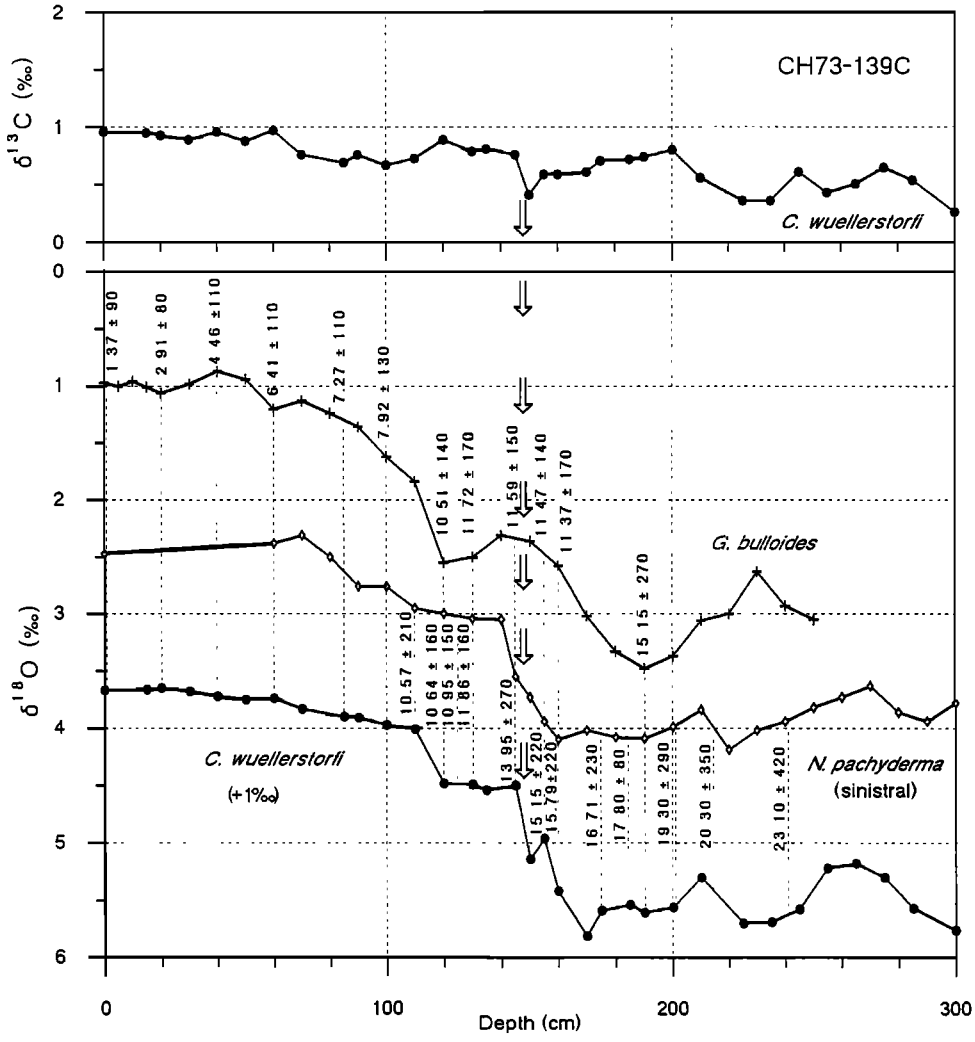

Figure 4. (continued)

interpolation of sediment thickness on the calendar age scale. This time slice depicts the spatial distribution of a short-lived epibenthic $\delta^{13}C$ minimum, the most pronounced excursion found in our high-resolution records (Figures 3 and 4; for example, cores 11944, 12328, 13289, 17045, Ocean Drilling Program (ODP) 658, V23-81, etc.). The minimum starts with the onset of termination Ia, culminates about 13,500 ^{14}C years ago [Sarnthein and Tiedemann, 1990], and parallels precisely a major planktonic $\delta^{18}O$ minimum in the Norwegian Sea [Weinelt et al., 1991; Sarnthein et al., 1992] and western North Atlantic [Keigwin et al., 1991] that is interpreted as a meltwater spike. The short-term $\delta^{13}C$ excursion is lost in about 1/3 of the records, where the sampling resolution and/or sedimentation rates are low (less than 2.5 cm kyr^{-1}).

The interval 14,800-15,800 ^{14}C years (18,300-19,300 cal years) ago records the oceanographic regime during the LGM, prior to its end. The time slice appears in most $\delta^{18}O$ curves as a ^{18}O maximum immediately below the pronounced $\delta^{18}O$ shift that marks the onset of glacial termination I (Figure 3).

The interval 18,000-20,000 ^{14}C years (21,500-23,500 cal years) ago was selected to study the paleoceanography during a central part of the LGM and to assess the trends in the evolution of deepwater circulation from the early to the late LGM.

The interval 24,800-26,000 ^{14}C years (28,300-29,500 cal years) ago records the ocean system response to the initial glacial advance during the first 1200 years of stage 2 after the moderately warm (interstadial) $\delta^{18}O$ event 3.1 and a (immediately preceding) short $\delta^{13}C$ minimum found in high-resolution records.

5. Results

5.1. Modern Water Masses in the East Atlantic: The $\delta^{13}C$ Record of Dissolved Inorganic Carbon Versus Oceanographic Data

A joint reevaluation of all $\delta^{13}C$ profiles measured on the total dissolved CO_2 (DIC) in the eastern Atlantic [Duplessy, 1972; Kroopnick, 1985; Erlenkeuser and Sarnthein, unpublished data, 1993] (Figure 5a) illustrates the present sources and spread of the major intermediate and deepwater masses and their gradual alteration, that is, the effect of ongoing physical mixing and chemical reactions within them. From 1200-1500 m to 3500 m depth, the most prominent feature in the modern

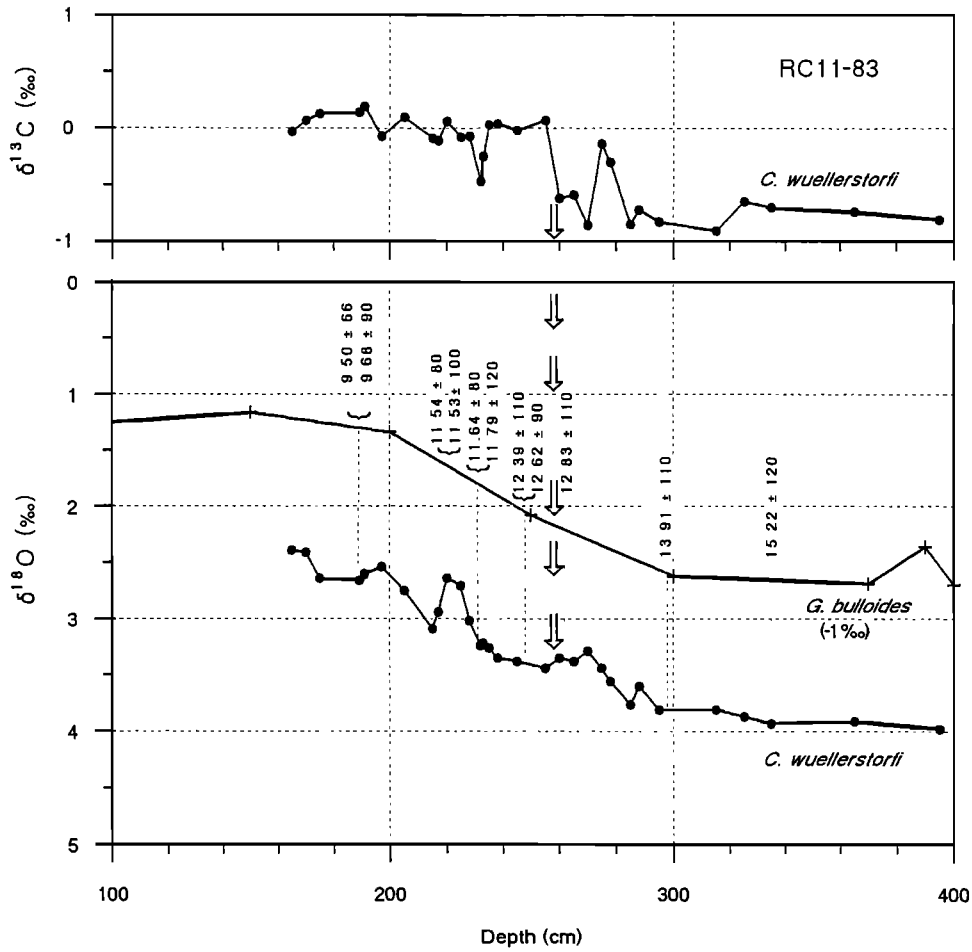

Figure 4. (continued)

eastern Atlantic is the NADW. A large portion of it, about 5-8 Sv [Saunders, 1982] spreads from the eastern to the western basin at 54°N through the Gibbs fracture zone (FZ) [Dickson et al., 1990]. Contrary to widespread belief, however, Saunders [1982] demonstrated that a further 6 Sv of NADW continues to flow south through the eastern basin and gradually crosses the Mid-Atlantic Ridge from east to west (not from west to east), with a flux approximately uniform with latitude (Figure 5b). At 32°N, the basinwide N-S flow still amounts to 2 Sv, while near 18°-20°N, its characteristic oxygen signal (more than 5.6 mL L^{-1}) fades out [McCartney et al., 1991]. Further south, especially south of the Sierra Leone Rise, the NADW signal in the east Atlantic is dominated by west to east geostrophic transport of NADW from the Brazil Basin across the Mid Atlantic Ridge, at 11°N through the Vema FZ and at 1°S through the Romanche and Chain FZ [McCartney et al., 1991].

At abyssal depths, below 3500-4000 m, cold dilute AABW (≤2°C) is supplied into the east Atlantic [Warren, 1981, Saunders, 1982, McCartney et al., 1991]. North of the Sierra Leone Rise, the bottom water debouches through the Vema FZ toward east and northeast into the Canary basins, which are bounded to the north by the east Azores FZ scarps. Here only two narrow passages with depths over 4500 m are cut through to the north [McCartney et al., 1991], which will be of great significance for understanding the features of LGM deepwater circulation (see section 5.4.). South of the Sierra Leone Rise, AABW debouches via the Romanche FZ into the southeast Atlantic abyssal basin. Hardly any AABW that fills the Cape Basin enters from south to north across the western end of the Walvis Ridge.

As expected from its high oxygen content, NADW in the east Atlantic is represented by high $\delta^{13}C$ values of 1.1-0.9‰, which dominate the north-south transect of Figure 5c between 2 and 5 km depth and 25°N and 10°S. Further south, the values decrease to 0.6/0.7‰ near 30°/40°S. This decrease reflects the gradual influence of both ongoing remineralization of ^{12}C-enriched POC and admixture of AABW from below.

North of 15°N, Figure 5c contains hardly any $\delta^{13}C$ data in the depth range of NADW, below 2000 m, over some 40° of latitude. At 50°-60°N, however, the E-W transect of Figure 5d depicts pronounced small-scale $\delta^{13}C$ variations (D0.5‰). West of the Rockall Plateau, the track of "juvenile" NADW is clearly traced near the seafloor by maximum $\delta^{13}C$ values of 1.25-1.3‰ down to 2300 m as compared with about 1.00‰ near 25°N (Figure 5c) (the track at 50°N is missing in Figure 5c, with data from east of the Rockall Plateau). Hence the ^{13}C values in NADW show an overall decrease by about 0.25‰ from 50° to 25°N, an alteration that matches a decrease in dissolved oxygen from about 6.0 to 5.6 mL L^{-1} [McCartney et al., 1991].

Near the equator, the local $\delta^{13}C$ values of NADW increase by

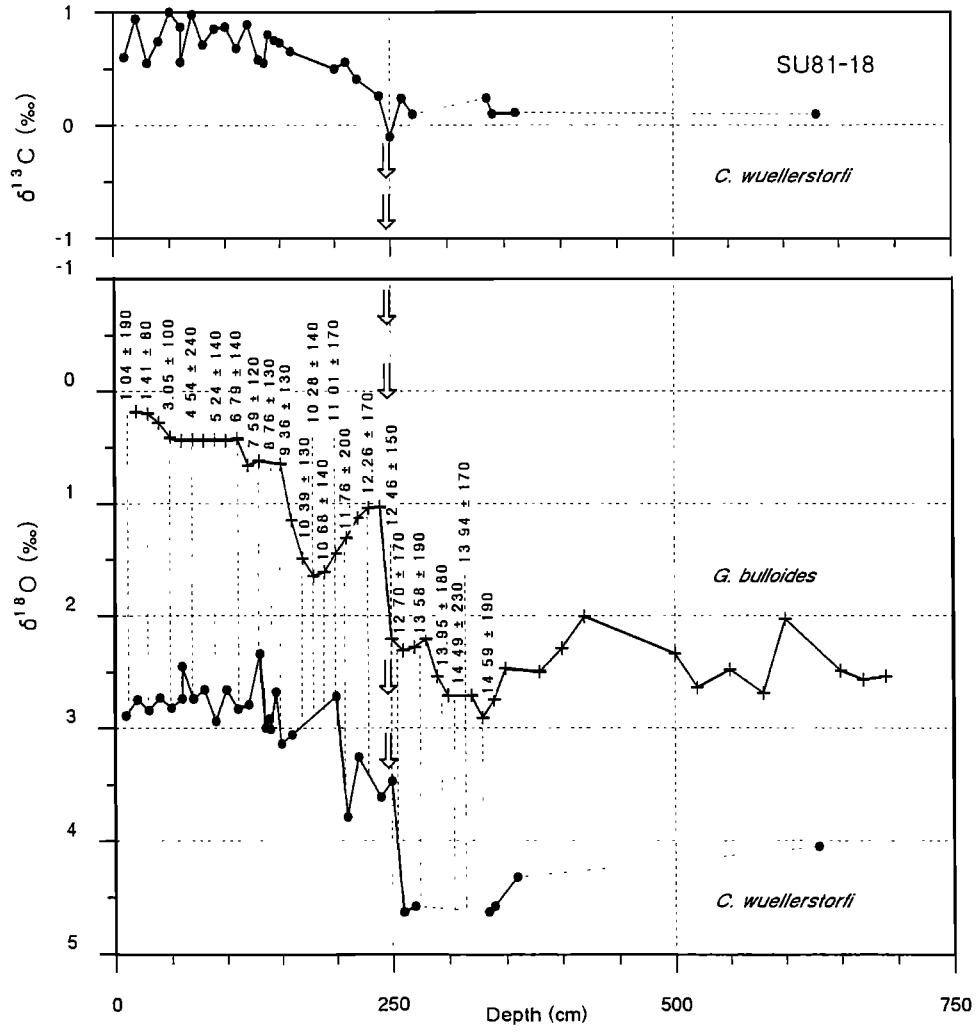

Figure 4. (continued)

about 0.25‰ from north to south (Figure 5c), contrary to the outlined general trend. This pattern is linked to west-east running currents along the equator through the Vema (11°N) and Romanche FZ at 0°N. Here it is the Equatorial Undercurrent within the top 1000 m depth and the incursion of better oxygenated NADW at 2000-4000 m; at the Vema FZ, AABW spreads from the western into the eastern Atlantic (Figure 5e). This interpretation is corroborated by a local increase in dissolved O_2 from 5.5 up to 6.0 mL L^{-1} [McCartney et al., 1991] and a decrease in phosphorus and CO_2 [Bainbridge, 1981].

The incursion of nutrient-enriched AABW (and/or lower Circumpolar Deep Water (CPDW)) into the South Atlantic Cape Basin is clearly reflected by low $\delta^{13}C$ values (Figure 5c), which parallel highs in the nutrient and CO_2 distribution [Bainbridge, 1981]. Minimum $\delta^{13}C$ values of 0.25‰ occur in the Cape Basin south of 40°S versus 0.4‰ in the west Atlantic off Brazil (Figure 5e). In the abyssal basins of the northeastern Atlantic, the modern presence of AABW is hardly seen (Figure 5c) except for a few low $\delta^{13}C$ values near the northern margin of the Sierra Leone Rise east of the Vema FZ.

The oxygenated Weddell Sea Bottom Water (WSBW), which downwells below the CPDW because of an extremely high density, is clearly traced in Figure 5c by intermediate $\delta^{13}C$ values, reaching 0.75-0.8‰ on the Antarctic basin floor, south of the mid ocean ridge (53°S) in the southern ocean.

Above 1500-2000 m, the outflow of nutrient-depleted Mediterranean outflow water (MOW) leads to a most pronounced, mesoscale $\delta^{13}C$ maximum (up to 1.3/1.4‰), extending from Gibraltar to the south and up to about 25°N (Figure 5c). The dominant flow toward north [Price et al., 1993] cannot be traced in Figure 5c because of a lack of data stations. The MOW signal is largely restricted to the eastern Atlantic margin but can still be recognized near the Mid-Atlantic Ridge south of the Azores [Käse et al., 1986; Duplessy, 1972]. The MOW is surrounded on either side by mesoscale water masses with $\delta^{13}C$ minima in the top 1000 m of the east Atlantic. In part, they reflect the position of the nutrient-enriched South Atlantic central water penetrating north up to 22°N [Labracherie, 1980]. Other minima result from remineralization of particulate organic matter below local zones of high plankton production in the surface water, such as in equatorial and coastal upwelling regions. The latter $\delta^{13}C$ minima are marked by small-scale local east-west gradients among the various $\delta^{13}C$ profiles [Duplessy, 1972; Kroopnick, 1985].

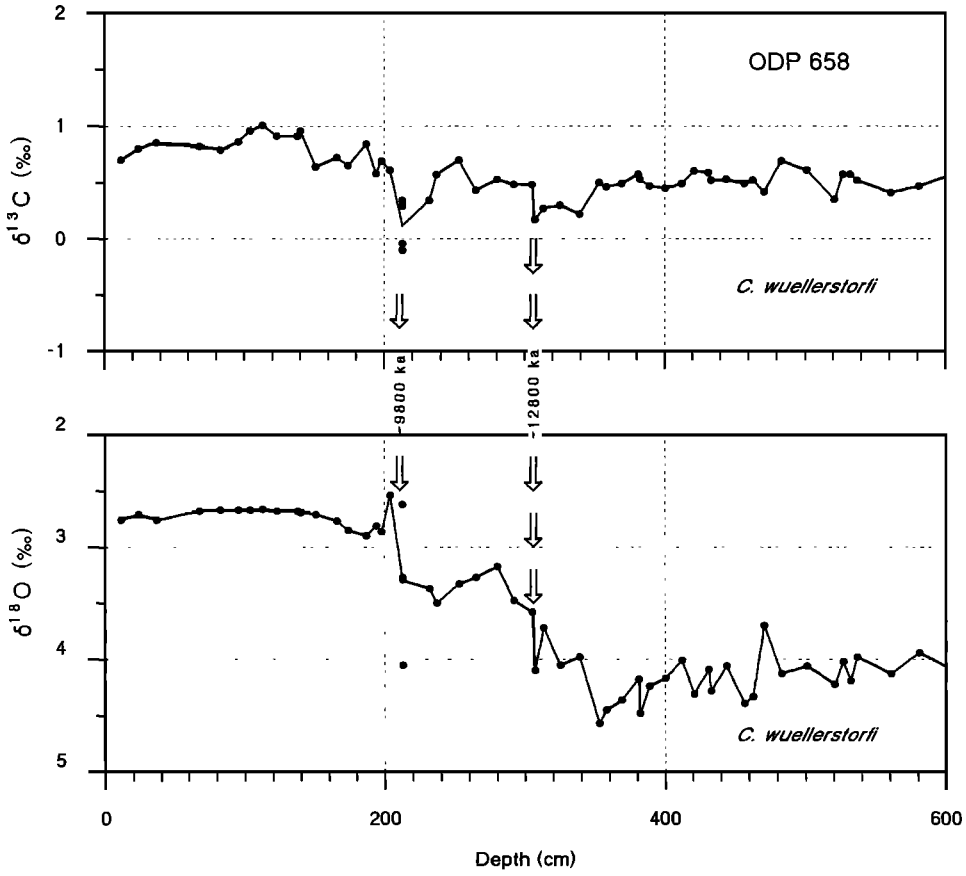

Figure 4. (continued)

5.2. Epibenthic $\delta^{13}C$ Record of Present Water Masses in the East Atlantic 0-3.6 ^{14}C kyr B.P. (= 0-4 Cal kyr)

The density of $\delta^{13}C$ contours in Figures 6 to 20, our main database, may appear controversial. In our view, however, the larger number of contours serves (1) to avoid an arbitrary overemphasis on any single $\delta^{13}C$ level that is subject to analytical noise, (2) to demonstrate more clearly the gradients in ocean chemistry between different water masses, and (3) to ease the comparability between the various time slices where different $\delta^{13}C$ levels dominate.

Most features of modern Atlantic deepwater circulation, displayed by the $\delta^{13}C$ record of DIC, also occur in the epibenthic $\delta^{13}C$ records of the average data of the last 4000 years (Figures 6a and 7). As in Figure 5c, the positive epibenthic $\delta^{13}C$ values in Figure 6a show the presence of NADW between 2 and 4 km depth and from 60°N-20°S, thus recording the most salient feature in the east Atlantic. The chemical alteration of NADW on its way from the Norwegian Sea to the south is minor. It is reflected by a two-step $\delta^{13}C$ shift from a maximum of >1.3‰ near the top of Rockall Plateau down to less than 1.2‰ south of 35°N and to values of less than 1.0-0.8‰ south of 0°-15°S. The benthic $\delta^{13}C$ data also appear to reflect details in chemical oceanography as small as a slight nutrient depletion near 3800 m at the equator, depicted as a minor positive $\delta^{13}C$ deviation. As in the DIC $\delta^{13}C$ record (Figure 5c), we relate this feature to more oxygenated deepwater advecting west to east through the Romanche FZ.

In contrast, local sample clusters with negative benthic $\delta^{13}C$ deviations, up to -0.3 to -0.45‰, occur in the depth range of NADW all along the African and Portuguese continental margin (dotted ovals in Figure 6a). They are linked, as previously suggested, to high fluxes of organic carbon to the seafloor (exceeding 2.0/2.5 g C m^{-2} y^{-1}) and fluff layers, induced by cells of coastal-upwelling productivity as deduced from high accumulation rates of total organic carbon TOC [Sarnthein and Winn, 1990]. Likewise, extremely low $\delta^{13}C$ values south of the equator near 1000 m depth, which strongly deviate from the local DIC data (Figure 6b), reflect the local impact of high TOC fluxes and productivity triggered by nutrients from tropical river mouths. It is not clear yet whether the extended $\delta^{13}C$ minimum at 2 km depth, marking the top of the NADW at 20°-40°N, is also an artifact of local high carbon fluxes or is related to an intermediate water mass advected from the south.

Below 3800 to 4400 m, more negative values of 0.6-0.8‰ reflect the northward incursion of dilute AABW into the Canary basin and further north, up to 50°N, east of Rockall Bank (Figures 6a and 7). Because a large portion of this abyssal geostrophic current flows along the east Atlantic continental margin [McCartney et al., 1991], the AABW is more clearly displayed in the epibenthic signal than in the few samples of the DIC record (Figures 5c and 5d). Between 800 and 1800 m

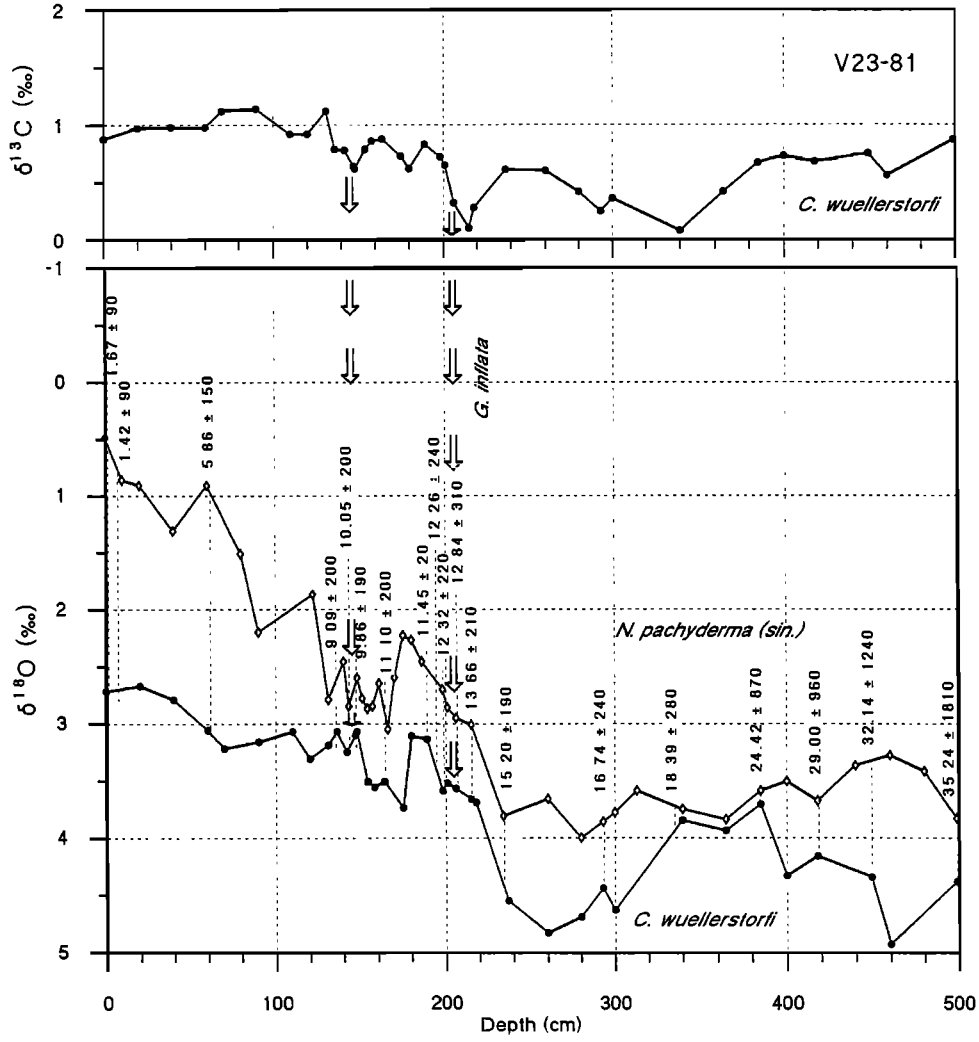

Figure 4. (continued)

depth southwest of Gibraltar (23-36°N) (Figure 6a), the small but pronounced $\delta^{13}C$ maximum of 1.2-1.25 ‰ matches the position of MOW, such as recorded in the $\delta^{13}C$ values of modern DIC.

In general, our benthic $\delta^{13}C$ record deviates from the $\delta^{13}C$ values of marine DIC (interpolated between nearby sample stations) by less than ± 0.2‰ (Figure 6b). The few outliers are linked either to local organic fluff layers or to an insufficient, too widely spaced coverage of DIC data. Boyle [1992] surmised that $\delta^{13}C$ values of epibenthic foraminifera, sampled in shallow water depths of less than 1000-2000 m, may systematicaly exceed the $\delta^{13}C$ values in marine DIC. Figure 8 demonstrates that two $\delta^{13}C$ values measured on "living" specimens of *C. wuellerstorfi* from 800-1000 m depth do not exceed the DIC-based $\delta^{13}C$ record by more than 0.2‰, a difference that also occurs at 2500-3000 m water depth and that does not appear to be statistically significant. Furthermore, the two outliers are derived from near Cape Blanc, a region with a particularly small-scale but strong variability of water masses, where the DIC profile of Figure 5c might have simply missed the local plume of MOW and/or picked a season with high values of remineralized POC. In summary, we consider the $\delta^{13}C$ values of benthic foraminifera as faithful recorders of ocean chemistry at all sites where the local flux of organic carbon is low, independent of water depth.

Having examined the most recent (modern 4 kyr) conditions, we discuss the evolution of deep water proceeding from older time slices (28.3-29.5 kyr) to younger.

5.3. Reconstruction of East Atlantic Deepwater Masses After the End of Moderately Warm Stage 3.1, 24.8-26.0 ^{14}C kyr B.P. (= 28.3-29.5 Cal kyr)

In the wake of stage 3, the $\delta^{13}C$ distribution patterns in Figures 9a and 10 (raw data uncorrected for any global $\delta^{13}C$ shift) and the corresponding main water masses still largely resemble the modern circulation pattern within the top 3500 m depth. Different features, however, appeared further down, the

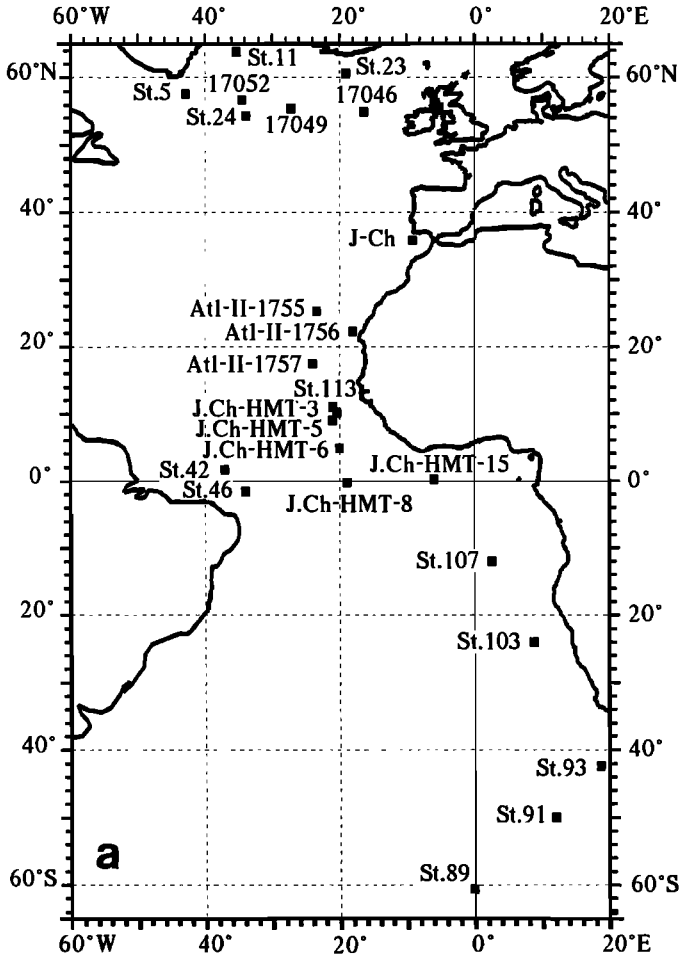

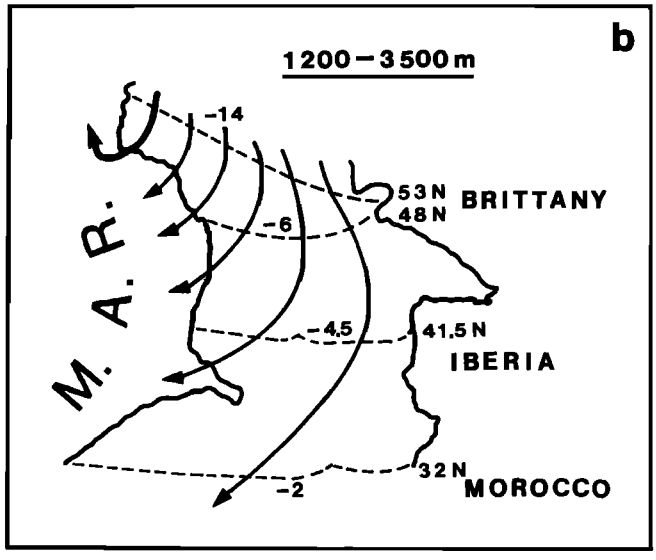

Figure 5. Profiles of $\delta^{13}C$ in dissolved inorganic carbon (DIC), and distribution of major water masses in the eastern Atlantic. (a) Location of water profiles. (b) Circulation of eastern North Atlantic at 1200-3500 m after Saunders [1982]. Transport is in sverdrup units of $10^6 m^3 s^{-1}$ (c) N-S $\delta^{13}C$ transect across the east Atlantic. (d) NW-SE transect across the northern Atlantic (NAD, North Atlantic Drift). (e) W-E transect across the equatorial Atlantic. For abbreviations of locations see Figure 2.

chemistry already anticipating the onset of the glacial regime of stage 2.

A tongue of ^{13}C-enriched values depicts a southward bound water mass between 2000 and 3500 m (Figures 9a and 10) similar as today. This water mass originated from north of Rockall Plateau, probably in the Norwegian-Greenland Sea (but not in the northwestern Atlantic off Greenland, where $\delta^{13}C$ values were as low as 0.22-0.76‰), and extended about as far south as today (0.6-0.84‰ $\delta^{13}C$ on top of the Sierra Leone Rise). This water mass is thus referred to, by analogy, as NADW. As compared to the present (Figures 6a and 7), the $\delta^{13}C$ values north of 40°N were little reduced, by only 0.1-0.25‰, especially west of Rockall Plateau. South of 35°-40°N, however, the $\delta^{13}C$ values were significantly lower, by -0.5 to -0.65‰ (Figure 9b). The steep N-S gradient in the NADW $\delta^{13}C$ values east of the Azores may have had various origins, including (1) a reduced N-S transport, (2) an increased mixing of ^{13}C-depleted abyssal water from below, and/or (3) an enhanced advection of ^{13}C-depleted POC from above.

At the same time, the incursion of MOW at Gibraltar was well oxygenated, showing a slight ^{13}C enrichment (by > 0.2‰) as compared to the present (Figure 9b). Outside the MOW and further south (possibly also further north), the intermediate water at 800-2000 m depth was slightly ^{13}C depleted by 0.1-0.3‰.

In contrast, the $\delta^{13}C$ values of the AABW incursion were strongly reduced, by up to -1.1‰ as compared to the present (Figure 9b). A ^{13}C reduction of more than 0.9‰ also occurs further west, on the Mid-Atlantic Ridge (site V25-59), outside the belt of high carbon flux below equatorial upwelling. This station suggests that the strong ^{13}C reduction observed in low-latitude abyssal waters below 3500 m was definitely a general, already glacial-style feature of AABW chemistry and not the result of a locally increased POC flux. The source of AABW, the CPDW, was also ^{13}C depleted by about 0.8‰ during this time [Duplessy et al., 1988].

AABW was at this time more advanced northward in the northeast Atlantic than today, up to 50°N, as was the case during the subsequent LGM. Moreover, the upper boundary of AABW lay slightly shallower, near 3500-3800 m. This enhanced abyssal circulation, when combined with the narrow passages cut through the scarps of the east Azores FZ, probably led to a significant upwelling of ^{13}C-depleted AABW east of the Azores. This would have led to the local dilution of the overlying NADW, as documented by the steep N-S gradient in $\delta^{13}C$ found in Figure 9.

5.4. Reconstruction of East Atlantic Water Masses During the LGM: 18.0-20.0 ^{14}C kyr B.P. (= 21.5-23.5 Cal kyr) and 14.8-15.8 ^{14}C kyr B.P. (= 18.3-19.3 Cal kyr)

The two time slices reconstructed for the LGM display very similar $\delta^{13}C$ records of east Atlantic deepwater masses. During both intervals, the northern east Atlantic north of 35°N was

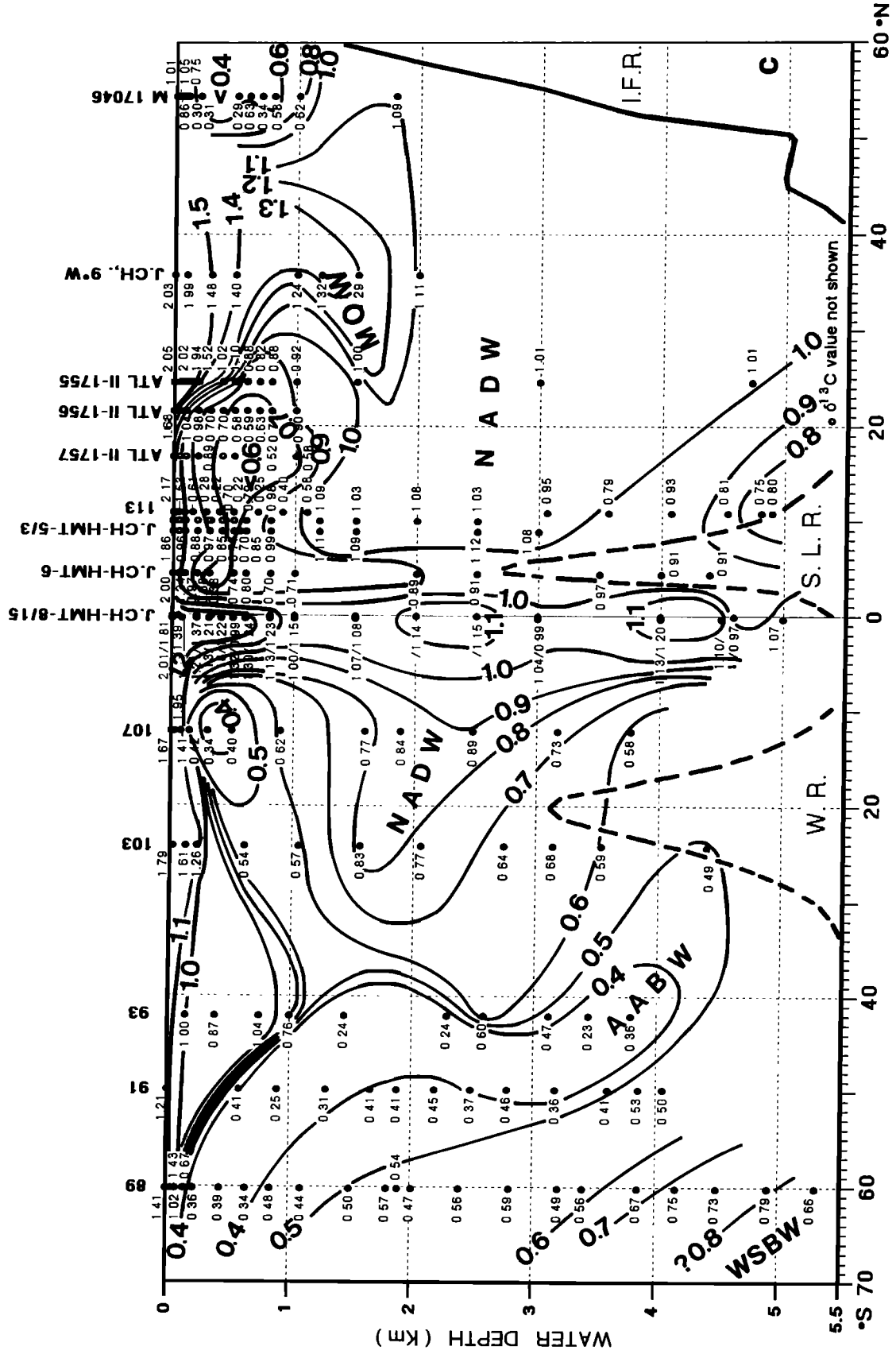
WATER DEPTH (km)
0
1
2
3
4
5
5.5
60°N
40
20
0
20
40
60
70°S
I.F.R.
C
S. L. R.
W. R.
N A D W
N A D W
A A B W
WSBW
M 17046
J.CH., 9°W
ATL II-1755
ATL II-1756
ATL II-1757
J.CH-HMT-5/3
J.CH-HMT-6
J.CH-HMT-8/15
δ13C value not shown

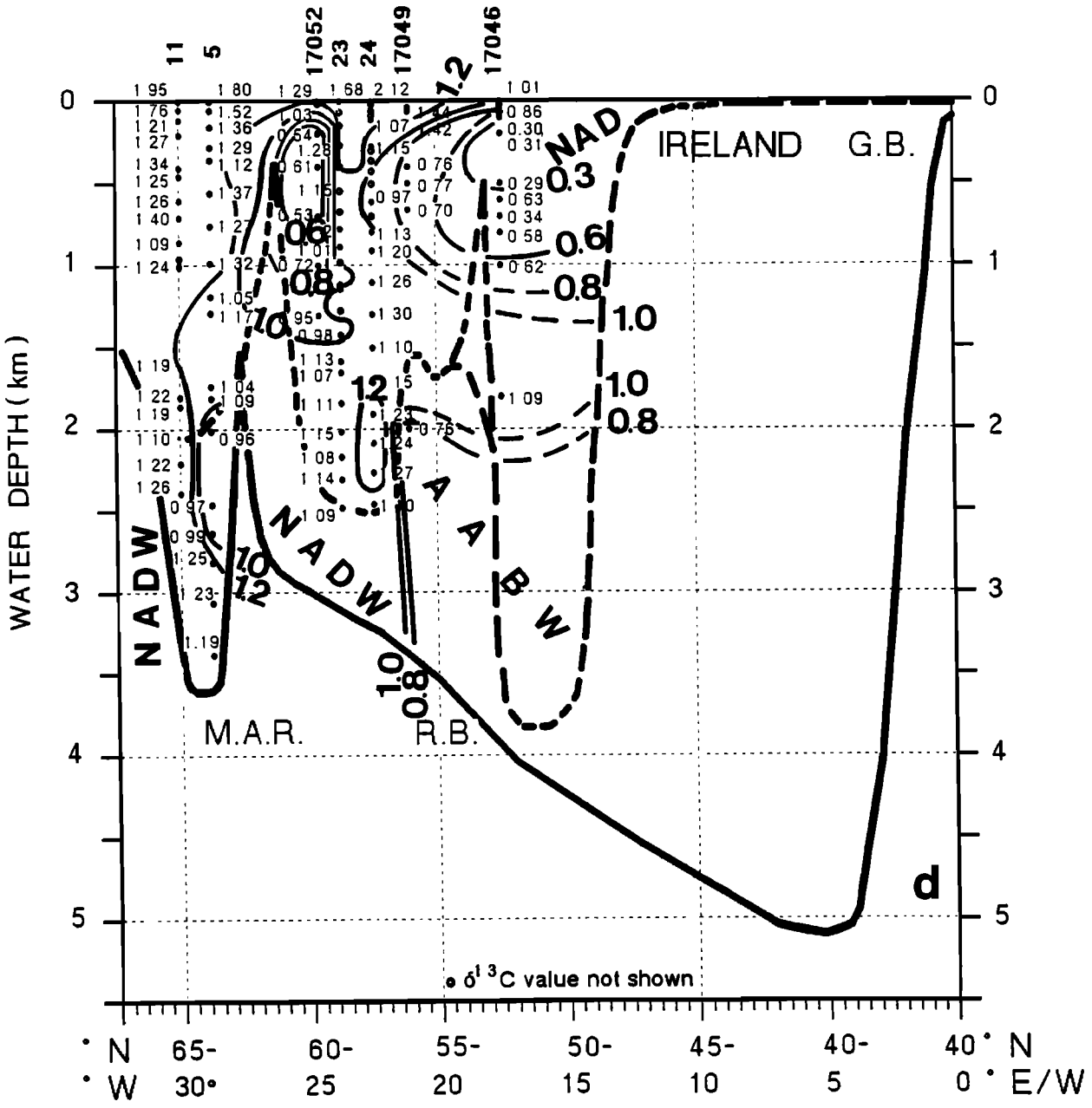

Figure 5. (continued)

dominated by a well defined tongue of high $\delta^{13}C$ values (0.7-1.2‰, uncorrected for any global $\delta^{13}C$ shift) (Figures 11a and 12a). As in the preceding time slice (Figure 9a), this tongue reflects the track of a southward bound water mass that started near Rockall Plateau (with $\delta^{13}C > 1.2$-1.7‰) which was downwelled to more than 3600 m depth at 35°-45°N in the east Atlantic (similar to that presented by Duplessy et al. [1988]). On its downward track it was increasingly diluted, and the $\delta^{13}C$ values became progressively lower by up to 0.7-0.8‰.

A more ^{13}C-depleted (i.e., more diluted and less oxygenated) branch of this water mass (0.4-0.5/0.6‰ $\delta^{13}C$) can be traced between 2000-3500 m depth from 35°N up to at least 10°S (Figures 11a and 12a), that is, approximately as far south as the 0.8-0.9‰ $\delta^{13}C$ contours of the present NADW (Figure 5a). This large-scale glacial circulation pattern only emerges after deleting a number of local $\delta^{13}C$ minima along the continental margin of west Africa and Portugal, patches that result from high fluxes of POC linked to upwelling productivity (dotted ovals in Figures 11a and 12a).

Contrary to previous models of a "glacial Atlantic Intermediate Water" [Duplessy et al., 1988; Boyle, 1992], our much enlarged new proxy data set allows us to reinterpret the large downwelled water mass in the northeast Atlantic as an embryonic version of North Atlantic *Deep* Water and the water mass between 35°N and 10°S as its strongly diluted continuation. This interpretation implies that a weakened salinity conveyor belt was active during the LGM.

During the earlier time slice of the LGM, the source of the

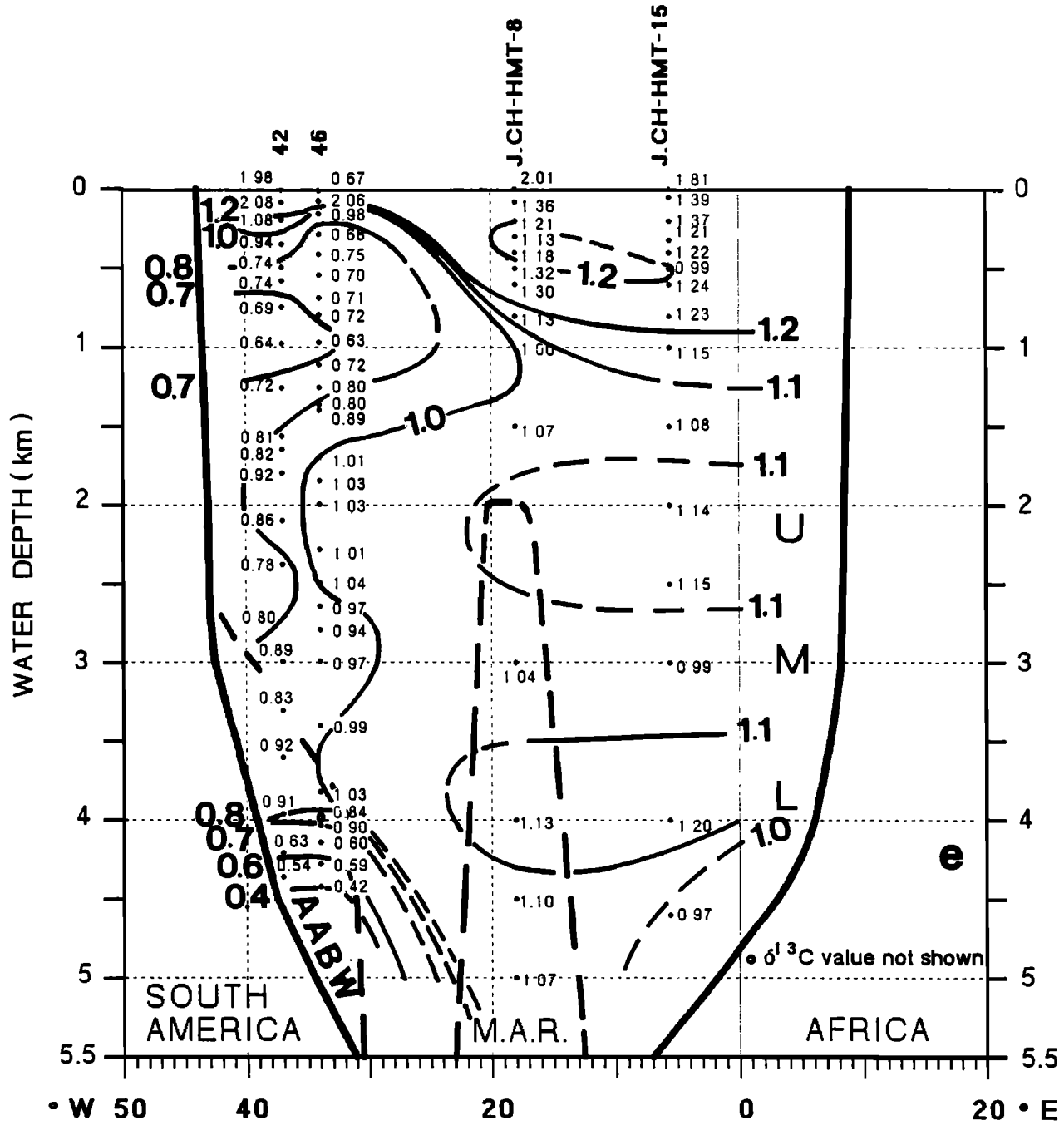

Figure 5. (continued)

NADW-style deep water lay between Rockall Plateau and Greenland (Figure 13a) (about 1.4‰ $\delta^{13}C$ at core location V28-14). Later, the main source region was confined to the central North Atlantic south of Iceland, near 55°-60°N (Figure 13b). This position fully matches the recent density-based model of deepwater formation by Labeyrie et al. [1992]. Unlike both the present and the end of stage 3.1, the glacial deep water did not originate from the Norwegian-Greenland Sea, because $\delta^{13}C$ values at site 552 are lowered, which lies at a "watchdog" position in the Iceland Basin within the present mainstream of the Norwegian Sea overflow [Dickson et al., 1990] (Figures 1 and 12). Note that in the glacial source regions of deepwater the initial $\delta^{13}C$ values reached 1.74‰ $\delta^{13}C$ (Figures 13a and b). Hence the amount of preformed nutrients in NADW may have differed little from the values found in modern downwelling regions of the Greenland Sea (1.7-1.8‰) (Figure 5d).

Below about 3500 m, the glacial east Atlantic was dominated by the incursion of a strongly ^{13}C-depleted, thick water mass of southern origin, such as was already noted in the time slice that followed stage 3.1 (Figure 9a). The $\delta^{13}C$ values of this glacial AABW decreased down to -0.8‰ at 41°S and to less than -0.4‰ near the equator. The ^{13}C-depleted AABW ad-

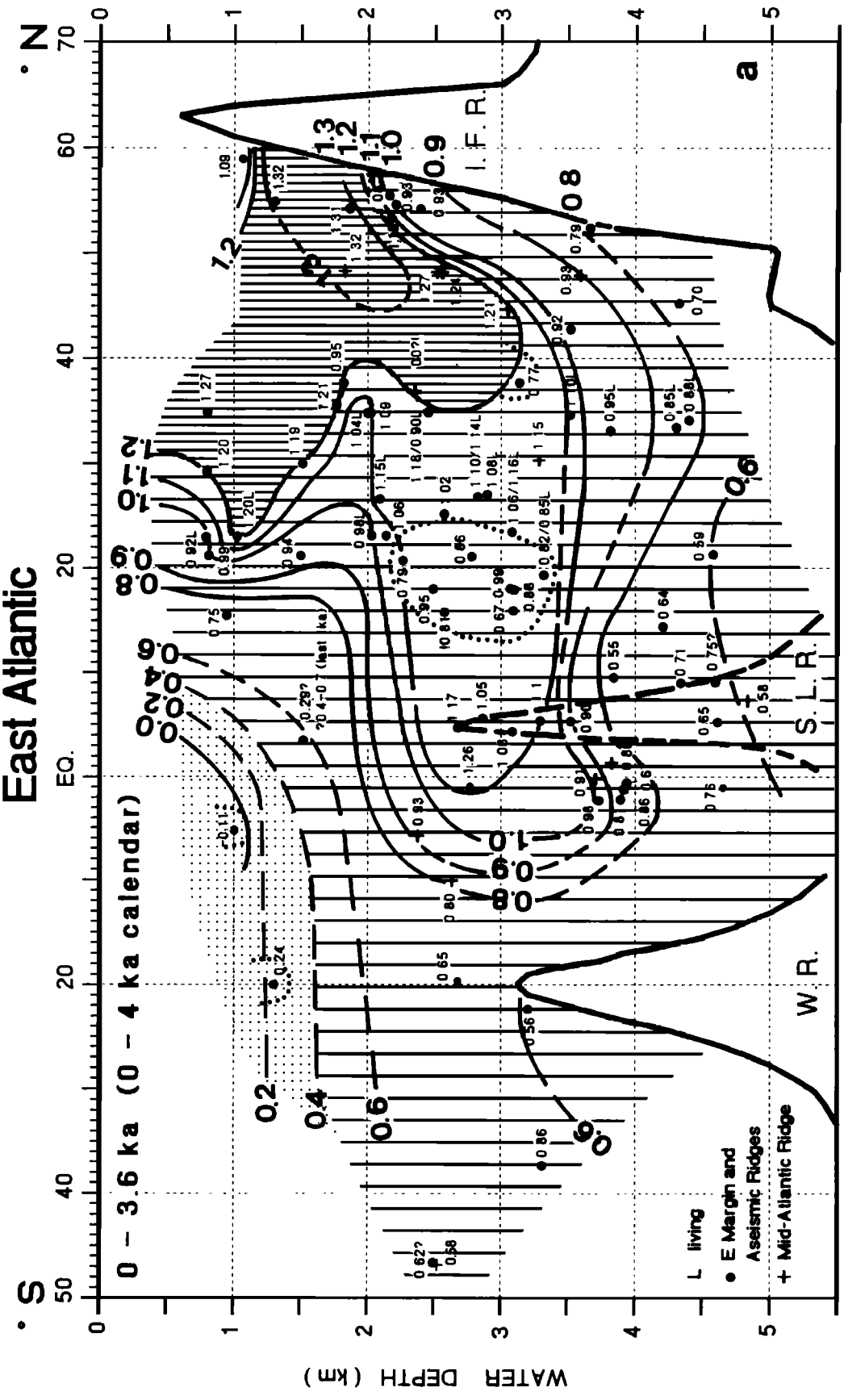

Figure 6. Benthic $\delta^{13}C$ profiles across the east Atlantic for the Recent time interval 0-3600 ^{14}C years B.P. (or 0-4000 calendar years). (a) N-S transect; L, "living" specimens of *C. wuellerstorfi*. (b) N-S transect of $\delta^{13}C$ anomalies: Recent epibenthic $\delta^{13}C$ values versus $\delta^{13}C$ values of modern DIC (differences between data of Figures 6a and 5c). For abbreviations of locations see Figure 2.

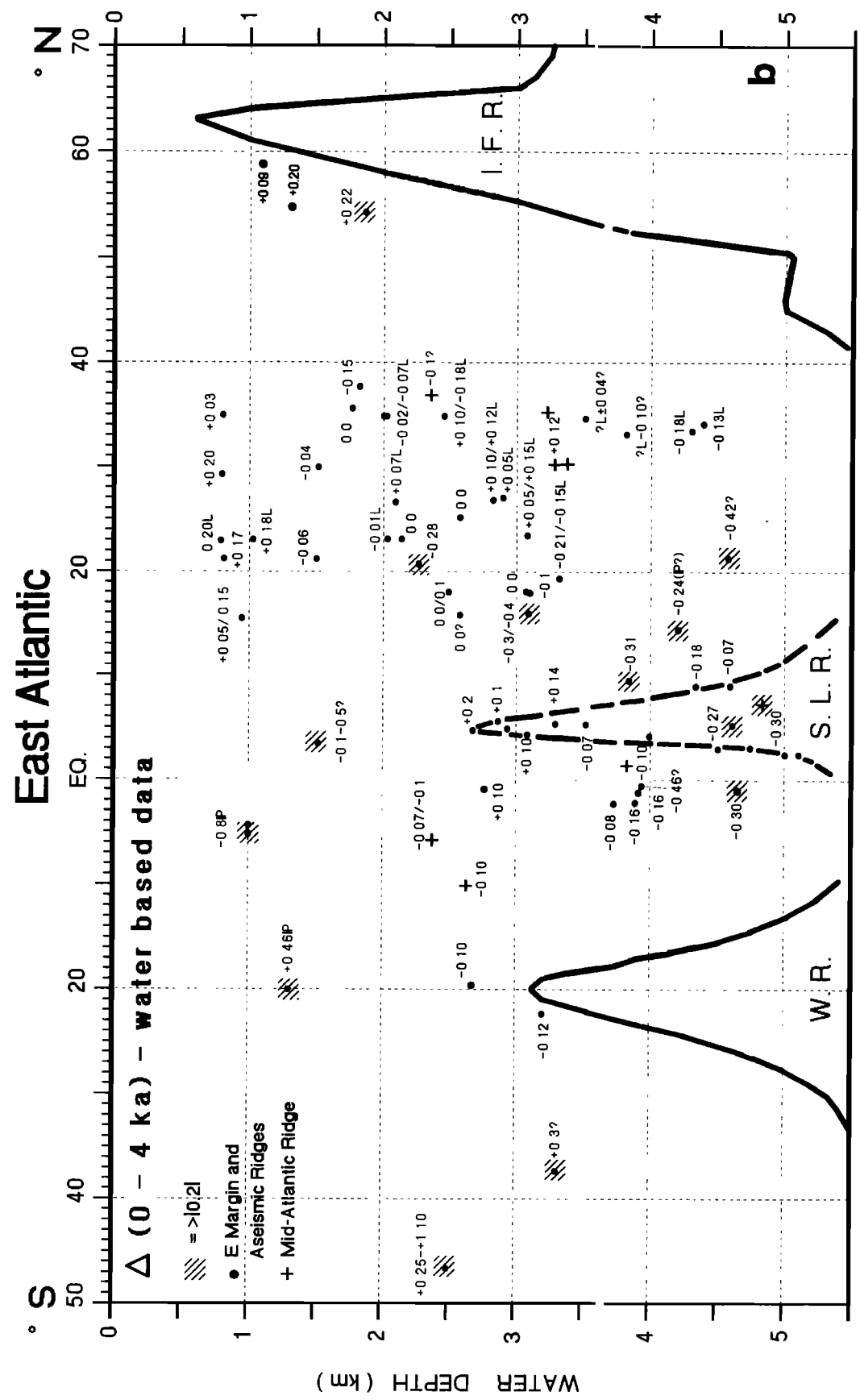
East Atlantic
Δ (0 – 4 ka) – water based data
= >|0.2|
E Margin and Aseismic Ridges
Mid-Atlantic Ridge
S. L. R.
I. F. R.
W. R.
b
° S
° N
EQ.
WATER DEPTH (km)

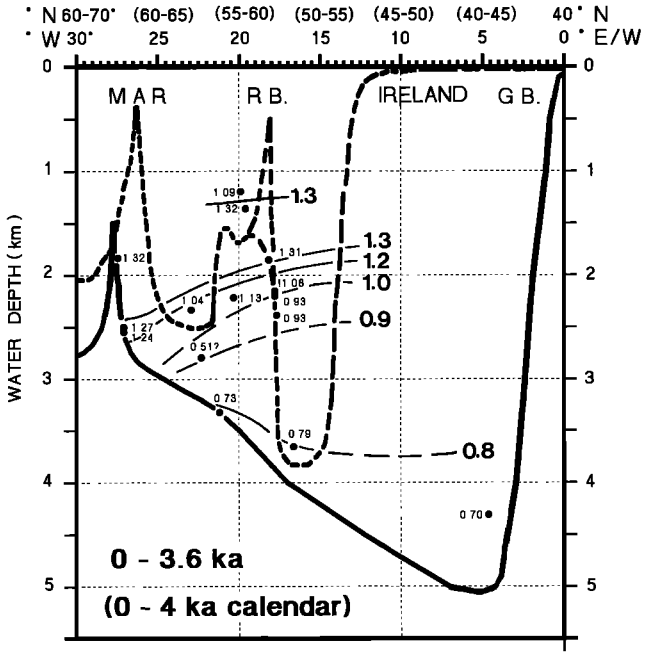

Figure 7. Benthic $\delta^{13}C$ profile running NW-SE across the North Atlantic. Average of last 3600 ^{14}C years = 4000 calendar years. Location of profile shown in Figure 1, for abbreviations of locations see Figure 2.

vanced in the east Atlantic up to 50°N, becoming gradually diluted, that is, ^{13}C enriched from -0.4/-0.2‰ up to more than 0.1/ 0.25‰ (Figures 11a and 12a). This trend represents a gradual admixture of ^{13}C- (and oxygen) enriched deepwater from above. In particular, the narrow deepwater passages cut through the east Azores FZ scarps may have acted as an effective barrier to the (enhanced) northward bound bottom water circulation, promoting the upwelling and admixture of AABW into the overlying deep water. Bottom morphology probably was thus the final cause of the marked N-S reduction in ^{13}C and dilution found in the glacial NADW derivative near 35°-40°N.

The third major feature of the glacial circulation in the east Atlantic was the $\delta^{13}C$ signal of the MOW. As first shown by Zahn et al. [1987], and in contrast to Boyle [1992], the conspicuous $\delta^{13}C$ signal of the MOW (up to 1.75‰) can be traced unambiguously at various sites close to the point source of the Straits of Gibraltar. From there, the MOW spread down to 1600 m depth and south to 20°N, approximately as far as today. Figures 11a and 12a show that it can be clearly distinguished from the embryonic NADW tongue that started near Rockall Plateau in the northern Atlantic. Moreover, the early glacial $\delta^{13}C$ values near the MOW source were slightly higher than those over the Rockall Plateau (Figure 11a), thus suggesting a gradient opposed to N-S flow. Compared to the Present, the MOW was ^{13}C enriched by up to >0.4‰ that is, extremely nutrient depleted (Figure 12b). This depletion, however, is no direct measure for the flux rate of the outflow [Zahn et al., 1987].

A comparison of Figures 11a and 12a and of Figures 13a and 13b, shows a number of interesting $\delta^{13}C$ anomalies, revealing the following differences in deepwater oceanography between the early and the late LGM: (1) The source area of ^{13}C-enriched NADW shifted slightly from the northwestern corner of the Atlantic, off southeast Greenland, to the east in the direction of Rockall Plateau. This shift, however, did not result in any change in the overall strength of the NADW signal. (2) The marked ^{13}C depletion of the AABW incursion decreased by about 0.2‰ both in the southern Cape Basin (from -0.81 to -0.67‰) near the equator and at 50°N. Below the equator, the maximum in benthic ^{13}C reduction had already occurred at the very beginning of stage 2, near 24 ^{14}C kyr (core 16772: -0.85‰ near the onset versus -0.22‰ at the end of the LGM). This shift toward higher $\delta^{13}C$ values appears to be linked in only a few cases to a decrease in the local carbon flux and productivity (e.g., cores 16772 and 16867). (3) The extremely high ^{13}C values of the MOW near Gibraltar decreased by about 0.2‰.

In summary, these trends suggest that the extremes in ^{13}C reduction or enrichment of the various glacial water masses occurred during the early LGM and diminished toward its end.

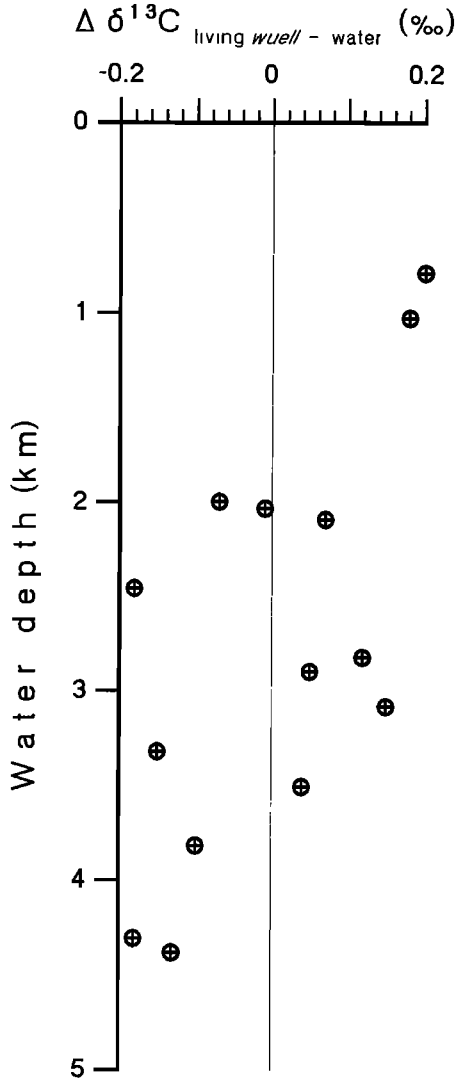

Figure 8. $\delta^{13}C$ anomalies between "living" (bengal rose stained) specimens of *C. wuellerstorfi* [Ganssen, 1983] and the ambient DIC plotted versus water depth.

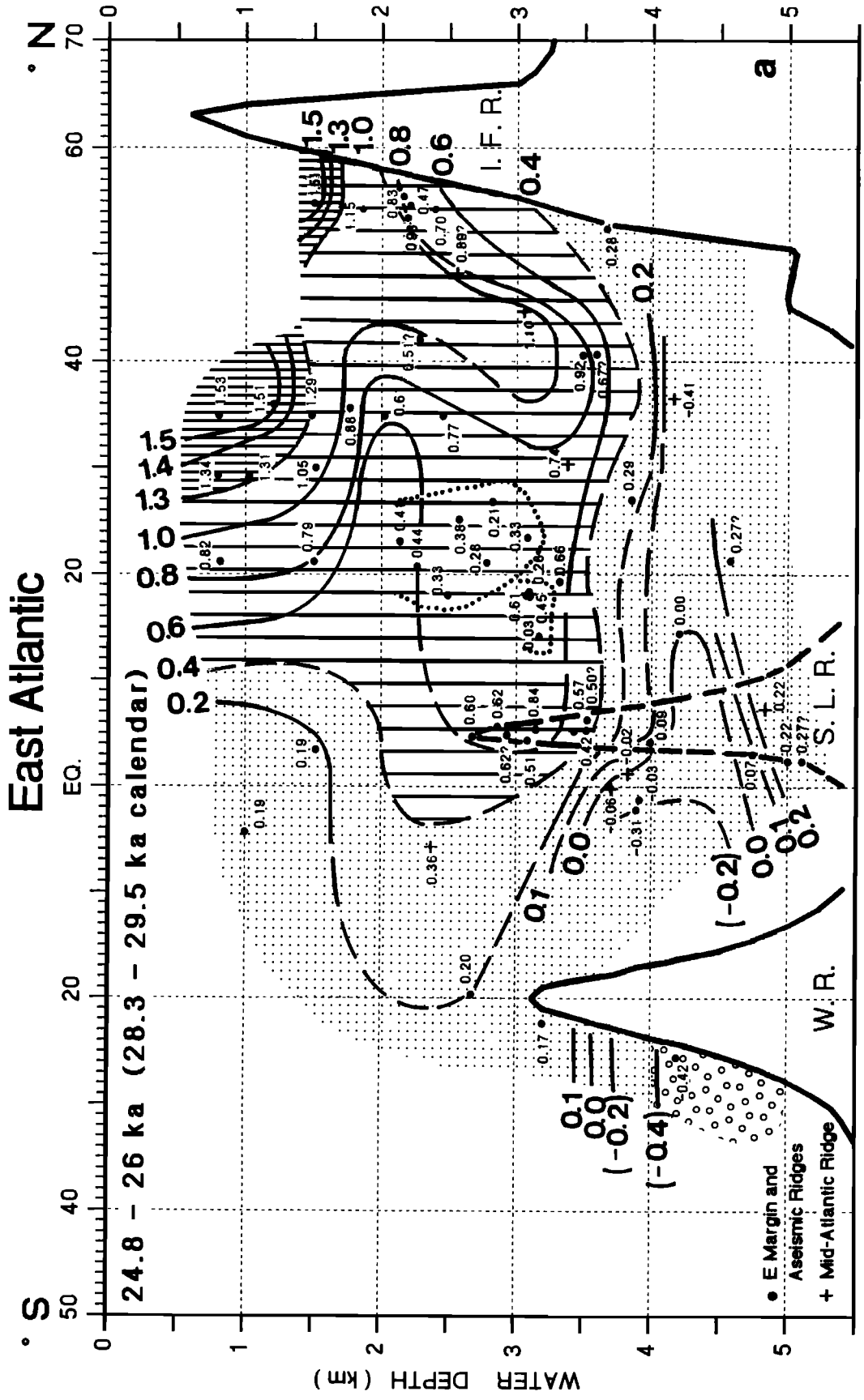

Figure 9. Benthic $\delta^{13}C$ profiles across the east Atlantic; 24,800-26,000 ^{14}C years = 28,300-29,500 calendar years ago. (a) N-S transect; (b) N-S transect of benthic $\delta^{13}C$ anomalies 24,800-26,000 ^{14}C years B.P. versus present (difference between data of Figures 9a and 6a). For abbreviations of locations see Figure 2.

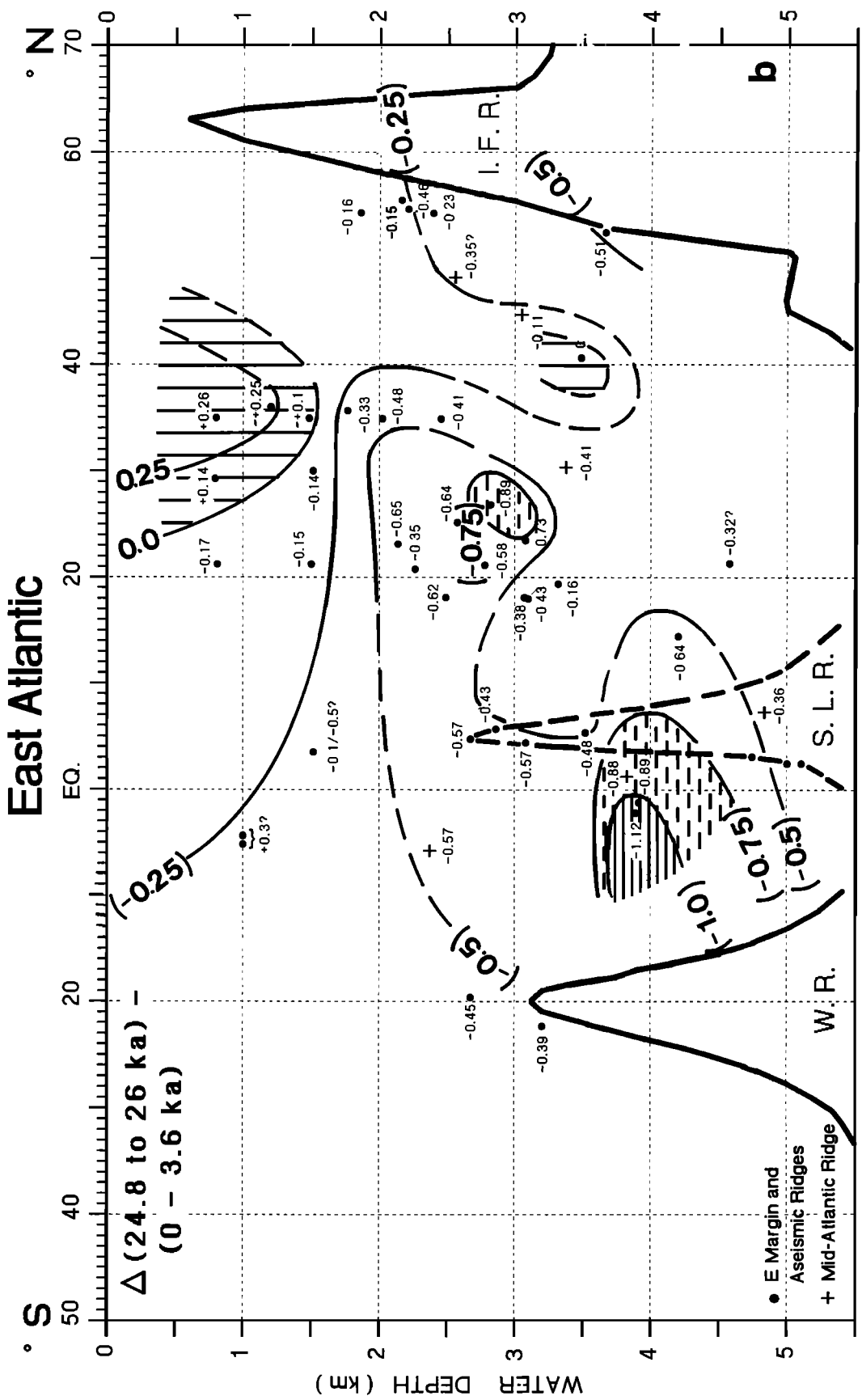
East Atlantic
° S
° N
EQ.
WATER DEPTH (km)
Δ (24.8 to 26 ka) – (0 – 3.6 ka)
b
I. F. R.
S. L. R.
W. R.
• E Margin and Aseismic Ridges
+ Mid-Atlantic Ridge

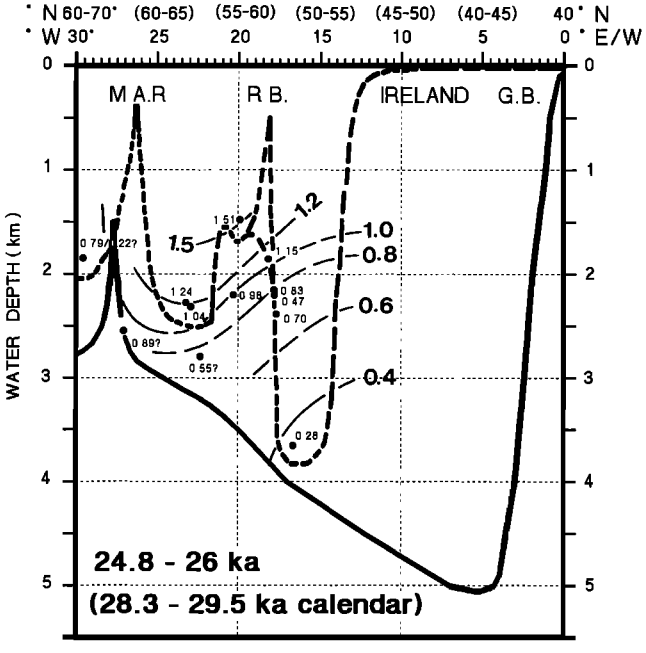

Figure 10. Benthic $\delta^{13}C$ profile running NW-SE across the North Atlantic; 24,800-26,000 ^{14}C years = 28,300-29,500 calendar years B.P. For abbreviations of locations see Figure 2.

5.5. The $\delta^{13}C$ record of East Atlantic Water Masses During Glacial Termination IA: Response to a Meltwater Spike 13.4-13.6 ^{14}C kyr B.P. (= 16.9-17.1 Cal kyr)

In spite of the difficulties in many cores of resolving this short time interval with the necessary stratigraphic resolution, Figures 4, 14, and 15 reveal various $\delta^{13}C$ features that are coherent and that clearly illustrate the exceptional deepwater regime about 13,500 ^{14}C years (17,000 cal years) ago, when both the western and northern North Atlantic were covered by meltwater lids originating from the Barents shelf and North America [Weinelt et al., 1991; Keigwin et al., 1991; Sarnthein et al., 1992; Bond et al., 1992].

Below 1600-2000 m, the $\delta^{13}C$ values in the east Atlantic were uniformly low at this time, constrained to a range of 0.40 to -0.28‰. The $\delta^{13}C$ value was as low as 0.63‰ even in core 17048, a key site on the Rockall Plateau for recording the formation of intermediate and deep water in the North Atlantic (Figures 14a and 15) (1860 m, 55°N). As compared to the end of the LGM, the $\delta^{13}C$ values were reduced by 0.35-0.6‰ in the most significant $\delta^{13}C$ records from the Rockall Plateau, the Moroccan continental margin, and the Mid-Atlantic Ridge (sites 15672, 17055, CHN 82-50-20, and SU 92-21), that is, at sites where the impact of local high carbon fluxes on $\delta^{13}C$ values was low. Hence we conclude that no more ventilated deep and intermediate waters spread from the North Atlantic to the south at that time, in contrast to the patterns of the preceding LGM. It is likely, however, that a poorly ventilated upper deep water flowed in from the south (some 0.15 and 0.3‰ contours between 2500 and 4000 m are weakly substantiated, because the local impact of paleoproductivity on the various $\delta^{13}C$ records is little known during this short time interval).

At this time, the $\delta^{13}C$ values below 4000 m, in the depth range of AABW, hardly differed from the LGM values. Exceptions to this are some extremely low $\delta^{13}C$ values in the Cape Basin (-0.81‰) and northeast of the Vema FZ in the abyssal Gambia and Canary basins (Figure 14a), and furthermore in a high-resolution record from the deep western basin of the North Atlantic (-0.78‰ in core EN 120-1 from Boyle and Keigwin [1985] with stratigraphy modified after our guidelines). In summary, it appears that the ^{13}C reduction and advection of AABW further increased below 4000-4500 m but decreased between 3500 and 4000 m after the LGM.

In contrast to the general $\delta^{13}C$ reduction below 1600 m depth, the $\delta^{13}C$ values within the top 1600 m were conspicuously high, reaching 1.0-1.35‰ near Gibraltar at 35°N (Figure 14a). These high values indicate an ongoing advection of MOW, possibly somewhat weaker than during the LGM. This suggests that the great circulation changes further below in the deep Atlantic occurred independently of the MOW advection.

In summary, the total east Atlantic between 1800 and 4500 m showed a fairly uniform $\delta^{13}C$ reduction by 0.75-1.00‰ as compared to today (Figure 14b), which we interpret as a response to the great meltwater incursion from the Barents Shelf that culminated about 13,500 ^{14}C years ago [Sarnthein et al.,1992] (first postulated by Berger [1977]). Extreme $\delta^{13}C$ reductions reached -0.85 to -1.15‰. In part, they reflect the chemistry of the water mass, in part an enhanced local carbon flux.

This striking deglacial minimum in Atlantic ventilation ended rapidly, as early as 12,700-13,200 ^{14}C years ago, as demonstrated by the first pronounced $\delta^{13}C$ increase in high-resolution isotope records (e.g., in cores 13289, 17055, 658, and RC 11-83) (Figures 3 and 4) that marks the start of postglacial NADW formation. A second increase in $\delta^{13}C$ values ended about 12,500 ^{14}C years ago (Figures 3 and 4), just prior to the great meltwater pulse described by Fairbanks [1989].

5.6. Reconstruction of East Atlantic Water Masses During the Younger Dryas: 10.35-10.8 ^{14}C kyr B.P. (= 12.3-12.8 Cal kyr)

Based on a comparison between the $\delta^{13}C$ distribution patterns of Figures 4, 16a, and 6a, and Figures 17 and 7, the late Holocene-style deepwater circulation and its intensity were established almost completely before and during most of the Younger Dryas cooling phase. The NADW flow was strongly developed with high $\delta^{13}C$ values of up to 0.9‰. It spread north-south between 2300 and 3700-4000 m depth from the Norwegian-Greenland Sea, passing close to Rockall Plateau and down to the equator. The boundary between NADW and AABW (slightly more distinct than in the Holocene) lay below 4000 m depth near the equator, which is about the same depth as today and 500 m deeper than during the LGM (Figures 11a and 12a). The west Atlantic basin off southeast Greenland was already as ^{13}C depleted as during the Holocene (Figure 17), which excludes any glacial-style deepwater formation in this region. Finally, the $\delta^{13}C$ values of the MOW were as high as in the late Holocene.

Outside the MOW source region, the intermediate water had $\delta^{13}C$ values about 0.15-0.30‰ lower than during the present. This applies to most parts of the eastern Atlantic, except for a

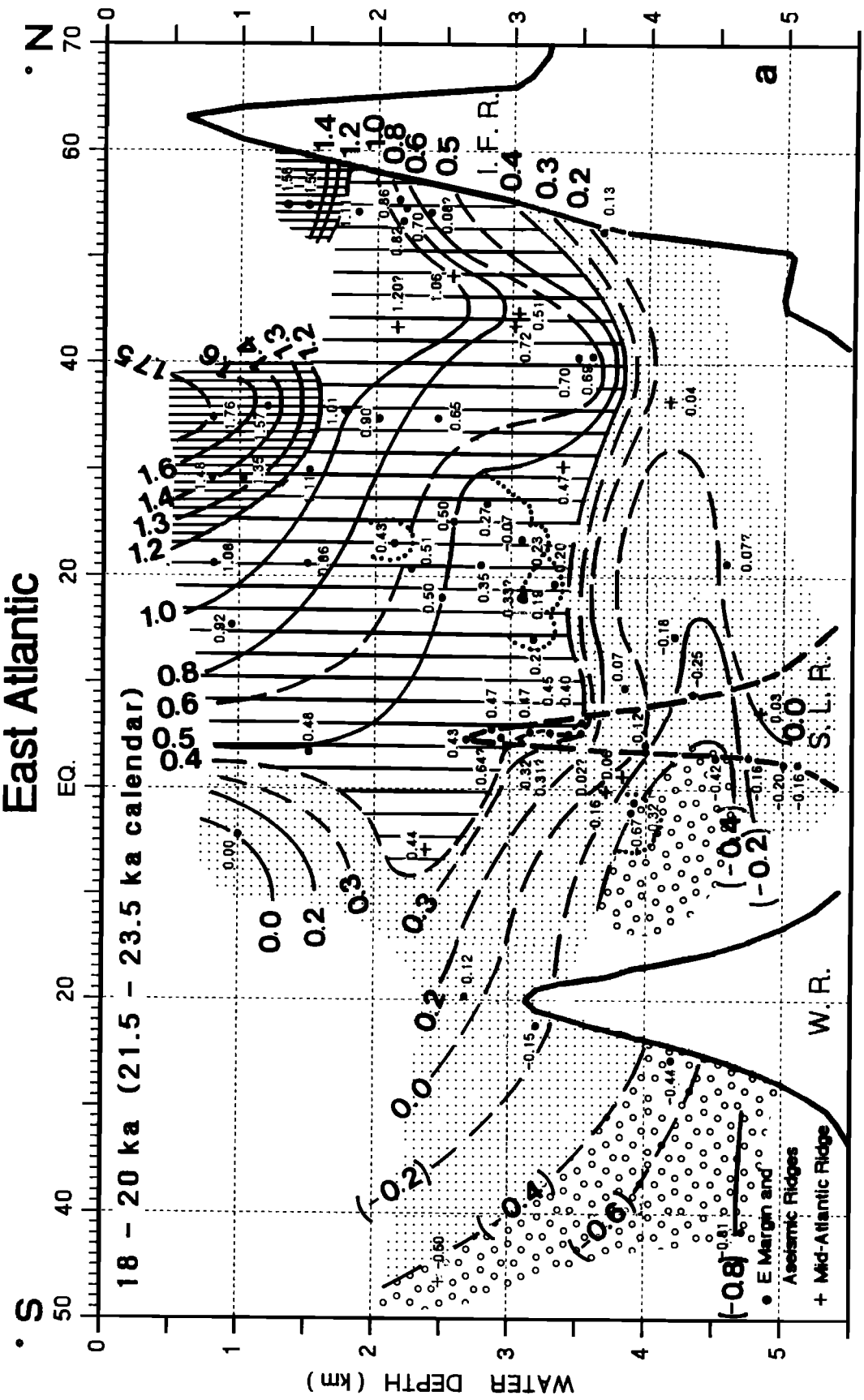

Figure 11. Benthic $\delta^{13}C$ profiles across the East Atlantic; 18,000-20,000 ^{14}C years = 21,500 -23,500 calendar years ago. (a) N-S transect; (b) N-S transect of benthic $\delta^{13}C$ anomalies 18,000-20,000 ^{14}C years BP versus present (difference between data of Figures 11a and 6a). For abbreviations of locations see Figure 2.

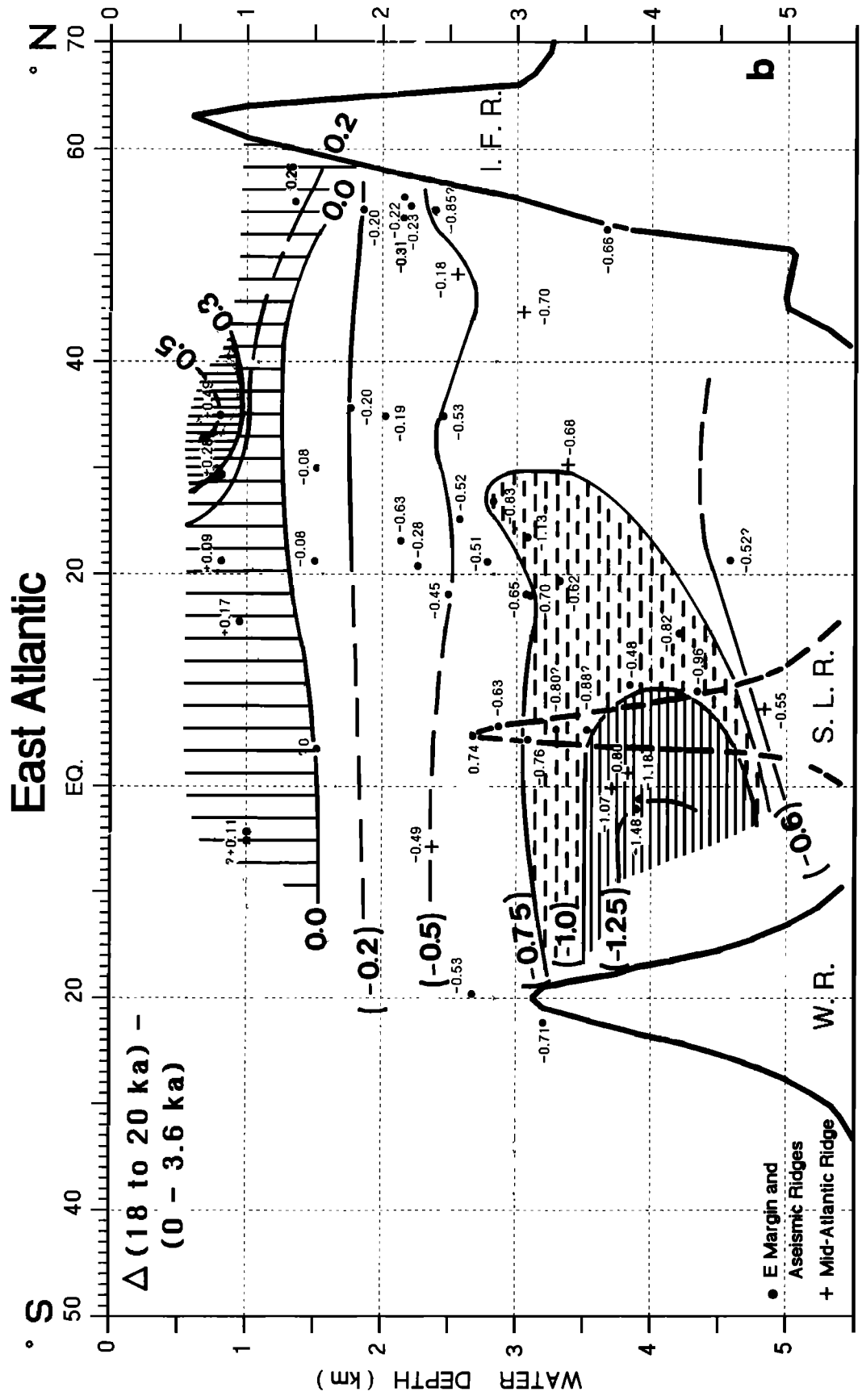
East Atlantic
° S
° N
EQ.
WATER DEPTH (km)
Δ (18 to 20 ka) – (0 – 3.6 ka)
I. F. R.
S. L. R.
W. R.
b
• E Margin and Aseismic Ridges
+ Mid-Atlantic Ridge

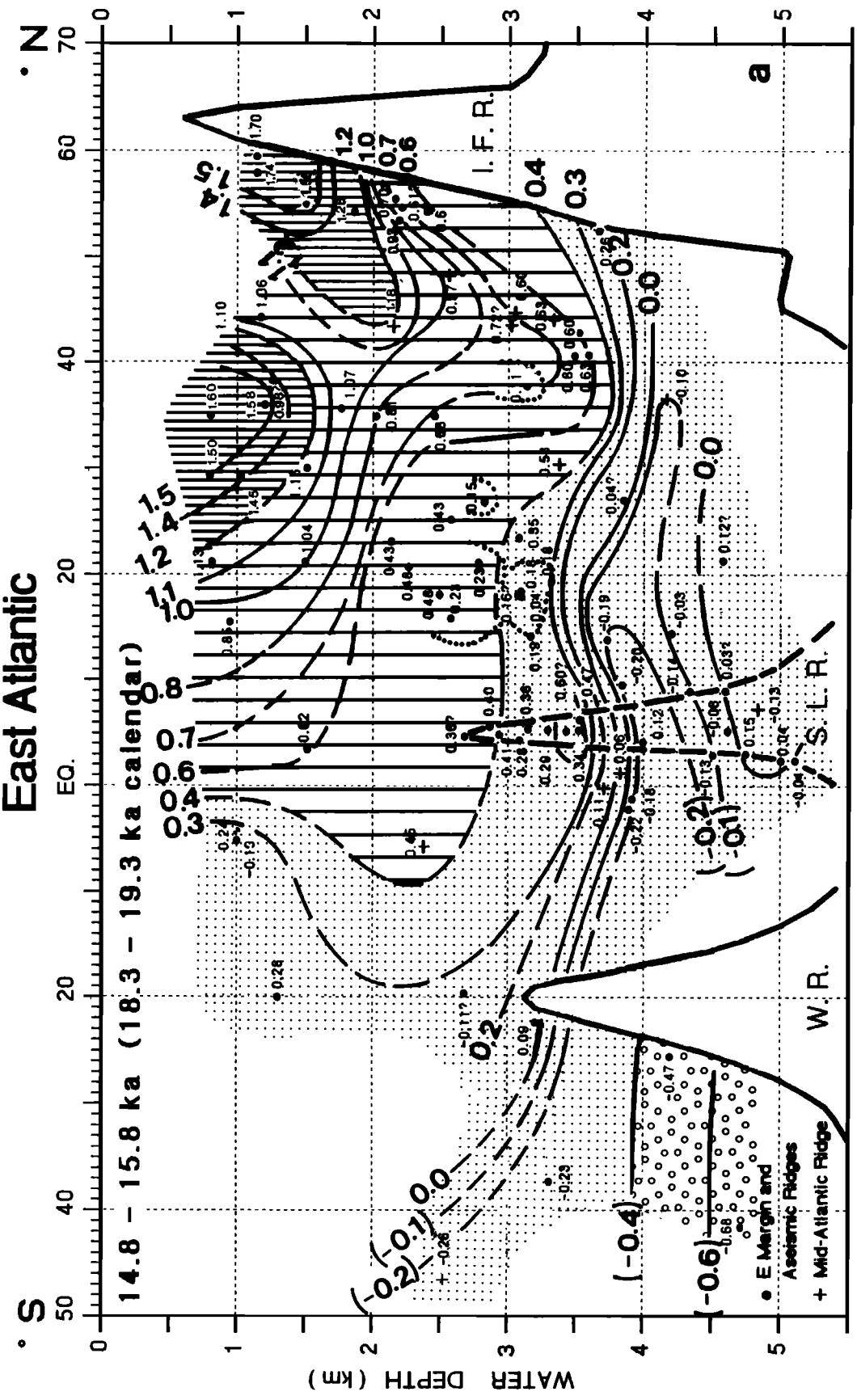

Figure 12. Benthic $\delta^{13}C$ profiles across the east Atlantic; 14,800-15,800 ^{14}C years = 18,300-19,300 calendar years ago. (a) N-S transect; (b) N-S transect of benthic $\delta^{13}C$ anomalies 14,800-15,800 ^{14}C years B.P. versus present (difference between data in Figures 12a and 6a). For abbreviations of locations see Figure 2.

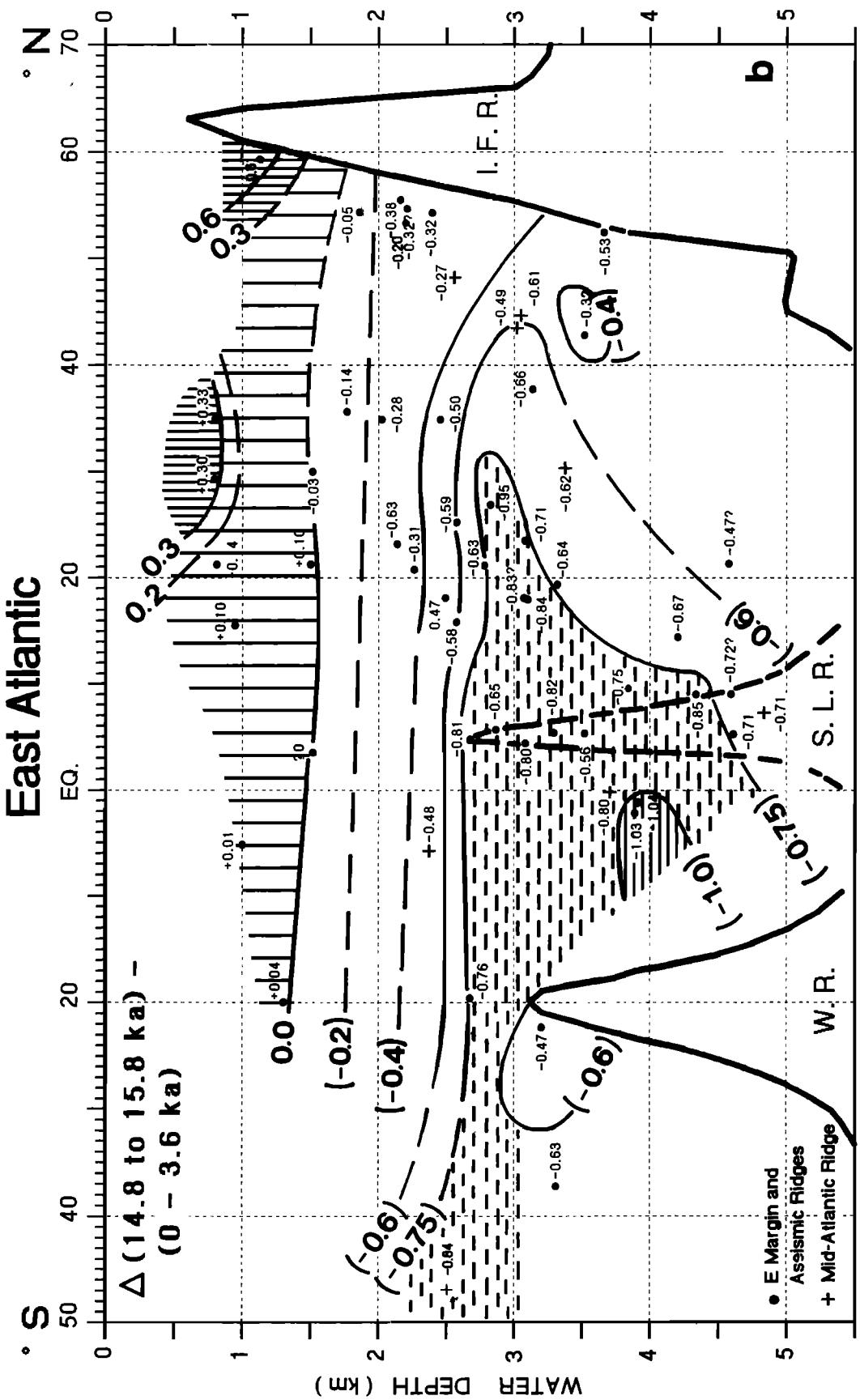
East Atlantic
Δ (14.8 to 15.8 ka) – (0 – 3.6 ka)
I. F. R.
S. L. R.
W. R.
b
• E Margin and Aseismic Ridges
+ Mid-Atlantic Ridge
WATER DEPTH (km)
° S
EQ.
° N

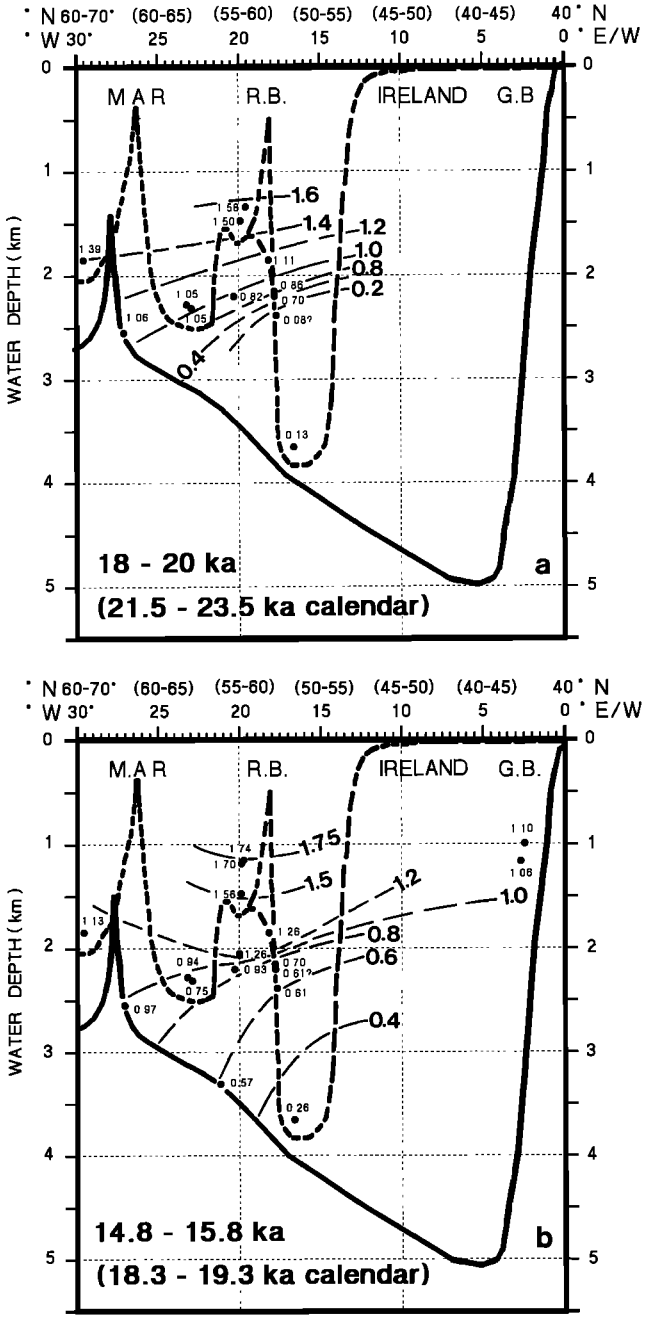

Figure 13. Benthic $\delta^{13}C$ profiles running NW-SE across the North Atlantic. (a) 18,000-20,000 ^{14}C years = 21,500-23,500 calendar years B.P. (b) 14,800-15,800 ^{14}C years = 18,300-19,300 calendar years B.P. For abbreviations of locations see Figure 2.

few particularly low $\delta^{13}C$ values at 20°-40°N (Figure 16b). At these sites either the local productivity-induced carbon flux then was particularly high or the stratigraphic resolution of the record was insufficient to fully separate the Younger Dryas from a subsequent $\delta^{13}C$ minimum.

This benthic $\delta^{13}C$ minimum covered a very short time span near the end and immediately subsequent to the Younger Dryas, about 10,200-9,500 ^{14}C years BP. It was as extreme as that during Termination IA about 13,500 ^{14}C years ago, but was only recorded in a small number of high-resolution sediment records (e.g., in cores 12310, 12347, 12379, 13289 (?), 16402, 16408, 16458, 17045, ODP 658, and V23-81) (see Figure 3 and in West Basin core EN 120-1 [Boyle & Keigwin, 1985]). Since the time span was as short as few 100 years and difficult to date because of a major ^{14}C "plateau" [Becker et al., 1991], the $\delta^{13}C$ minimum remained unresolved in most sediment cores and cannot be reconstructed as a time slice. Note that no such minimum occurred in our $\delta^{13}C$ records prior to the Younger Dryas, which was rather preceded by a $\delta^{13}C$ increase.

5.7. Holocene Variability of East Atlantic Water Masses: 8.35 - 9.1 ^{14}C kyr B.P. (9.25-9.8 Cal kyr), 6.1-7.2 ^{14}C kyr B.P. (7-8 Cal kyr), and Present

After the onset of Holocene peak interglacial conditions, the benthic $\delta^{13}C$ patterns (Figures 18-20) differed only little from the present, that is, from the average of the last 4000 years (Figures 6 and 7). Similar to the present, the main stream of NADW from the Norwegian-Greenland Sea passed west of the Rockall Plateau to the Mid-Atlantic Ridge (along sites 552 and 17055, 1.2-1.3‰ $\delta^{13}C$) (Figure 20). Further northwest, site V28-14 lay in poorly ventilated intermediate water (0.32-0.69‰ $\delta^{13}C$) between the Mid-Atlantic Ridge and Greenland south of the Denmark Strait, distal from deepwater formation and advection.

The early Holocene chemistry of the NADW (Figure 18) matched closely the late Holocene pattern (Figure 6a), perhaps more than the pattern of the early mid-Holocene (Figure 19). The base of the early Holocene NADW (0.8-0.9‰) lay a few 100 m deeper, suggesting that the NADW advection was intensive. In contrast, the $\delta^{13}C$ signal of the AABW was less negative 8350-9100 ^{14}C years ago than in the early mid-Holocene, that is, the abyssal circulation increased slightly about 6500 ^{14}C years ago. The marked early Holocene $\delta^{13}C$ maximum (0.85-0.9‰) in the deep Sierra Leone Basin below 4500 m clearly exceeded the values of the present. An extended $\delta^{13}C$ minimum near 4300-4600 m (0.25-0.6‰) remains unexplained.

Near 7000 ^{14}C years B.P., the $\delta^{13}C$ values in the central NADW were slightly reduced (by 0.1-0.2 ‰ versus the present) over a large region extending from the Azores down to the equator near 2000-3000 m depth (Figure 19b). The $\delta^{13}C$ signal of the lower part of the NADW then was clearly confined to the west of Rockall Plateau in the North Atlantic (Figure 20b) and remained basically unchanged. The ventilation and possibly the advection of middle and upper NADW were thus somewhat reduced in the middle Holocene, but the lower NADW had $\delta^{13}C$ values such as in the early Holocene and today. Further below, at more than 4000 m depth, the middle Holocene $\delta^{13}C$ values in the bottom water were lowered by more than 0.1-0.2‰ versus the present, more than in the early Holocene. This pattern suggests that the circulation of AABW then was slightly enhanced, possibly a response to the weakened NADW flux (Figure 19a and 19b). Possibly, these intrawarm stage variations in deepwater ventilation were a joint result of variations in northern high-latitude precipitation [Weaver et al., 1991], as discussed in section 6.3.

In contrast to the deep water, the $\delta^{13}C$ values of the interme-

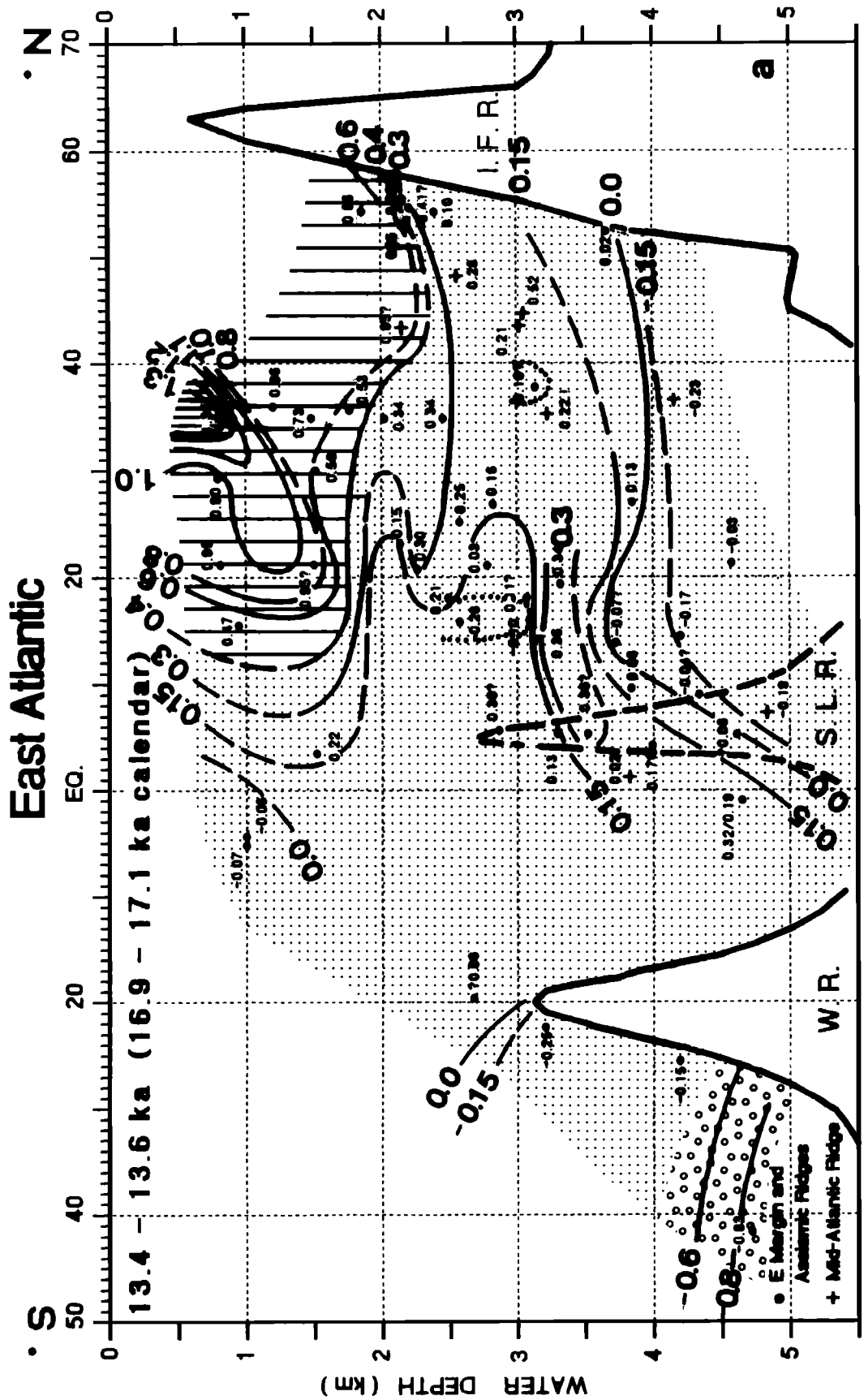

Figure 14. Benthic $\delta^{13}C$ profiles across the east Atlantic; 13,400-13,600 ^{14}C years = 16,900-17,100 calendar years ago. (a) N-S transect; (b) N-S transect of benthic $\delta^{13}C$ anomalies 13,400-13,600 ^{14}C years B.P. versus present (difference between data of Figures 14a and 6a). For abbreviations of locations see Figure 2.

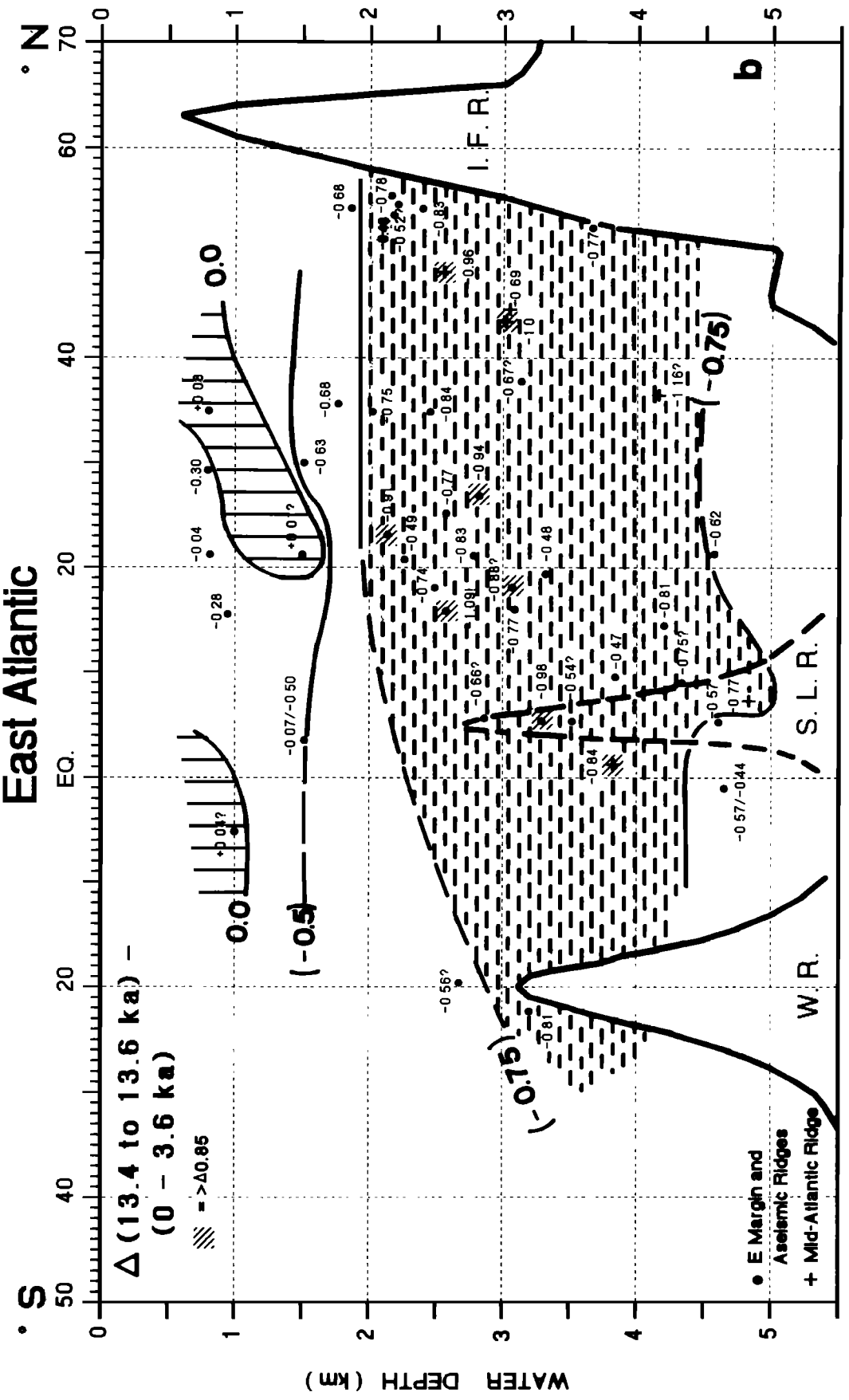
East Atlantic
°S
EQ.
°N
WATER DEPTH (km)
Δ (13.4 to 13.6 ka) – (0 – 3.6 ka)
= >Δ0.85
0.0
(-0.5)
(-0.75)
I. F. R.
S. L. R.
W. R.
b
• E Margin and Aseismic Ridges
+ Mid-Atlantic Ridge

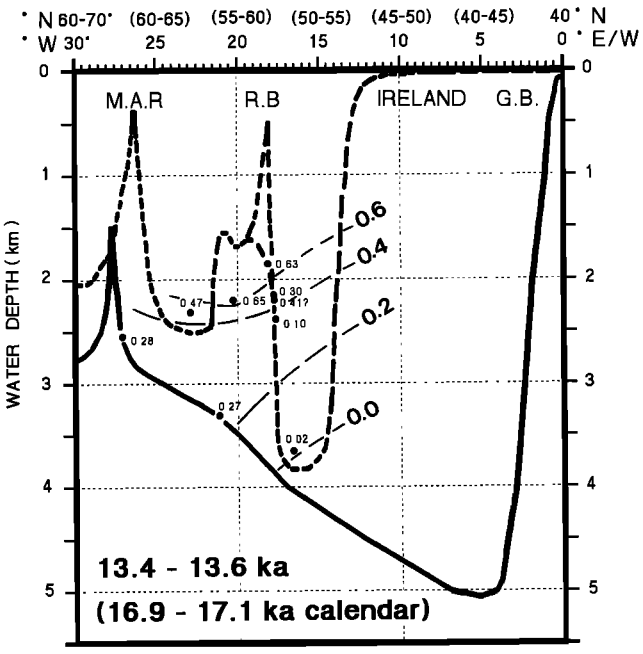

Figure 15. Benthic $\delta^{13}C$ profile running NW-SE across the North Atlantic 13,400-13,600 ^{14}C years = 16,900-17,100 calendar years ago. For abbreviations of locations see Figure 2.

diate water at 1000-1800 m depth clearly reached a minimum during the early Holocene. At the position of the MOW, west of Gibraltar they were lowered by up to 0.4‰ versus the present (and by up to 0.75‰ versus the LGM). Furthermore, the local productivity-controlled $\delta^{13}C$ minima offshore tropical African rivers reached extremes during this time. Both patterns are in harmony with abundant evidence for pluvial conditions in North Africa during the earliest Holocene [Sarnthein et al., 1982; Rossignol-Strick et al., 1982; Hooghiemstra, 1989]. The strong monsoonal precipitation triggered both an increased discharge of fluvial nutrients to the coast of tropical Africa and a reduction in Mediterranean deepwater formation and outflow.

The early middle Holocene $\delta^{13}C$ values of MOW at 1000-1800 m increased slightly relative to the early Holocene, but were still lower than today. This $\delta^{13}C$ increase paralleled the continental sediment record of increased African aridity during this time [Fontes and Gasse, 1991; Sarnthein, 1978; Sarnthein et al., 1982], which led to enhanced deepwater formation in the Mediterranean.

6. Discussion

6.1. Significance of Epibenthic $\delta^{13}C$ Records for Reconstructing Large-Scale and Mesoscale Features of Deepwater Paleoceanography

The main thrust of this paper is to reconstruct past changes in the thermohaline circulation of the Atlantic, as recorded by proxies for variations in ocean chemistry. Such reconstructions may lead to a better understanding of past changes in both climate and atmospheric chemistry. Moreover, they provide a basis for testing ocean general circulation models which simulate and attempt to predict the physical processes of climatic change, such as, the response to increasing atmospheric carbon dioxide.

Our reconstructions are based on benthic $\delta^{13}C$ records, widely regarded as "established" tracers of ocean paleochemistry [Duplessy, 1982; Broecker and Peng, 1982; Duplessy et al., 1984, 1988; Zahn et al., 1986, 1987, 1991; Curry et al., 1988]. Three problems, however, that may strongly affect the significance of this reconstruction technique need to be discussed: (1) Discrepancies that were found between the two main proxies of ocean paleochemistry, $\delta^{13}C$ and Cd/Ca [Charles and Fairbanks, 1990; Boyle, 1992; Zahn et al., 1991], may imply that these were variations in high-latitude gas exchange between ocean and atmosphere, altering the preformed $\delta^{13}C$ distributions of downwelled surface water. (2) During the LGM, the global average decrease in benthic foraminiferal $\delta^{13}C$ of about 0.3-0.35‰ may have been induced by a substantial transfer of organic carbon from the continents to the ocean. (3) The technique of projecting benthic $\delta^{13}C$ values from the margin onto a transect across the central basin may lead to spurious results, missing the actual tracks of circulation.

With regard to problem (1), possible changes in gas exchange, our basin-wide data permit us to precisely trace past variations in the primary $\delta^{13}C$ composition of DIC in North Atlantic surface waters at the time of convection. Today, the freshly downwelled surface waters in the Iceland and Greenland Seas show $\delta^{13}C$ values of 1.7-1.8‰ [Weinelt, 1993]. After the NADW has passed through the Färöer Channel, the values are diluted to 1.25-1.3‰ (Figure 5d). These $\delta^{13}C$ values persisted as long as the Norwegian overflow through the Färöe Channel was active, that is, in the wake of stage 3.1, during the Younger Dryas, and in the Holocene (Figures 10, 17, and 20). During the LGM, high $\delta^{13}C$ values also persisted directly below the convergence zone. However, it then occurred west of Rockall Plateau (Figures 11, 12, and 13). These glacial values south of Iceland reached a maximum of 1.6-1.74‰ similar to those of the modern Norwegian-Greenland Seas. East of Greenland, maximum $\delta^{13}C$ values amounted to 1.38-1.45‰ during the early LGM (Figure 13a).

Based on ^{14}C results in the Pacific [Shackleton et al., 1988], the ventilation of the LGM deep ocean may have decreased because of widespread perennial ice coverage in the North Atlantic and the Norwegian-Greenland Seas [CLIMAP, 1981] that reduced the rate of deepwater production. From our evidence, however, we conclude that in the northern North Atlantic itself, no noticeable change took place in preformed $\delta^{13}C$ (and, possibly, in the local gas exchange) of the downwelled surface waters over the last 30,000 years. Based on the work of Duplessy et al. [1991], the downwelled waters during LGM mostly originated from a sort of rudimentary North Atlantic drift, then running to the north in the central Atlantic. During this time, therefore, $\delta^{13}C$ variations in the Atlantic deep and intermediate waters should form a reliable record of the progressive increase in DIC as deep-ocean water flowed away from the convection sites, because of (1) the continued input and oxidation of ^{13}C-depleted marine organic carbon and (2) the lateral and vertical mixing of different oceanic water masses more strongly enriched in DIC. In contrast, the history of preformed $\delta^{13}C$ is as yet unknown for water masses

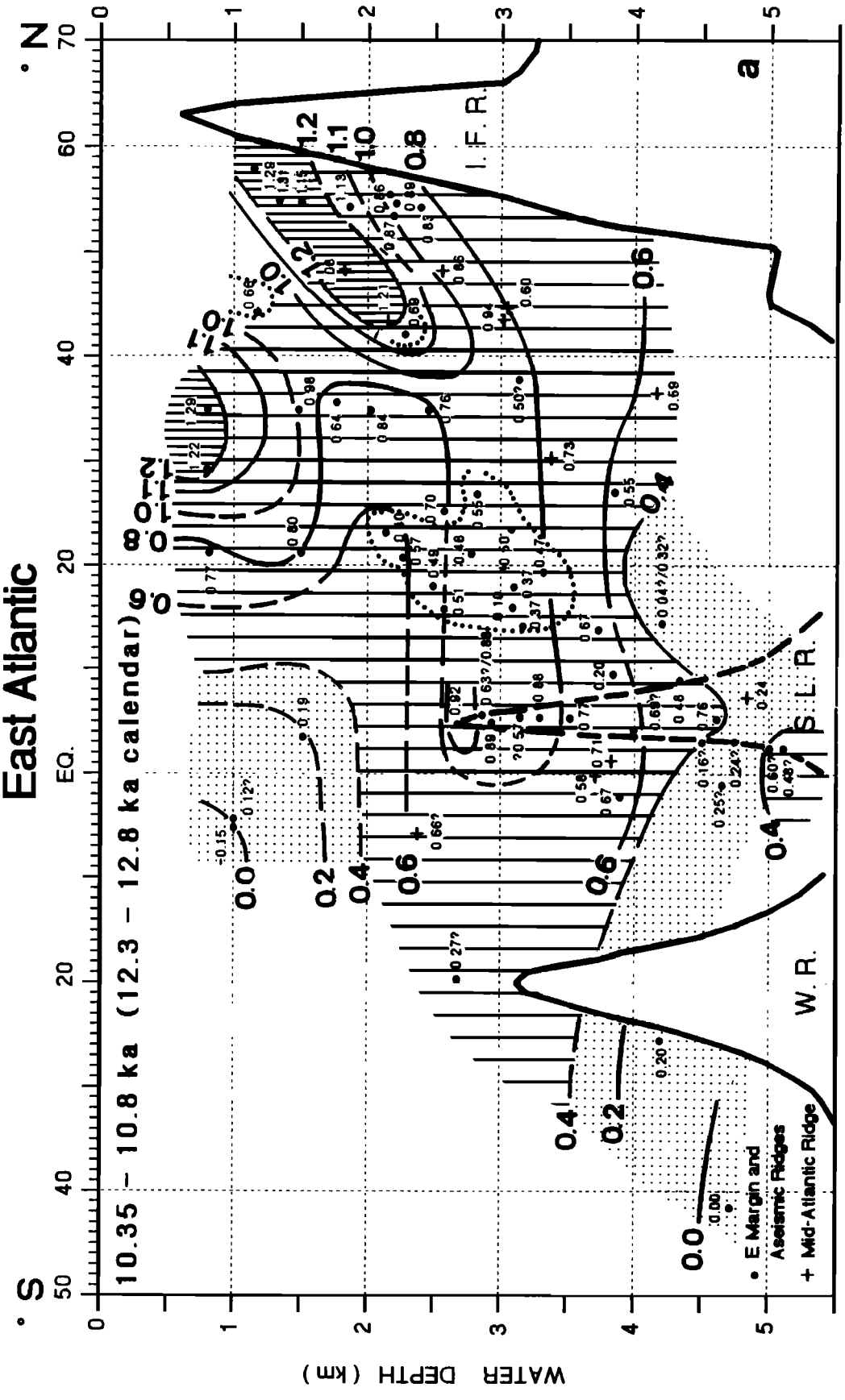

Figure 16. Benthic $\delta^{13}C$ profiles across the east Atlantic; 10,400-10,800 ^{14}C years = 12,300-12,800 calendar years B.P. (a) N-S transect; (b) N-S transect of benthic $\delta^{13}C$ anomalies 10,400-10,800 ^{14}C years B.P. versus present (difference between data of Figures 16a and 6a). For abbreviations of locations see Figure 2.

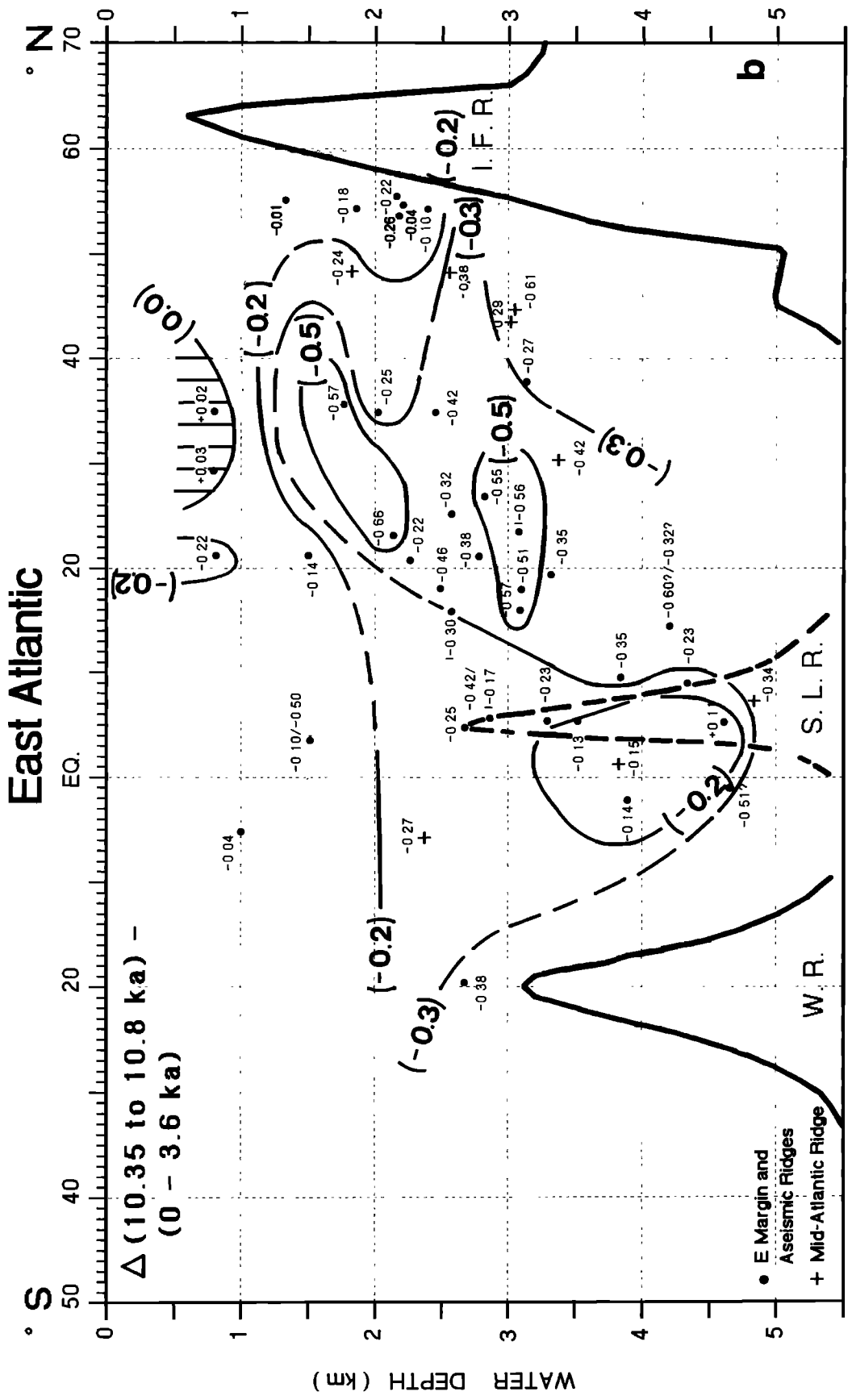
East Atlantic
Δ (10.35 to 10.8 ka) – (0 – 3.6 ka)
b
I. F. R.
S. L. R.
W. R.
EQ.
° S
° N
WATER DEPTH (km)
E Margin and Aseismic Ridges
Mid-Atlantic Ridge

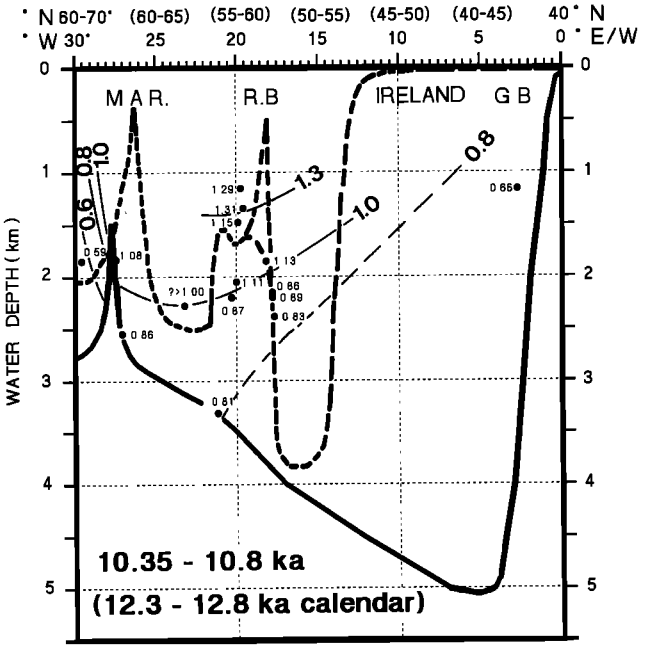

Figure 17. Benthic $\delta^{13}C$ profile running NW-SE across the North Atlantic; 10,400-10,800 ^{14}C years = 12,300-12,800 calendar years B.P. For abbreviations of locations see Figure 2.

downwelled in the southern ocean [Charles and Fairbanks, 1990].

Regarding problem (2), as proposed by Shackleton [1977], Curry et al. [1988], and Duplessy et al. [1988], the global decrease in the mean $\delta^{13}C$ content of the LGM ocean by about 0.3-0.35‰ may result from a large-scale transfer of ^{13}C-depleted carbon from the continental biosphere to the ocean during glacials. This portion of the total $\delta^{13}C$ shift, which actually is linked to continental organic carbon, should be subtracted from any oceanic $\delta^{13}C$ differences between the LGM and today (Figures 11b and 12b) prior to interpreting the $\delta^{13}C$ variations of specific water masses in the east Atlantic in terms of changes in deep-ocean circulation and the biological pump.

The magnitude of this continental carbon transfer is still highly controversial. Many factors, such as the conversion of vegetational carbon into soil carbonate, are unknown and estimates of the postglacial increase in terrestrial biomass range from zero up to 1300 gigatons (Gt) C [Prentice and Fung, 1990; Prentice and Sarnthein, 1993; Kern and Schlesinger, 1992]. Moreover, terrestrial carbon enriched in ^{12}C is characteristicaly inert and hardly dissolves in ocean water [Tissot and Welte, 1984]. Recent new insights have come from Leuenberger et al. [1992], who produced the first $\delta^{13}C$ estimates of glacial atmospheric CO_2 from air bubbles in ice cores. These values were about 0.3‰ more negative than in pre-industrial time, compared with -0.7‰ measured on paleo-C4 plant material [Marino et al. 1992]. As expected, this shift parallels the $\delta^{13}C$ difference found in the ocean but also does not explain it.

More arguments arise from comparing the high Holocene $\delta^{13}C$ values of NADW with data from stage 5.5 [Sarnthein and Tiedemann, 1990; Zahn et al., 1986], when atmospheric CO_2 was as high [Barnola et al., 1987] and land vegetation was as well developed as during the early Holocene [e.g., Hooghiemstra, 1989]. The $\delta^{13}C$ values of NADW, however, were at that time reduced by about 0.5‰. In summary, this evidence is unlikely to support a simple linkage between the general $\delta^{13}C$ shifts in the deep ocean and the transfer of continental carbon.

Other factors can be invoked to explain the mean ocean glacial-to-interglacial benthic $\delta^{13}C$ shift of 0.3‰. From the Atlantic up to the Pacific, the $\delta^{13}C$ decrease may simply reflect an increase in the overall residence time of deep water, that is, a reduced turnover rate of organic matter and nutrients during the LGM paralleled by enhanced formation of upper intermediate water. A more sluggish glacial deepwater circulation is well documented by age differences between glacial deep and surface water, which increased significantly, by about 500 years, as compared to the Holocene [Shackleton et al., 1988]. This increased residence time must have increased the alkalinity and thus the potential to absorb remineralized marine organic carbon in deepwater, sufficiently to produce the given global $\delta^{13}C$ shift by 0.32‰. Recent modeling of Ku and Luo [1992] indeed shows that circulation effects may account for as much as two thirds of the 0.32‰ shift in the Atlantic and the southern ocean. Moreover, a reduction by 0.3‰ $\delta^{13}C$ may already occur after time spans as short as several hundred years. This estimate can be derived in the Atlantic from the modern flux rates of POC, the distribution of modern deepwater ages at 3000 m depth [Broecker et al., 1988], and the present rate of deepwater flow. Based on these considerations, we decided to assess directly the glacial-to-interglacial variability in water mass chemistry from the local Atlantic $\delta^{13}C$ anomalies, irrespective of any impact of the transfer of continental carbon.

Regarding problem (3), our reconstructions of deepwater masses may suffer, provided that the age controls are correct, from the straightforward technique employed to project benthic $\delta^{13}C$ values from the ocean margins and ridges horizontally onto imaginary profiles across the central basin. This assumes a horizontal stratified water mass from east to west across the east Atlantic. Both the distribution of modern DIC-based $\delta^{13}C$ values [Duplessy, 1972] and the fact that benthic isotopic data from the eastern continental margin and the Mid-Atlantic Ridge largely match (where unbiased by local fluxes of organic carbon) indeed suggest a largely uniform horizontal water mass stratification in low and middle latitudes. This does not apply, however, to extrapolations from the eastern to the western Atlantic, where NADW is more ^{13}C-enriched (see GEOSECS data of Bainbridge [1981] and Kroopnick [1985]). North of about 40°N the east-west differences and small-scale effects become more pronounced because of enhanced Coriolis forcing. At 55°N, mesoscale patterns already dominate the distribution of deepwater masses in an east-west direction (Figures 5b, 7, 10, etc.).

Additional small-scale circulation patterns also occur near the equator where better-ventilated deep water flows from the west into the east Atlantic through the Romanche FZ (Figure 5e) and less ventilated AABW spreads through the Vema FZ. These modern features are recorded to a similar extent in most time slices of the past. For example, $\delta^{13}C$ values from the Sierra Leone Rise usually exceed the values from sites further north by up to 0.25‰ and thus depict the local advection of

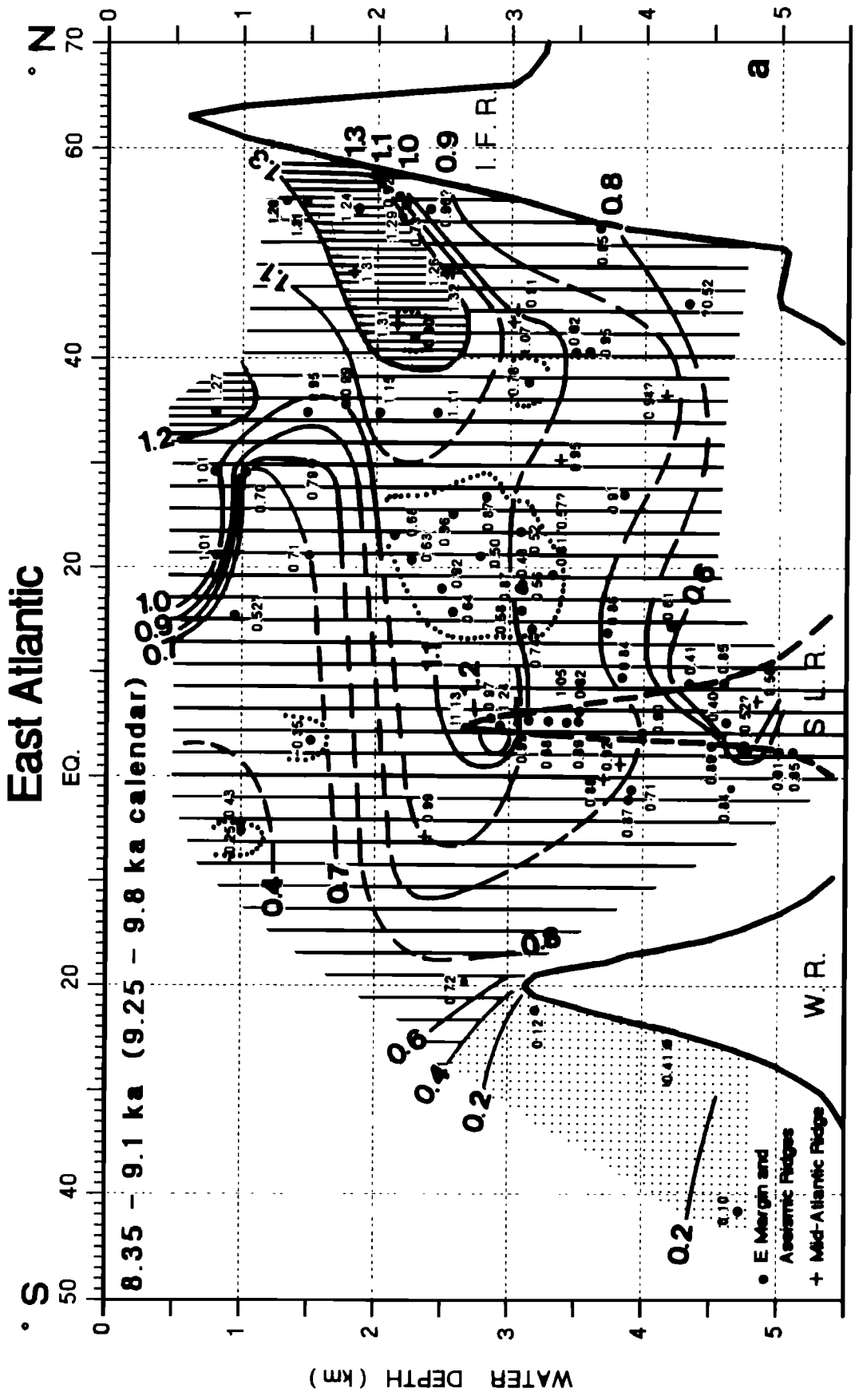

Figure 18. Benthic $\delta^{13}C$ profiles across the east Atlantic; 8350-9100 ^{14}C years = 9250-9800 calendar years ago. (a) N-S transect; (b) N-S transect of benthic $\delta^{13}C$ anomalies 8350-9100 ^{14}C years B.P. versus present (difference between data of Figures 18a and 6a). For abbreviations of locations see Figure 2.

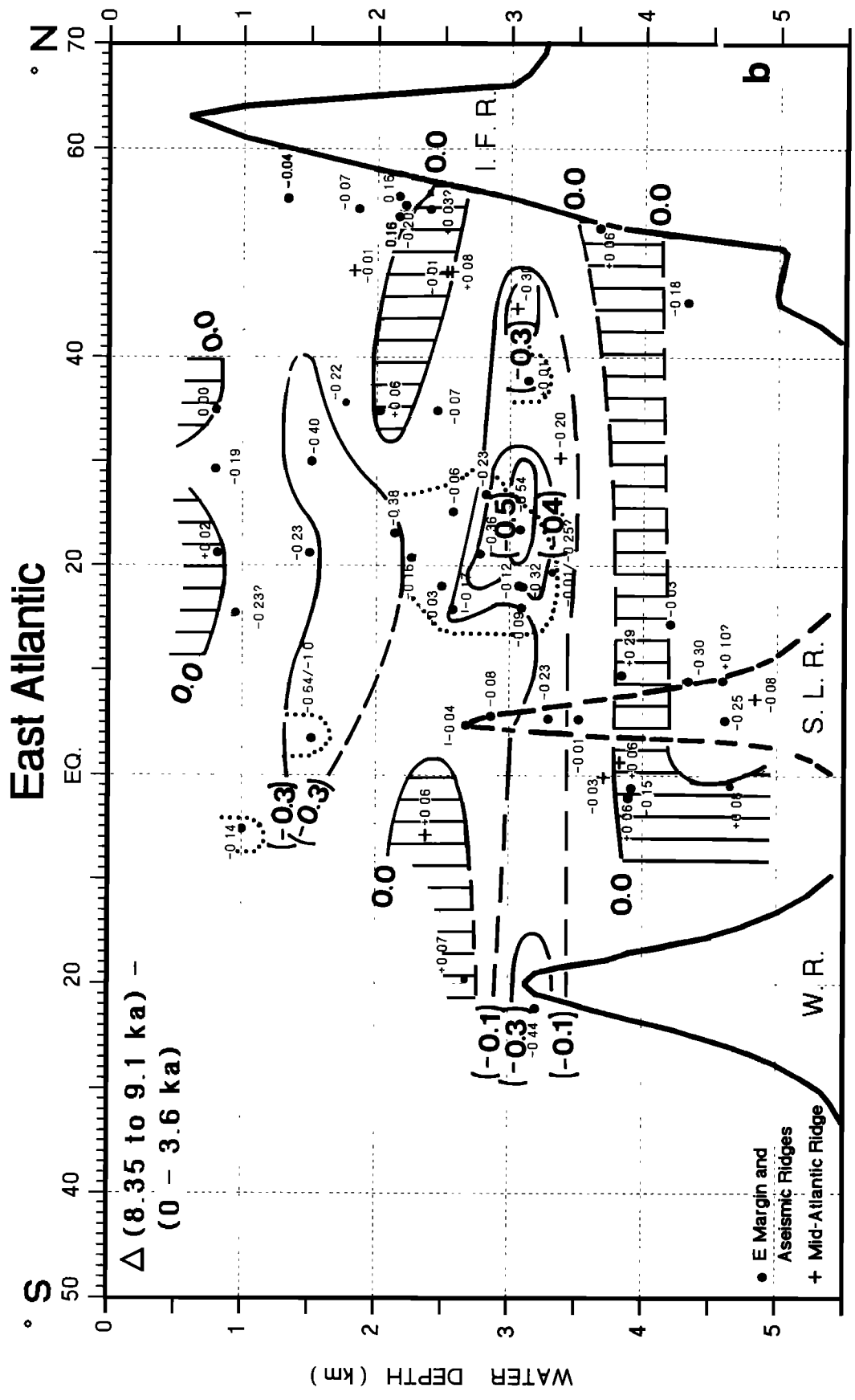
East Atlantic
Δ (8.35 to 9.1 ka) – (0 – 3.6 ka)
° S
° N
EQ.
WATER DEPTH (km)
I. F. R.
S. L. R.
W. R.
b
• E Margin and Aseismic Ridges
+ Mid-Atlantic Ridge

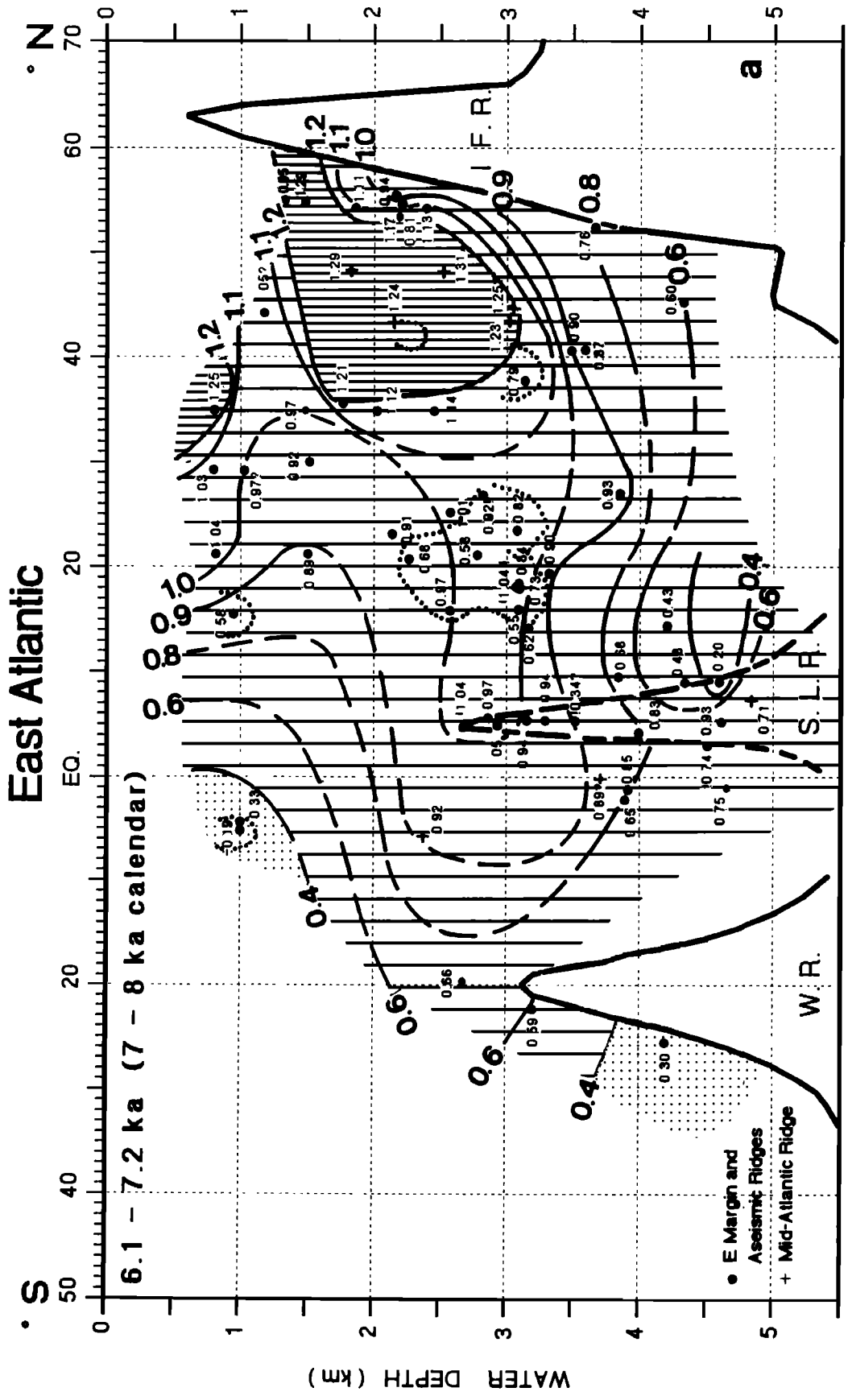

Figure 19. Benthic $\delta^{13}C$ profiles across the east Atlantic; 6100-7200 ^{14}C years = 7000-8000 calendar years ago. (a) N-S transect; (b) N-S transect of benthic $\delta^{13}C$ anomalies 6100-7200 ^{14}C years B.P. versus present (difference between data of Figures 19a and 6a). For abbreviations of locations see Figure 2.

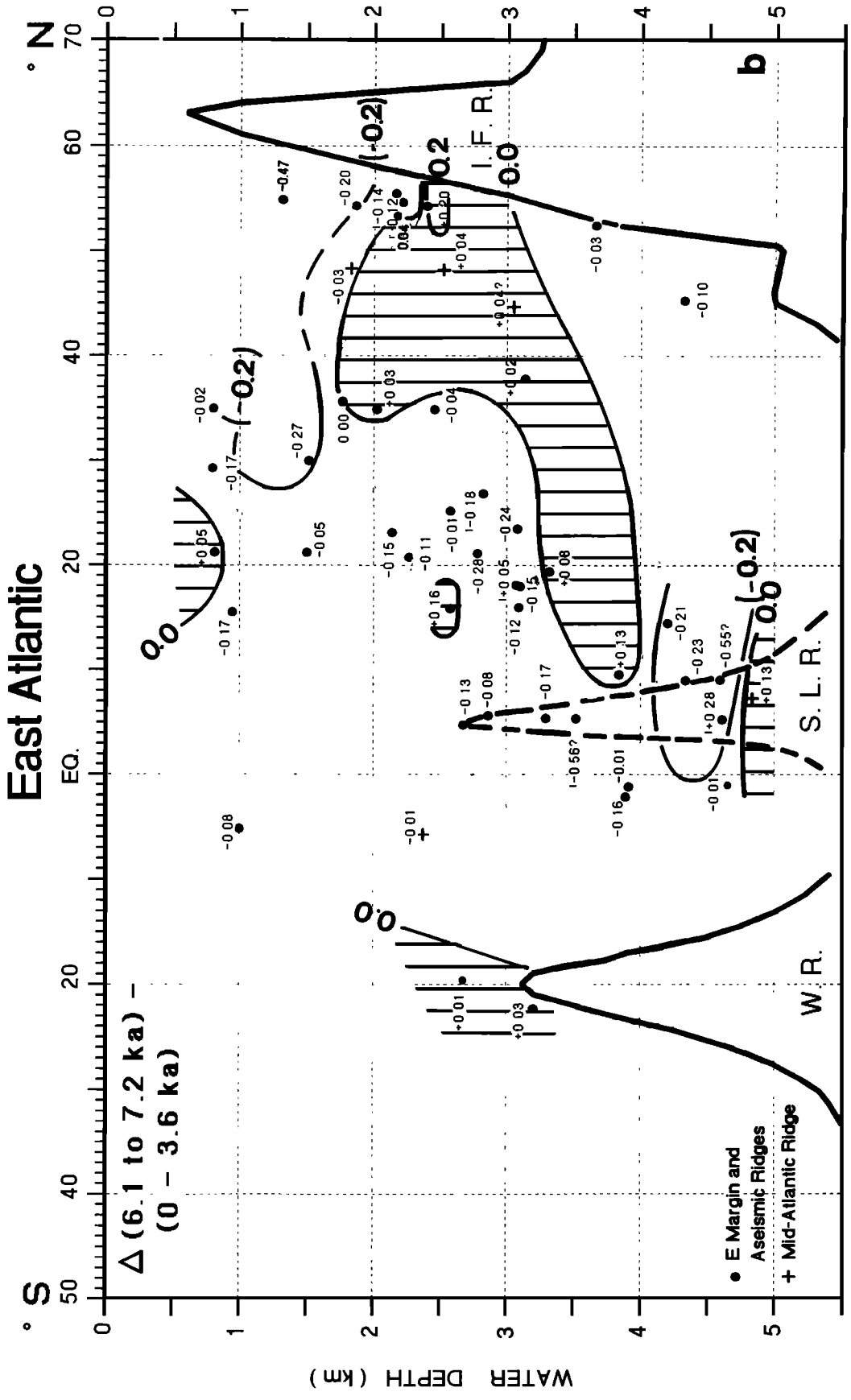
East Atlantic
° S
° N
EQ.
WATER DEPTH (km)
Δ (6.1 to 7.2 ka) – (0 – 3.6 ka)
• E Margin and Aseismic Ridges
+ Mid-Atlantic Ridge
I. F. R.
S. L. R.
W. R.
b

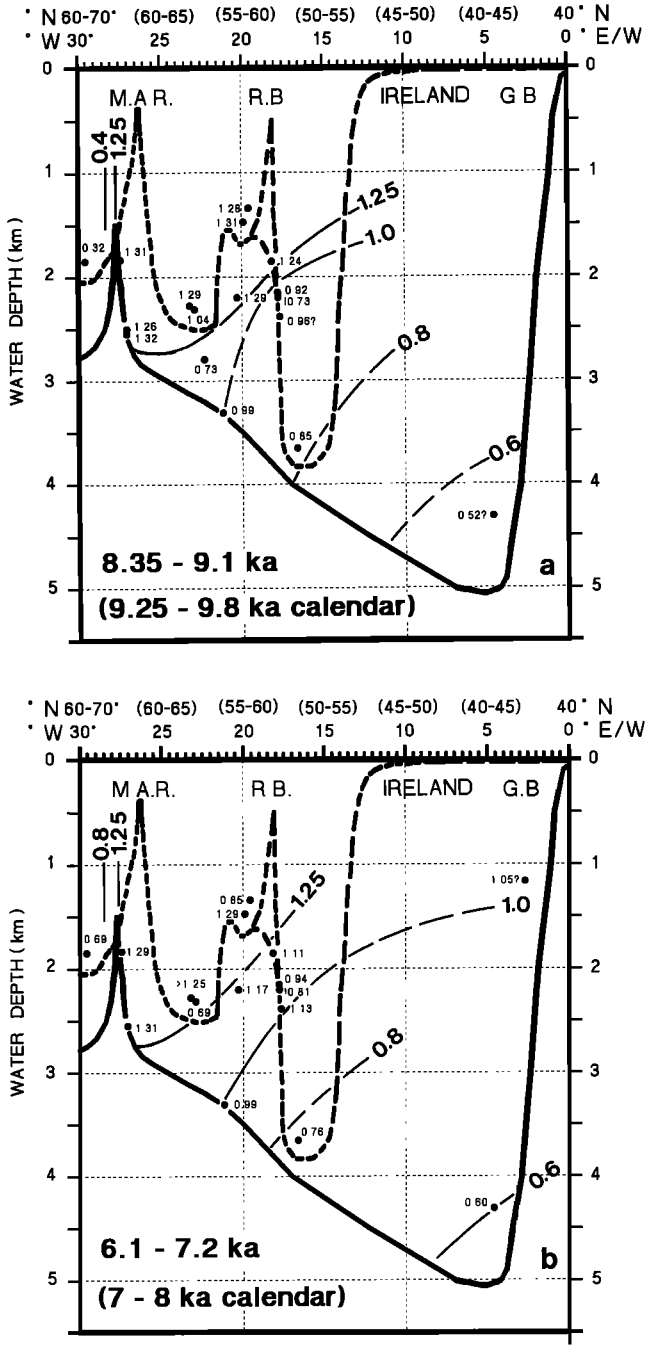

Figure 20. Benthic $\delta^{13}C$ profiles running NW-SE across the North Atlantic. (a) 8350-9100 ^{14}C years = 9250-9800 calendar years B.P. (b) 6100-7200 ^{14}C years = 7000-8000 calendar years B.P. For abbreviations of locations see Figure 2.

water masses superimposed on the basin-wide circulation features.

6.2. Modes of Atlantic Deepwater Circulation

Based on the assumptions outlined above, the paleo-$\delta^{13}C$ transects reconstructed in Figures 9-20 can be used to address the crucial issue of whether there were two or three distinct states of thermohaline deepwater circulation that can be identified over the last glacial-to-interglacial cycle. The possibility of different modes of circulation in the modern and the LGM ocean was first postulated by Stommel [1961]. Our reconstructions can also serve to test models suggesting that the LGM mode of Atlantic circulation is characterized by (1) reduced NADW flow compared to AABW flow, (2) enhanced intermediate water (IW) flux, (3) a sharp separation between IW that was been more oxygenated than today and deep waters that were less ventilated, and (4) significantly lower deepwater temperatures [Peltier et al., 1993].

The eight time slices presented in Figures 6,7, and 9-20 clearly suggest grouping the distribution of east Atlantic water masses into three different states of deepwater circulation.

The Holocene/interglacial mode. This interval is marked by strong southward bound NADW flow in the northeast Atlantic, originating from the Norwegian-Greenland Sea, similar to the present (Figures 6 and 7). The mode applies with minor variations to the last 9000 ^{14}C years (mode 1a in Figures 18 and 19). It also applies to the Younger Dryas (Figures 16 and 17) and, with a weakened NADW flow, to the stage 3-2 boundary (mode 1b in Figures 9 and 10).

The glacial mode. This second mode of circulation differs only in quantitative terms from the Holocene mode and includes a southward bound, although much reduced, NADW end-member. However, its well-oxygenated core is formed south of Iceland and reaches down to 3600 m depth east of the Azores, that is, clearly below the level of IW. Further south, however, the glacial NADW end-member, which continues up to the equator between 2000 and 3500 m, is strongly diluted (Figures 11-13). Below 3500 m, the incursion of very cold, oxygen-depleted AABW is clearly enhanced and can be traced north up to Rockall trough. A large portion of the AABW appears to upwell near the scarps of the east Azores FZ, thereby markedly diluting the overlying NADW from below.

The only significant flux of well-oxygenated IW in the (east) Atlantic is linked to the Mediterranean outflow. This glacial mode lasted from the early LGM until after its end, and it was succeeded by mode 3.

The meltwater mode . This mode is characterized by poorly ventilated and weakly differentiated deepwater masses below 2000 m, that is, by stagnation or, more likely, by inflow of poorly ventilated deep water from the southern ocean (Figure 14). The outflow of oxygenated IW from the Mediterranean was also reduced. This third mode is encountered twice. The first time it occurred was during early termination Ia, about 13,800-12,800 ^{14}C years ago (Figures 3 and 14), when a major meltwater pulse came from the Barents ice sheet [Sarnthein et al., 1992]. This event is recognized as a salinity minimum down to Rockall Plateau and off Portugal [Duplessy et al., 1992]. A second case occurred immediately after the Younger Dryas, during early termination Ib, about 10,300-9,600 ^{14}C years ago (Figures 3 and 4) (not compiled as a time slice).

6.3. History and Chemical Budgets of the Salinity Conveyor Belt

Figure 21 and Table 2 summarize a time series scheme of the three different circulation modes, especially of the variations in NADW flow and, presumably, in the salinity conveyor belt (SCB) over the last 26,000 ^{14}C years. The anomalies shown in

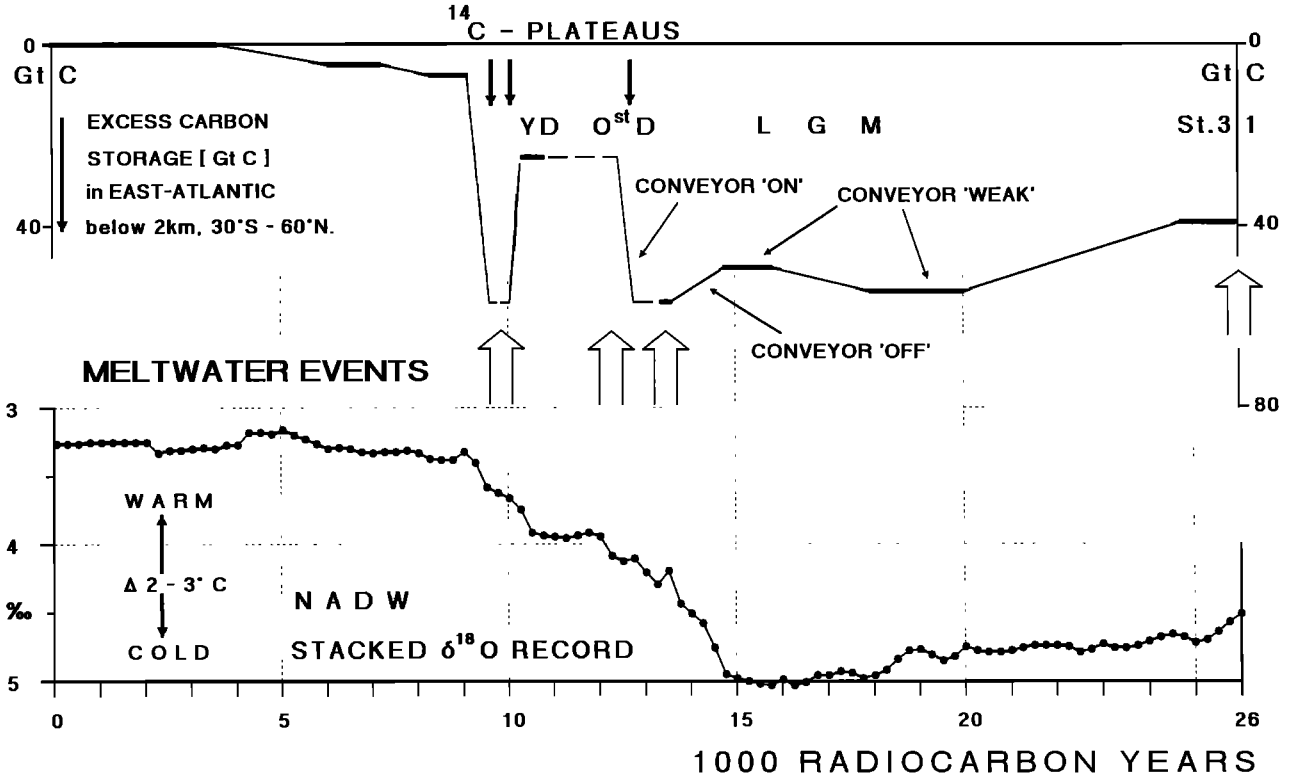

Figure 21. Reconstruction of variations in the salinity conveyor belt (SCB) over the last 30,000 calendar years. SCB intensity is deduced from $\delta^{13}C$ differences between past time slices and the Recent, converted into gigatons of carbon stored in excess of today in the east Atlantic below 2000 m depth (see Table 2). The $\delta^{18}O$ curve is based on six stacked high-resolution benthic records from the same depth range in the eastern Atlantic. Thin arrows mark positions of ^{14}C plateaus, and wide arrows indicate meltwater events.

carbon storage in the east Atlantic are calculated from the $\delta^{13}C$ anomalies between the various past time slices (Figures 9-20) and the Recent (Figure 6a). The $\delta^{13}C$ anomalies between 60°N and 30°S were converted into Gt of (dissolved) carbon using an equation of Broecker and Peng [1982] (abbreviated):

$$1‰\ \Delta\delta^{13}C = 1.4 * 10^{-6}\ \text{kg C (kg } H_2O)^{-1}. \quad (1)$$

East Atlantic water volumes (in km^3) were compiled between the Mid-Atlantic Ridge and the eastern continental margin on a grid of 10° latitude by 500 m water depth. Our estimates of past anomalies in carbon storage ignore a possible global $\delta^{13}C$ shift linked to a LGM transfer of continental biomass (see previous discussion) and any possible variations in carbonate compensation. Accounting for the global $\delta^{13}C$ shift of 0.3‰, however, would lead approximately to a reduction in the LGM storage anomalies below 2000 m depth by about 1/3 and to an increase in the relative carbon release from the top 2000 m by up to a factor of 2.

Contrary to widespread assumptions (reviewed by Peltier et al. [1993]), large parts of stage 3 and the stage 3-2 boundary (subsequent to stage 3.1) were still characterized by a largely Holocene-style mode of deepwater circulation that hardly reflects the massive growth of continental ice taking place at this time, except for a significant $\delta^{13}C$ depletion below 3500 m depth, interpreted as a conspicuous increase in the northward bound advection of AABW and its upwelling east of the Azores (Figures 9a and b). Hence the glacial (AABW) signal from the south clearly led the signal from the north. As compared to the present, the total amount of carbon sequestered in the deep Atlantic was higher, by about 10 Gt C below 4000 m and by 34 Gt C above (Table 2 and Figure 21).

Only after the $\delta^{18}O$ increase 26,000-24,500 ^{14}C years B.P. was the glacial mode of deepwater circulation established (Figure 3). Near its beginning, this mode showed the maximum $\delta^{13}C$ reduction, with $\delta^{13}C$ values increasing slightly toward the end of the LGM. As compared to the present, the ^{13}C reduction of east Atlantic deep water during the LGM reflects an additional storage of about 38-43 Gt C (D35-37.5 Gt C at 2-4 km, δ^{1}2.515.5 Gt C below 4 km depth) (details in Table 2). This additional carbon storage parallels the glacial minimum in atmospheric pCO_2 [Barnola et al., 1987]. We assume that the accelerated glacial $\delta^{13}C$ decrease and alteration of the southward bound NADW water mass east of the Azores mainly resulted from the enhanced admixture of ^{13}C-depleted southern source bottom water (AABW) from below, that is, from a reversed SCB in the abyssal Atlantic, as outlined in sections 5.4. and 6.2. Further important factors include (1) increased vertical flux rates of degrading POC induced by higher paleoproductivity in midlatitudes near the Azores [Curry et al., 1988; Sarnthein et al., 1988; Mix, 1989] and (2) a slowed down horizontal flow rate of NADW, which was linked to reduced dynamics of NADW formation and thus a weakened SCB.

In contrast to the deep eastern Atlantic, the glacial IW (0-2

Table 2. Anomalies of Carbon Storage in the East Atlantic Deep Water and Intermediate Water Over the Last 30,000 Years in Exess to Today

Water mass	6.1-7.2 ^{14}C ka	8.35-9.1 ^{14}C ka	10.35-10.8 ^{14}C ka	13.4-13.6 ^{14}C ka	14.8-15.8 ^{14}C ka	18-20 ^{14}C ka	24.8-26 ^{14}C ka
0-2 km	3.7	8.2	7.7	14.0	*-4.9*	*-5.1*	6.0
2-4 km	2.4	5.6	18.8	43.8	36.3	38.7	29.0
	(2.0)	(4.5)	(17.4)	(42.6)	(35.3)	(37.6)	(28.0)
>4 km	2.2	1.2	5.9	12.7	12.6	15.5	10.0
						(15.4)	
Total	8.3	15.0	32.4	70.5	44.0	49.1	45.0
	(7.9)	(13.9)	(31.0)	(68.3)	(43.0)	(47.9)	(44.0)

Figures in parantheses exclude data influenced by local high fluxes of organic carbon. Negative values marked by italics. See text for explanation.

km; more precisely, 0-1.5 km) became more δ^{13}C and oxygen enriched (Figures 11 and 12), as first suggested by Duplessy et al. [1988], and lost about 5 Gt C of total dissolved carbon. This number originates from the effects of both the advection of highly oxygenated Mediterranean water (-3 Gt C) [Zahn et al., 1987] and the NADW end-member formed near Rockall Plateau (as also proposed by Labeyrie et al. [1992]).

After the LGM, the estimated variations in East Atlantic carbon storage (Figure 21) record in detail the sequence of short-term events in Atlantic paleoceanography linked to the last deglaciation and suggest important insights into the internal driving mechanisms of climatic forcing. This record of carbon storage across termination I has benefitted especially from the new precision in the chronostratigraphic interpolations of the various short-lived isotopic oscillations in between the isotopic events, when based on the strict use of converted calendar years instead of non-linear ^{14}C years for age interpolations of undated sediment intervals (see section 3.).

The onset of the δ^{18}O decrease that marks the early deglaciation of termination I (Figures 3 and 4) directly paralleled a large benthic δ^{13}C reduction that appears in all medium- to high-resolution records below 1800 m and that reflects the absolute minimum level of ventilation of both east and west Atlantic deep waters over the last 30,000 cal years. This δ^{13}C minimum probably resulted from a short-term advection of poorly ventilated deep water from the Southern Ocean. At greater depths, the generally low ventilation of AABW did not further decrease during this time.

The Atlantic storage of carbon culminated about 13,600±100 (reconverted) ^{14}C years B.P., right when the benthic foraminiferal δ^{18}O record reached its first postglacial minimum. This age matches precisely the culmination of a major meltwater incursion into the northeast Atlantic [Weinelt, 1993; Sarnthein et al., 1992; Duplessy et al., 1992; Bond et al., 1992] and hence suggests a strong causal relationship between the two events, as proposed by the model of Maier-Reimer and Mikolajewicz [1989]. During this time, the advection of ventilated Mediterranean IW continued, but also decreased abruptly, absorbing 6 Gt C (as compared to D 19 Gt C in the total IW layer). The early pulse of deglaciation may thus have had a similar influence on the formation of Mediterranean IW as it did on the downwelling of NADW in the North Atlantic, possibly via north Russian (via the Black Sea) and Alpine meltwater.

In total, the east Atlantic DIC exceeded the present DIC by about 70 Gt C (27 Gt C more than during the late LGM) (Table 2). This additional transfer of carbon into the deep Atlantic cannot be properly compared yet with variations in atmospheric pCO_2, because the ice core records are still insufficient [Barnola et al., 1987; Dansgaard and Oeschger, 1989; B. Stauffer, personal communication, 1993]. Perhaps, the atmospheric pCO_2 record deduced from carbon isotopes in peat [White et al., 1994] may reveal the expected signal.

In harmony with various models, the complete shutdown of the SCB implied by the δ^{13}C data resulted in an immediate stop of heat transport to the North Atlantic, especially to northern and central Europe. The response is documented by (1) extremely low sea surface temperature in the northeastern Atlantic, which persisted in a number of high-resolution faunal records until about 13,000 ^{14}C years B.P [Bard et al., 1987; Duplessy et al., 1992; Veum et al., 1992; H. Schulz, Ph.D. thesis in preparation, 1994] and (2) a marked short-term cooling and glacial readvance in Europe, summarized as the Oldest Dryas event [Lotter et al., 1992].

The meltwater mode of east Atlantic deepwater circulation ended abruptly, about 12,800-12,500 ^{14}C years ago. The benthic δ^{13}C values then increased to the level of the Younger Dryas and record an abrupt return of oxygenated NADW simultaneously in the northeastern North Atlantic (e.g., AMS ^{14}C dated cores 17045, NA 87-22, and V23-81) (Figures 3 and 4), the Norwegian-Greenland Sea [Veum et al., 1992], and in the southern ocean (core RC 11-83). Here the age of the δ^{13}C rise matches precisely the ages in the North Atlantic when based on the age interpolation of converted calendar years, contrary to a younger age estimate of 12,200-12,600 years B.P. interpolated from conventional ^{14}C years [Charles and Fairbanks,

1992]. The meltwater pulse in the Norwegian-Greenland Sea, the pacemaker of the antecedent $\delta^{13}C$ minimum, stopped a few hundred years earlier, prior to 13,100 ^{14}C years B.P. [Weinelt, 1993; Sarnthein et al., 1992] (Figure 21). In total, the renewal of NADW circulation about 12,800-12,500 years ago led to the sudden release of almost 40 Gt C from the east Atlantic (difference between time slices 13,600-13,400 years B.P. and 10,800-10,350 years B.P.) (Table 2). Note that this pronounced release of carbon precisely paralleled the abrupt pre-Bölling onset of warm climate about 14,650 cal years equal to 12,650 ^{14}C years ago as recorded in the Greenland ice core record of Taylor et al. [1993].

The turning on of the SCB thus did not parallel [Charles and Fairbanks, 1992] but immediately preceded a second meltwater incursion centered in the Bölling near 12,500-12,300 y B.P. that was the main meltwater pulse according to Fairbanks [1989]. It was less conspicuous within the Norwegian-Greenland Sea [Weinelt, 1993; Sarnthein et al., 1992], the crucial site of deepwater formation. Hence, this second pulse, although generally larger, did not impede the deepwater ventilation in most parts of the east Atlantic, unlike the meltwater input 13,500 y ago.

Contrary to many models [Broecker et al., 1988; Broecker, 1992] (see the recent review in the work by Berger [1990]), Figures 4 and 16a show that no shutdown of deepwater ventilation occurred in the east Atlantic for more than 1500 years prior to and during the (early) Younger Dryas cooling episode, the origin of which remains an enigma. The observation that deepwater ventilation was well developed at this time is documented in most high- to medium-resolution records in Figure 3 and also in core RC 11-83 from the southern ocean. Altogether, the total carbon storage in east Atlantic deepwater and intermediate water masses exceeded the present DIC only by 32 Gt C (Table 2).

Subsequent to the Younger Dryas (and near its end), a further conspicuous shutdown (mode 3) emerged in east Atlantic deepwater circulation, which paralleled the climatic amelioration of early termination Ib near 10,200-9,600 years B.P. This event is only documented in a few $\delta^{13}C$ records (enumerated in section 5), the resolution of which exceed about 10-15 cm kyr.$^{-1}$ The stratigraphic correlation is based on details in the sequence of $\delta^{18}O$ and $\delta^{13}C$ records (Figure 4) and is well substantiated. Although the number of carbon isotope records that contain this short-term minimum in deepwater ventilation is insufficient for reconstructing a complete oceanic transect, the event can be clearly traced all over the deep and abyssal Atlantic. Hence, it was incorporated into the carbon record of Figure 21 per analogy with the event near 13,500 years B.P. The striking synchrony between the short-term preboreal ventilation low of Atlantic deep water and the strong preboreal meltwater pulse of Fairbanks [1989] suggests a direct causal relationship analogous to that discussed for the event 13,500 years ago.

About 9,500-9,100 ^{14}C years ago, the Holocene mode of deepwater circulation was fully established. Since then, the east Atlantic carbon budgets have differed little from the present (+15 Gt C near 9000 years B.P. and +8.3 Gt C about 6500 years ago). Minor Holocene variations in the carbon budget at 2-4 km depth (D3.5-5.5 Gt C) are ascribed to both variations in the SCB because of precipitation changes in the high-latitude Atlantic [Broecker et al., 1990; Weaver et al., 1991] and an incursion of AABW, which increased during the middle Holocene. A ventilation minimum of MOW emerged 9000 years ago (+8.4 Gt C).

6.4. Deepwater Circulation and ^{14}C Plateaus

During this study, it has proved difficult to precisely radiocarbon date the end and/or beginning of these various modes of deepwater circulation. Especially difficult was defining when the SCB was renewed both at about 12,800-12,500 ^{14}C years ago and prior to 9,600-9,500 ^{14}C years ago (Figures 3 and 4). Problems occurred because these two intervals directly matched "^{14}C plateaus," times when the ^{14}C ages remained constant over several hundred calendar years. The existence of these "plateaus" has been recently reported by Bard et al. [1990, 1993], Stuiver et al. [1991], Kromer and Becker [1992], and Lotter et al. [1992]. Based on tree ring chronology, Kromer & Becker [1992] defined a first plateau at 9600 ^{14}C years B.P., extending over about 400 cal years, and a second plateau at about 10,100 ^{14}C years ago, lasting for more than 400 cal years. Varve counts of Lotter et al. [1992] confirmed the duration of the first two plateaus as 428 and 356 cal years, respectively, and revealed a third plateau at about 12,700-12,600 ^{14}C years ago that extended over more than 300 cal years subsequent to the Oldest Dryas, prior to the Bölling starting 14,600 cal years ago [Taylor et al., 1993] equal to 12,600 ^{14}C years B.P. These age ranges largely agree with the age ranges revealed by U/Th dating [Bard et al., 1990].

The striking contemporaneity between the ^{14}C plateaus and the now much better constrained ages for the "switch-ons" of the SCB strongly suggests a joint origin of these features (although the link to plateaus 1 and 2 needs more precise datings in the future). Based on Table 2, the east Atlantic between 60°N and 30°S alone released about 40 Gt C over the short time span of ^{14}C plateau 3 when NADW circulation started. The total Atlantic (eastern plus western basin plus the circum Antarctic Ocean) must have then released at least two to three times as much, that is, about one third to one half of a glacial atmospheric carbon unit (about 300 Gt C, disregarding any effects of carbonate compensation). Similarly, the same amount of DIC was probably released along with ^{14}C plateau 1 (possibly together with plateau 2), based on a rough conversion of the extreme $\delta^{13}C$ excursions during these intervals. We surmise that the large amount of fossil carbon expelled at these times from the deep ocean to the atmosphere induced abrupt oscillations in atmospheric CO_2, by now poorly documented in ice cores [Barnola et al., 1987; B. Stauffer, personal communication, 1993]. However, a high-resolution atmospheric pCO_2 record from carbon isotopes in peat [White et al., 1994] clearly presents the "missing link", that is two prominent CO_2 spikes in the atmosphere precisely at the times of Atlantic CO_2 exhalation. Thus, we conclude that the abrupt carbon transfer to the ocean surface has led to a short-term decrease in the global atmospheric ^{14}C budget, producing a relative increase of planktonic ^{14}C ages over the time span of the ^{14}C plateaus.

Both ^{14}C plateau 3 and the renewal of Atlantic deepwater ventilation after the first breakdown of the SCB 12,800-12,500 ^{14}C years ago may be linked to a further exceptional

feature of ocean history, that is, the short-term minimum in Pacific deepwater age (451-520 years versus 1500-2000 years) lasting approximately from 14,340-14,020 to >12,000 ^{14}C years B.P., as reported by Shackleton et al. [1988]. The abrupt changes in Pacific deepwater ages clearly reflect a fast decrease and increase in the oceanic carbon budget. Because of insufficient age correlations, however, the precise cause and effect relationships between the changes in Pacific and Atlantic paleochemistry are not yet fully understood.

In summary, we conclude that the oscillations in Atlantic deepwater circulation have been a major cause of variations in the ^{14}C balance of the atmosphere and the ocean during termination I and hence of the hitherto unexplained ^{14}C plateaus.

7. Conclusions

Our reconstructions of east Atlantic deepwater circulation demonstrate that both the salinity conveyor belt (SCB) and the abyssal incursion of AABW into the east Atlantic were highly variable during the last 30,000 years. Basically, three modes of deepwater circulation can be distinguished. During the present interglaciation, the Norwegian-Greenland Sea has been the dominant site of North Atlantic deepwater formation. The same mode was still active, although strongly reduced, near the stage 3-2 boundary, the time of major glacial advance (mode 1b). At this time, the abyssal incursion of ^{13}C-depleted AABW had already reached a maximum similar to the glacial mode and hence led to changes in glacial deepwater circulation originating in the north.

During the glacial mode, the source region of the NADW end-member shifted to the south of Iceland and resulted in a much weakened, but still recognizable, southward bound flow of NADW up to the equator. East of the Azores, it was strongly diluted by upwelled AABW, which was at its maximum extent during early stage 2. In total, the glacial east Atlantic absorbed about 44-50 Gt C below 2000 m, whereas the IW above 2000 m released about 5 Gt C. In these estimates no glacial transfer of continental biomass into the ocean is considered. Moreover, no noticeable changes are found in preformed ^{13}C, that is, in the gas exchange of downwelled water in the North Atlantic during glacial times versus the present.

The early deglaciation led to a major meltwater pulse in the northeast Atlantic culminating 13,500 ^{14}C years ago, which induced the third mode of Atlantic deepwater circulation with a massive ventilation minimum below 1800 m and a reduced ventilation of the IW. NADW flow at that time was probably fully replaced by an advection of deep water from the south. This short-term reversal of the SCB resulted in a major European cooling episode, the Oldest Dryas. A similar shutdown of NADW formation occurred right after the Younger Dryas, about 10,200-9600 ^{14}C years B.P. In both cases, the subsequent renewal of NADW formation required only a few hundred years and was synchronous with the recently discovered ^{14}C plateaus near 12,800-12,500 years and at 10,000 and 9600 ^{14}C years B.P., furthermore, with abrupt global warming. The sudden release of fossil carbon of an order of magnitude of 1/3 of a glacial atmospheric carbon unit from the Atlantic (2x40 Gt C expelled from the east and west Atlantic plus, perhaps, about 40 Gt C from the South Atlantic and southern ocean) is proposed as the main cause for observed variations in the atmospheric ^{14}C balance and global ^{14}C ages.

During the Younger Dryas, the Atlantic deepwater circulation and the SCB largely approached the interglacial mode. Intra-Holocene variations include a marked minimum in the Mediterranean outflow about 9000 years ago and a slight increase in the advection of AABW about 6500 ^{14}C years B.P.

More efforts are clearly required to reconstruct the circulation in the western basin of the Atlantic and also in the South Atlantic where the variability of incursions from the southern ocean should be traced more precisely. Future high-resolution records of changes in ocean paleochemistry will contribute to a more precise documentation of the reversals in past deep-ocean circulation that obviously took place within intervals as short as a few hundred years or less.

Acknowledgments. This paper was largely prepared during the first author's tenure as a visiting scientist at the CNRS-CEA Centre de Faibles Radioactivites at Gif-sur-Yvette in France. We are grateful to F. Schott, G. Siedler, and M. Rhein for valuable information and comments in the field of regional oceanography of the east Atlantic and to the reviewers of the manuscript for numerous constructive suggestions, especially to Mark Maslin for correcting the English. This study received substantial support from the German National Program of Climate Research, from the EPOCH project of the EC, the Sonderforschungsbereich 313 at Kiel University (publication 180), and from the Centre National de la Récherche Scientifique, the Institut National des Sciences de l'Universe, and Comissariat a l'Energie Atomique joint support to C.F.R./Gif-sur-Yvette.

References

Altenbach, A., Verbreitungsmuster benthischer Foraminiferen im Arktischen Ozean und in glazialen und interglazialen Sedimenten des Europäischen Nordmeeres, Habilitation thesis, 111 pp., University of Kiel, Kiel, Germany, 1992.

Altenbach, A., and M. Sarnthein, Productivity record in benthic foramini- fera, in *Productivity of the Ocean, Present and Past*, edited by W.H. Berger, V.S. Smetacek, and G. Wefer, pp. 255-269, John Wiley, New York, 1989.

Bainbridge, A.E., GEOSECS Oceanographic Data. Atlantic Expedition, vol. 2, National Science Foundation, Washington, D.C., 1981.

Bard, E., M. Arnold, P. Maurice, J. Duprat, J. Moyes and J.-C. Duplessy, Retreat velocity of the North Atlantic polar front during the last deglaciation determined by ^{14}C accelerator mass spectrometry, *Nature, 328*, 791-794, 1987.

Bard, E., B. Hamelin, R.G. Fairbanks, and A. Zindler, Calibration of the ^{14}C timescale over the past 30,000 years using mass spectrometry U-Th ages from Barbados corals, *Nature, 345*, 405-410, 1990.

Bard, E., M. Arnold, R.G. Fairbanks and B. Hamelin, ^{230}Th-^{234}U and ^{14}C ages obtained by mass spectrometry on corals, *Radiocarbon, 35*, 191-200, 1993.

Barnola, J.M., D. Raynaud, A. Neftel, Y.S. Korotchevich, and C., Lorius, Vostok ice core provides 160,000-years record of atmospheric CO_2, *Nature, 329*, 408-414, 1987.

Becker, B., B. Kromer and P. Trimborn, A stable isotope tree-ring timescale of the late Glacial/Holocene boundary, *Nature, 353*, 647-649, 1991.

Berger, W.H., Deep-sea carbonate: The deglaciation preservation spike in pteropods and foraminifera, *Nature, 269*, 301-304, 1977.

Berger, W.H., The Younger Dryas cold spell - A quest for

causes, *Palaeogeogr. Palaeoclimat. Palaeoecol.*, *89*, 219-237, 1990.

Berger, W.H. and E. Vincent, Deep-sea carbonates: reading the carbon-isotope signal, *Geol. Rundsch.*,*75*, 249-270, 1986.

Bond, G., H. Heinrich, S. Huon, W.S. Broecker, L. Labeyrie, J. Andrews, J. McManus, S. Clasen, K. Tedesco, R. Jantschik, C. Simet, and K. Mieczyslawa, Evidence for massive discharges of icebergs into the glacial northern Atlantic, *Nature*, 360,245-249, 1992.

Boyle, E.A., Cadmium: Chemical tracer of deepwater, *Paleoceanography*, *3*, 471-490, 1988.

Boyle, E.A., Cadmium and $\delta^{13}C$ paleochemical ocean distributions during the stage 2 glacial maximum, *Annu. Rev. Earth Planet. Sci.*, *20*, 245-287, 1992.

Boyle, E.A., and L.D. Keigwin, Comparison of Atlantic and Pacific paleo-chemical records for the last 215,000 years: Changes in deep ocean circulation and chemical inventories, *Earth Plant. Sci. Lett.*, *76*, 135-150, 1985.

Boyle, E.A. and L. Keigwin, North Atlantic thermohaline circulation during the last 20,000 years: Link to high latitude surface temperature, *Nature*, *330*, 35-40, 1987.

Broecker, W.S., The strength of the nordic heat pump, The Last Deglaciation: Absolute and Radiocarbon Chronologies, edited by E. Bard and W.S. Broecker *NATO ASI Ser., SER. I*, 2, 173-182, 1992.

Broecker, W.S., and T.-H. Peng, *Tracers in the Sea*, pp. 1-690, Eldigio, Palisades, New York, 1982.

Broecker, W.S., and T.-H. Peng, The oceanic salt pump. Does it contribute to the glacial-interglacial difference in atmospheric CO_2 content?, *Global Biochem. Cycles*, 3, 215-239, 1989.

Broecker, W.S., and T.-H. Peng, Interhemispheric transport of carbon dioxide by ocean circulation, *Nature*, *356*, 587-589, 1992.

Broecker, W.S., M. Andree, G. Bonani, W. Wölfli, H. Oeschger, M. Klas, A. Mix and W. Curry, Preliminary estimates for the radiocarbon age of deep water in the glacial ocean, *Paleoceanography*, *3*, 659-669, 1988.

Broecker, W.S., A. Mix, M. Andree, and H. Oeschger, Radiocarbon measure-ments on coexisting benthic and planktic foraminifera shells: Potentialfor reconstructing ocean ventilation times over the past 20,000 years, *Nucl. Instrum. Methods Phys. Res.*,Sect. B, *5*, 331-339, 1984.

Broecker, W.S., D.M. Peteet, and D. Rind, Does the ocean-atmosphere system have more than one stable mode of operation?, *Nature*, *315*, 21-26, 1985a.

Broecker, W.S., C. Rooth, and T.-H. Peng, Ventilation of the deep northeastern Atlantic, *J. Geophys. Res.*, *90*, 6940-6944, 1985b..

Broecker, W.S., G. Bond, M. Klas, G. Bonani, and W. Wölfli, A salt oscillator in the Glacial Atlantic?, 1, The concept, *Paleoceanography*, *5*, 469-478, 1990.

Bryan, F., High-latitude salinity effects and interhemispheric thermohaline circulations, *Nature*, *323*, 301-304, 1986.

Charles, C.D., and R.G. Fairbanks, Glacial to interglacial changes in theisotopic gradients Southern Ocean surface water, *Geological history of the Polar Oceans: Arctic versus Antarctic*, edited by U. Bleil and J. Thiede, pp. 519-538,Kluwer Academic. Norwell, Mass., 1990.

Charles, C.D., and R.G. Fairbanks, Evidence from Southern Ocean sediments for the effect of North Atlantic deepwater flux on climate, *Nature*, *355*, 416-419, 1992.

Climate: Long-Range Investigation, Mapping and Prediction Project Members, Seasonal reconstructions of the Earth's surface at the last glacial maximum, *Map. Chart Ser.Geol. Soc. Am.*, MC-36, 1981.

Curry, W.B., J.-C. Duplessy, L.D. Labeyrie, and N.J. Shackleton, Changes in the distribution of $\delta^{13}C$ of deep water SCO_2 between the last Glaciations and the Holocene, *Paleoceanography*, *3*, 317-342, 1988.

Curry, W.B., and G.P. Lohmann, Carbon isotopic changes in benthic foraminifera from the western South Atlantic: Reconstruction of glacial abyssal circulation patterns, *Quat. Res.*, 18, 218-235, 1982.

Curry, W.B. and G.P. Lohmann, Carbon deposition rates and deepwater residence time in the equatorial Atlantic Ocean throughout the last 160,000 years, in The Carbon Cycle and Atmospheric CO_2: Natural Variations Archean to Present, *Geophys. Monogr. Ser. ,Vol. 32*, edited by E.T. Sundquist, and W.S. Broecker pp. 285-302, AGU, Washington, D.C.,1985.

Dansgaard, W., and H. Oeschger, Past environmental long-term records from the Arctic, in *The Environmental Record in Glaciers and Ice Sheets* , edited byH. Oeschger and C.C. Langway, Jr., pp. 287-318, Wiley-Interscience, New York, 1989.

Dickson, R.R., E.M. Gmitrowicz, and A.J. Watson, Deep-water renewal in the northern North Atlantic, *Nature*, *344*, 848-850, 1990.

Duplessy, J.-C., La géochemie des isotopes stables du carbone dans la mer, Ph.D. thesis, 195 p. d'Etat es Sciences Physics, Paris, 1972.

Duplessy, J.-C., North Atlantic deep water circulation during the last climatic cycle, *Bull. Inst. Géol. Bassin Aquitaine*, *31*, 379-391, 1982.

Duplessy, J.-C., L. Labeyrie, M. Arnold, M. Paterne, J. Duprat, and T.C.E. van Weering, Changes in surface salinity of the North Atlantic Ocean during the last deglaciation, *Nature*, *358*, 485-488, 1992.

Duplessy, J.-C., L. Labeyrie, A. Juillet-Leclerc, F. Maitre, J. Duprat, and M. Sarnthein, Surface salinity reconstruction of the North Atlantic ocean during the last glacial maximum, *Ocean. Acta*, *14*, 311-324, 1991.

Duplessy, J.-C., N.J. Shackleton, R.K. Matthews, W. Prell, W.F. Ruddiman, M. Caralp, and C.H. Hendy, ^{13}C record of benthic foraminifera in the last Interglacial ocean: Implications for the carbon cycle and the global deep water circulation, *Quat. Res.*, *2*, 225-243, 1984.

Duplessy, J.-C., N.J. Shackleton, R. Fairbanks, L. Labeyrie, D. Oppo, and N. Kallel, Deep water source variations during the last climatic cycle and their impact on the global deepwater circulation, *Paleoceanography*, *3*, 343-360, 1988.

Emiliani, C., C. Rooth, and J.J. Stipp, The late Wisconsin Flood into the Gulf of Mexiko, *Earth Plant. Sci. Lett.*, *41*, 159-162, 1978.

Fairbanks, R.G., A 17,000-years glacio-eustatic sea level record: Influence of glacial melting rates on the Younger Dryas event and deep-ocean circulation, *Nature*, *342*, 637-642, 1989.

Fontes, J.C., and F. Gasse, Palhydaf (Palaeohydrology in Africa) program: Objectives, methods, major results, *Palaeogeogr. Palaeoclimat. Palaeoecol.*, *84*, 191-215, 1991.

Ganssen, G., Isotopic Analysis of Foraminifera Shells, *Palaeogeogr. Palaeoclimat. Palaeoecol.*, *33*, 271-276, 1981.

Ganssen, G., Dokumentation von küstennahem Auftrieb anhand stabiler Isotope in rezenten Foraminiferen vor Nordwest-Afrika, *Meteor Forschungsergeb.*, Reihe C, *37*, 1-46, 1983.

Graham, D.W., B.H. Corliss, M.L. Bender, and L.D. Keigwin

Jr., Carbon and oxygen isotopic disequilibria of Recent deep-sea benthic foraminifera, *Mar. Micropaleontol., 6*, 483-497, 1981.

Hodell, D.A., Late Pleistocene paleoceanography of the South Atlantic sector of the Southern Ocean: Ocean Drilling Program hole 704A, *Paleoceanography, 8*, 47-68, 1993.

Hooghiemstra, H., Variations of the NW African trade wind regime during the last 140,000 years: Changes in pollen flux evidenced by marine sediment records, *NATO ASI Ser.*, Ser. C, *2*, 733-770, 1989.

Hut, G., Consultants' group meeting on stable isotope reference samples for geochemical and hydrological investigations, in 1-42, International Atomic Energy Agency Vienna, 1987.

Jansen, E., and T. Veum, Two-step deglaciation: Timing and impact on North Atlantic deep water circulation, *Nature, 343*, 612-616, 1990.

Käse, R.H., J.F. Price, P.L. Richardson, and W. Zenk, A quasi-synoptic survey of the thermocline circulation and water mass distribution within the Canary Basin, *Journal of Geophysical Research, 91/C8*, 9739-9748, 1986.

Keigwin, L.D., G.A. Jones, S.J. Lehman, and E.A. Boyle, Deglacial meltwater discharge, North Atlantic deep circulation, and abrupt climate change, *J. of Geophys.Res., 96* , 16,811-16,826, 1991.

Kern, R.A., and W.H. Schlesinger, Carbon stores in vegetation, *Nature, 357*, 447-448, 1992.

Kromer, B. and B. Becker, Tree-ring ^{14}C calibration at 10.000 BP, in The Last Deglaciation: Absolute and Radiocarbon Chronologies, edited by Bard, E.A. and W.S. Broecker, *NATO ASI Ser., Ser. I, 2*, 3-12,1992.

Kroopnick, P., The distribution of ^{13}C of ΣCO_2 in the world oceans, *Deep Sea Res., 32*, 57-84, 1985.

Kroopnick, P., R.F. Weiss, and H. Craig, Total CO_2, ^{13}C, and dissolved oxygen-^{18}O at Geosecs II in the North Atlantic, *Earth Plant. Sci. Lett., 16*, 103-110, 1972.

Ku, T.L., and S. Luo, Carbon isotopic variations on glacial-to-interglacial time scales in the ocean: Modeling and implications, *Paleoceanography, 7*, 543-562.

Labeyrie, L.D., J.C. Duplessy, and P.L. Blanc, Variations in mode of formationand temperature of oceanic deep waters over the past 125,000 years, *Nature, 327*, 477-483, 1987.

Labeyrie, L.D., J.-C. Duplessy, J. Duprat, A. Juillet-Leclerc, J. Moyes, E. Michel, N. Kallel, and N.J. Shackleton, Changes in the vertical structure of the North Atlantic Ocean between glacial and modern times, *Quat. Sci. Rev., 11*, 401-414, 1992.

Labracherie, M., Les Radiolaires temoins de l'évolution hydrogeologique depuis le dernier maximum glaciaire au large du Cap Blanc (Afrique du Nord-Ouest), *Palaeogeogr. Palaeoclimat. Palaeoecol., 32* , 163-184, 1980.

Leuenberger, M., U. Siegenthaler, and C.C. Langway, Carbon isotope compostion of atmospheric CO_2 during the last ice age from an Antarctic core, *Nature, 357*, 488-490, 1992.

Linke, P. and G.F. Lutze, Microhabitats preference of benthic foraminfera - A static concept or a dynamic adaptation to optimize food acquisition?, *Mar. Micropaleontol., 20*, 215-234, 1993.

Lotter, A.F.., B. Ammann, J. Beer, I. Hajdas, and M. Sturm, A step towards an absolute time-scale for the Late-Glacial: Annually laminated sediments from Soppensee (Switzerland), in The Last Deglaciation: Absolute and Radiocarbon Chronologies, edited by E.A. Bard and W.S. Broecker *NATO ASI Ser. I, 2*, 45-68, 1992.

Lutze, G.F. and H. Thiel, *Cibicidoides wuellerstorfi* and *Planulina ariminensis*, elevated epibenthic foraminifera, *Ber. 6, pp.1-86* Sonderforschungsbereich 313, University of Kiel, Germany, 1987.

Lutze, G.F. and H. Thiel, Epibenthic foraminifera from elevated microhabitats (*Cibicidoides wuellerstorfi, Planulina ariminensis*), *J. Foraminiferal. Res., 19*, 153-158, 1989.

Maier-Reimer, E. and U. Mikolajewicz, Experiments with an OGCM on the cause of the Younger Dryas, Rep. 39, pp.1-13, Max-Planck-Institute für Meteorologie, Hamburg, Germany, 1989.

Marino, B.D., M.B. McElroy, R.J. Salawitch, and W.G. Spaulding, Glacial to inter-glacial variations in $\delta^{13}C$ for atmospheric CO_2, *Nature, 357*, 461-465, 1992.

McCartney, M.S., S.L. Bennett, and M.E. Woodgate-Jones, Eastward flow through the Mid-Atlantic Ridge at 11°N and its influence on the abyss of the Eastern Basin, *J. Phys. Oceanogr., 21*, 1089-1121, 1991.

McCorkle, D.C., L.D. Keigwin, B.H. Corliss, and S.R. Emerson, The influence of microhabitats on the carbon isotopic composition of deep-sea benthic foraminifera, *Paleoceanography, 5*, 161-185, 1990.

Michel, E., L'ocean ou dernier maximum glaciaire: Le cycle du carbone et la circulation. Contraintes isotopiques et modelisation, Ph.D. thesis, 191pp. Univ. de Paris-Sud, Centre d'Orsay, Orsay France, 1991.

Mix, A.C., Pleistocene paleoproductivity: Evidence from organic carbon and foraminferal species, in *Productivity of the Ocean: Present and Past*, edited by W.H. Berger, V.S. Smetacek, and G. Wefer pp. 313-340, John Wiley, New York ,1989.

Mix, A.C., and W.F. Ruddiman, Structure and timing of the last deglaciation: Oxygen-isotope evidence, *Quat. Sci. Rev., 4*, 59-109, 1985.

Mix, A.C., and R.G. Fairbanks, North Atlantic surface-ocean control of Pleistocene deep-ocean circulation, *Earth Planet. Sci. Lett., 73*, 231-243, 1985.

Oppo, D., and R.G. Fairbanks, Variability in the deep and intermediate water circulation of the Atlantic Ocean during the past 25,000 years: Northern hemisphere modulation of the southern ocean, *Earth Planet. Sci. Lett., 86*, 1-15, 1987.

Oppo, D., and R.G. Fairbanks, Mid-depth circulation of the subpolar North Atlantic during the last glacial maximum, *Science, 259*, 1148-1152, 1993.

Peltier, W.R., et al., How can we use paleodata for evaluating the internal variability and feedback in the climate system?, in *Global Changes in the Perspective of the Past, edited by J. Eddy and H. Oeschger*, pp. 239-262, John Wiley, New York, 1993.

Prentice, I.C. and M. Sarnthein, Self-regulatory processes in the biosphere in the face of climate change, in: *Global changes in the Perspective of the Past, edited by J. Eddy and H. Oeschger*, pp. 29-38, John Wiley, New York, 1993.

Prentice, K.C. and I.Y. Fung, The sensitivity of terrestrial carbon storage to climate change, *Nature, 346*, 48-51, 1990.

Price, J.F., M. O'Neil Baringer, R.G. Lueck, G.C. Johnson, I. Ambar, G. Parilla, A. Cantos, M.A. Kennelly, T.B. Sanford, Mediterranean outflow mixing and dynamics, *Science, 259*, 1277-1282, 1993.

Reid, J.L., On the contribution of the Mediterranean Sea outflow to the Norwegian-Greenland Sea, *Deep Sea Res., 26*, 1199-1223, 1979.

Rooth, C., Hydrology and ocean circulation, *J. Phys. Oceanogr., 11*, 131-149, 1982.

Rossignol-Strick, M., W. Nesteroff, P. Olive, and C.

Vergnaud-Grazzini, After the deluge: Mediterranean stagnation and sapropel formation, *Nature, 295*, 105-110, 1982.

Sarnthein, M., Sand deserts during glacial maximum and climatic optimum, *Nature, 271*, 43-46, 1978.

Sarnthein, M., and R. Tiedemann, Younger Dryas-style events at glacial Terminations I-IV: Associated benthic $\delta^{13}C$ anomalies at ODP Site 658 constrain meltwater hypothesis, *Paleoceanography, 6*, 1041-1055, 1990.

Sarnthein, M. and K. Winn, Reconstruction of low and mid latitude export productivity, 30,000 y B.P. to Present: Implications for global carbon reservoirs, in Climate-Ocean Interaction, edited by M. Schlesinger, pp.319-342, Kluwer Academic Publ., Norwell, Mass., 1990.

Sarnthein, M., J. Thiede, U. Pflaumann, H. Erlenkeuser, D. Fütterer, B. Koopmann, H. Lange, and E. Seibold, Atmospheric and oceanic circulation patterns off NW-Africa during the past 25 million years, in *Geology of the Northwest African Continental Margin,* edited by U. Rad et al. , pp.545-604 Springer Verlag, New York, 1982.

Sarnthein, M., K. Winn, and R. Zahn, Paleoproductivity of oceanic upwellingand the effect on atmospheric CO_2 and climatic change during deglaciation times, in Abrupt Climatic Change, edited by W.H. Berger and L.D. Labeyrie, *NATO ASI Ser., Ser. C*, 216 , 311-337, 1987.

Sarnthein, M., K. Winn, J.-C. Duplessy, and M.R. Fontugne, Global variationsof surface ocean productivity in low and mid latitudes: Influence on CO_2, *Paleoceanography, 3*, 361-399, 1988.

Sarnthein, M., E. Jansen, J.-C. Duplessy, H. Erlenkeuser, A. Flatoy, T. Veum, E. Vogelsang, and M.S. Weinelt, $\delta^{18}O$ time-slice reconstruction of meltwater anomalies at Termination I in the North Atlantic between 50 and 80°N, in The Last Deglaciation: Absolute and Radiocarbon Chronologies, edited by E.A. Bard, and W.S. Brocker , *NATO ASI Ser., Ser, I, 2*, 183-200, 1992.

Saunders, P.M., Circulation in the eastern North Atlantic, *J. Mar. Res., 40*, 641-657, 1982.

Shackleton, N.J., Carbon-13 in *Uvigerina*: Tropical rainforest history and the equatorial Pacific carbonate dissolution cycles, in *The Fate of Fossil Fuel in the Oceans*, edited by N.R. Andersen and A.Malahoff, pp. 401-447, Plenum Press New York, 1977.

Shackleton, N.J., and M.A. Hall, Oxygen and carbon isotope stratigraphy of Deep-Sea Drilling Project Hole 552A: Plio-Pleistocene glacial history, *Initial Rep. Deep Sea Drill. Proj., 81*, 599-601, 1984.

Shackleton, N.J., J.-C. Duplessy, M. Arnold, P. Maurice, M.A. Hall, and J. Cartlidge, Radiocarbon age of last glacial Pacific deep water, *Nature, 335*, 708-711, 1988.

Stocker, T.F., and D.G. Wright, A zonally averaged ocean for the thermohaline circulation, II, Interocean circulation in the Pacific-Atlantic Basin system, *J. Phys. Oceanogr., 21*, 1725-2739, 1991.

Stommel, H., Thermohaline convection with two stable regimes of flow, *Tellus, 13*, 224-230, 1961.

Stuiver, M., T. Braziunas, B. Becker, and B.,Kromer, Climatic, solar, oceanic, and geomagnetic influences on late-Glacial and Holocene atmospheric $^{14}C/^{12}C$ change, *Quat. Res., 35*, 1-24, 1991.

Taylor, K.C., G.W. Lamorey, G.A. Doyle, R.B. Alley, P.M. Grootes, P.A. Mayewski, J.W.C. White, and L.K. Barlow, The 'flickering switch' of late Pleistocene climate change, *Nature, 361*, 432-436, 1993.

Tiedemann, R., Acht Millionen Jahre Klimageschichte von Nordwest-Afrika und Paläo-Ozeanographie des angrenzenden Atlantiks: Hochauflösende Zeitreihen von ODP Sites 658-661, Ph.D. thesis, pp. 1-127, University. of Kiel, Kiel, Germany, 1991.

Tissot, B.P., and D.H. Welte, *Petroleum Formation and Occurrence*, 699 pp., Springer-Verlag, New York, 1984.

Veum, T., E. Jansen, M. Arnold, J. Beyer, and J.-C. Duplessy, Watermass exchange between the North Atlantic and the Norwegian Sea during the past 28,000 years, *Nature, 356*, 783-788, 1992.

Warren, B.A., Deep water circulation in the world ocean, in *Evolution of Physical Oceanography*, edited by B.A. Warren, and C. Wunsch, pp.6-41, MIT Press, Cambridge, Mass., 1981.

Weaver, A.J., E.S. Sarachik, and J. Marotzke, Freshwater flux forcing of decadal and interdecadal oceanic variability, *Nature, 353*, 836-838, 1991.

Weinelt, M., Schmelzwasser-Episoden in der Norwegisch-Grönländischen See während der letzten 60 000 Jahre, Ph.D. thesis, 105 pp., University of Kiel, Kiel, Germany, 1993.

Weinelt, M.S., M. Sarnthein, E. Vogelsang, and H. Erlenkeuser, Early decay of the Barents Shelf Ice Sheet Spread of stable isotope signals across the Eastern Norwegian Sea, *Nor. Geol. Tidsskrift*, (3), *71* 137-140, 1991.

White, J.W.C., P. Ciais, R.A. Figge, R. Kenny, and V. Markgraf, A high-resolution atmospheric pCO_2 record from carbon isotopes in peat, *Nature, 367*, 153-156, 1994.

Winn, K., Sarnthein, M. and H. Erlenkeuser, $\delta^{18}O$ stratigraphy and age control of Kiel sediment cores in the East Atlantic, *Ber. 45, pp. 1-99,* Geol. Paläont. Inst. University of Kiel, *45*, 1-99, 1991.

Zahn, R., M. Sarnthein, and H. Erlenkeuser, Benthos isotopic evidence for changes of the Mediterranean outflow during the late Quaternary, *Paleoceanography, 2*, 543-559, 1987.

Zahn, R., K. Winn, and M. Sarnthein, Benthic foraminiferal $\delta^{13}C$ and accumulation rates of organic carbon: *Uvigerina peregrina* group and *Cibicidoides wuellerstorfi, Paleoceanography, 1* (1), 27-42, 1986.

Zahn, R., A. Rushdi, N.G. Pisias, B.D. Bornhold, B. Blaise, and R. Karlin, Carbonate deposition and benthic $\delta^{13}C$ in the subarctic Pacific: Implications for changes of the oceanic carbonate system during the past 750,000 years, *Earth Plant. Sci. Lett. 103*, 116-132, 1991.

J.-C. Duplessy and L. Labeyrie, Centre des Faibles Radioactivités, Laboratoire mixte CNRS-CEA, Parc du CNRS, F-91198 Gif-sur Yvette Cedex, France.

H. Erlenkeuser, C-14 Laboratory, University of Kiel , D-24098 Kiel, Germany.

G. Ganssen, Institut voor Aardtwetenschappen, Vrije Universiteit, NL-1007 MC Amsterdam, Netherlands.

S.J.A. Jung, M. Sarnthein, K. Winn, Geologisch-Paläontologisches Institut, University of Kiel, D-24098 Germany.

(Received January 29, 1993; revised November 9, 1993; accepted November 18, 1993)